# Role of FAM57B2 and Lactosylceramide in Chondrogenesis

# Lilit Antonyan

Department of Human Genetics, Faculty of Medicine McGill University, Montréal, Québec, Canada

## February 2018

A thesis submitted to McGill University in partial fulfillment of the requirements of the degree of Master of Science in Human Genetics.

Copyright © Lilit Antonyan, 2018

#### Abstract

Chondrogenesis is critical for the healing of fractured bones. After an initial inflammation stage, a "soft callus" composed of chondrocytes bridges the injury site, to be later mineralized and substituted by bone. When studying bone healing in mice deficient for *Cyp24a1*, which cannot synthesize the vitamin D metabolite, 24,25(OH)<sub>2</sub>D<sub>3</sub>, a significant and reproducible impairment in callus formation is observed. We used callus tissue of *Cyp24a1* knockout mice to clone *Fam57b2* (*Family with sequence similarity 57, member B*), which encodes a transmembrane protein that specifically interacts with 24,25(OH)<sub>2</sub>D<sub>3</sub>. Previous work from our laboratory revealed 24,25(OH)<sub>2</sub>D<sub>3</sub>-dependent production of lactosylceramide (LacCer) by FAM57B2. We hypothesized that LacCer acts as a signaling molecule to regulate chondrocyte differentiation or function.

Mutagenesis was performed to identify the binding pocket for 24,25(OH)<sub>2</sub>D<sub>3</sub> and the topology of FAM57B2. The structure-function analysis for the 24,25(OH)<sub>2</sub>D<sub>3</sub> binding site remain inconclusive but additional strategies have been identified and are discussed. Immunofluorescence detection of epitope-tagged mutants allowed to conclude that FAM57B2 localizes to the endoplasmic reticulum, with both the N- and C-termini facing the cytosolic compartment. We propose a protein topology with one membrane loop and 4 transmembrane domains.

LacCer had no effect on adhesion, migration or apoptosis of chondrogenic ATDC5 cells. However, LacCer treatment decreased proliferation and adhesion to fibronectin, and potentiated differentiation of chondrocytes when cultured in media containing insulin, transferrin, and selenium (ITS). Similarly, ATDC5 cells stably overexpressing *Fam57b2* showed a significant increase of expression of chondrogenic markers. Our results indicate that FAM57B2 and LacCer are important regulators of chondrocyte biology.

#### Résumé

La chondrogenèse est essentielle pour la guérison des fractures. Après la réponse inflammatoire initiale, le cal 'mou' composé de chondrocytes relie les extrémités de la lésion, pour être ensuite minéralisé et substitué par de l'os. Lors de l'étude de la cicatrisation osseuse chez des souris mutantes pour *Cyp24a1*, déficientes en 24,25(OH)<sub>2</sub>D<sub>3</sub>, une altération de la formation du cal est observée. À partir du cal de souris mutantes *Cyp24a1*, nous avons cloné *Fam57b2* (famille avec similitude de séquence 57, membre B), encodant une protéine transmembranaire qui interagit spécifiquement avec la 24,25(OH)<sub>2</sub>D<sub>3</sub>. Des travaux antérieurs de notre laboratoire ont révélé une production de lactosylcéramide (LacCer) suite à l'interaction de 24,25(OH)<sub>2</sub>D<sub>3</sub> avec FAM57B2. Nous avons testé l'hypothèse selon laquelle LacCer agit comme second messager pour influencer la différenciation et/ou la fonction des chondrocytes.

L'analyse structure-fonction par mutagénèse de FAM57B2 afin d'identifier le site de liaison de la 24,25(OH)<sub>2</sub>D<sub>3</sub> fut non concluante mais des stratégies supplémentaires ont été identifiées et sont discutées. L'immunodétection de mutants marqués par un épitope a permis de conclure que FAM57B2 se localise au réticulum endoplasmique, avec les extrémités N- et C-terminales du côté cytosolique. Nous proposons une topologie protéique comprenant une boucle membranaire et 4 domaines transmembranaires.

LacCer n'a démontré aucun effet sur l'adhésion, la migration ou l'apoptose de cellules chondrogéniques de la lignée ATDC5. Cependant, LacCer a diminué la prolifération et l'adhésion à la fibronectine, et a potentialisé la différenciation chondrocytaire en présence d'insuline, de transferrine et de sélénium (ITS). De même, les cellules ATDC5 surexprimant *Fam57b2* ont montré une augmentation significative de l'expression des marqueurs chondrogéniques. Nos résultats indiquent que FAM57B2 et LacCer sont des régulateurs importants de la biologie des chondrocytes.

# Table of Contents

Abstract	2
Résumé	3
Table of Contents	4
List of Abbreviations	6
List of Figures	8
List of Tables	9
Acknowledgements	10
Chapter I: Introduction, Hypothesis and Aims	11
1. Introduction	11
1.1 Bone Physiology	11
1.1.1 Intramembranous Ossification	13
1.1.2 Endochondral Ossification.	13
1.2 Chondrocyte Physiology and Differentiation	15
1.3 Fracture Repair Stages	18
1.4 Vitamin D	21
1.4.1 Forms and Pathway	21
1.4.2 Role in Calcium Homeostasis	24
1.5 CYP24A1 and 24,25(OH) <sub>2</sub> D <sub>3</sub>	25
1.6 Cyp24a1-Gene Deficient Mice	28
1.7 FAM57B	32
1.8 Ceramides	37
1.8.1 Lactosylceramide	39
Hypothesis	43
Aims	43
Chapter II: Materials and Methods	44
2.1 Cell lines, Antibodies, and Reagents	44
2.2 Plasmids, Vector Cloning and Mutagenesis	46
2.3 Transfection of HEK293 and Infection of ATDC5 cells with Target DNA	47
2.4 FAM57B2 Protein Expression	49

2.5 Chondrocyte Cell Regulation Assays	49
2.5.1 Proliferation	49
2.5.2 Differentiation	49
2.5.3 Adhesion	50
2.5.4 Cell Migration	51
2.5.5 Apoptosis	52
2.5.6 Reactive Oxygen Species	52
2.6 Immunofluorescence	52
2.7 Enzymatic Assay and Thin Layer Chromatography	53
2.8 Real-Time RT-PCR (RT-qPCR)	54
2.9 Statistical Analysis	55
2.10 Tables	56
Chapter III: Results	57
3.1 FAM57B2 WT and Mutant Protein Outline	57
3.2 FAM57B2 Protein Expression	58
3.3 24,25(OH) <sub>2</sub> D <sub>3</sub> -dependent Production of Lactosylceramide	59
3.4 Cellular Localization and Topology of FAM57B2	61
3.5 Fam57b2-overexpression in ATDC5 Cells	67
3.6 Fam57b2-overexpression in ATDC5 Cells and 24,25(OH) <sub>2</sub> D <sub>3</sub> Effect on ATDC5	
Differentiation	68
3.7 Lactosylceramide Effect on Cell Differentiation, Proliferation, Adhesion,	
Migration and Apoptosis	69
3.8 Signal Transduction	74
Chapter IV: Discussion	78
Chapter V: Conclusions and Future Directions	89
Chanter VI: References	93

#### List of Abbreviations

AA Amino acid Ab Antibody

ATDC5 Chondrogenic cell line derived from mouse teratocarcinoma AT805

**BSA** Bovine serum albumin

BMP Bone morphogenetic protein

**Calcifediol** 25(OH)D<sub>3</sub> or 25-hydroxyvitamin D<sub>3</sub>

**Calcitriol** 1,25(OH)<sub>2</sub>D<sub>3</sub> or 1,25-dihydroxyvitamin D<sub>3</sub> **cDNA** Complimentary deoxyribonucleic acid

**Cholecalciferol** Vitamin D<sub>3</sub>

Col2a1Gene encoding mouse collagen type II  $\alpha$ I chainCol10a1Gene encoding mouse collagen type X  $\alpha$ I chain

CYP24A1 25-hydroxyvitamin D<sub>3</sub>-24-hydroxylase
 CYP27A1 Mitochondrial vitamin D<sub>3</sub>-25-hydroxylase
 CYP27B1 25-hydroxyvitamin D<sub>3</sub>-1-α-hydroxylase
 CYP2R1 Microsomal vitamin D<sub>3</sub>-25-hydroxylase

**DBP** Vitamin D-binding protein

DMSO Dimethyl sulfoxide
DNA Deoxyribonucleic acid
ECM Extracellular matrix
ER Endoplasmic reticulum
ESC Embryonic stem cell

**FAM57B** Family with sequence similarity 57 member B

**FAM57B2** Family with sequence similarity 57 member B isoform 2

FGF Fibroblast growth factor GAG Glycosaminoglycan

HEK293 Human embryonic kidney cell line
HVDRR Hereditary vitamin-D-resistant rickets

IF Immunofluorescence

IGF-I Insulin-like growth factor 1
ITS Insulin-transferrin-selenium

kDa Kilodalton KO Knockout

LacCer Lactosylceramide

MAPK Mitogen-activated protein kinase
M-CSF Macrophage colony-stimulating factor

MEK Mitogen-activated protein kinase kinase or MAPK/ERK Kinase

MSC Mesenchymal stem cell
mRNA Messenger ribonucleic acid

**NF-κB** Nuclear factor kappa-light-chain-enhancer of activated B cells

OE-PCR Overlap-extension PCR
PBS Phosphate-buffered saline
PCR Polymerase chain reaction
PDGF Platelet-derived growth factor

PFA Paraformaldehyde
PKC Protein kinase C
PLA<sub>2</sub> Phospholipase A<sub>2</sub>

**PPAR-**γ Peroxisome proliferator-activated receptor gamma

**PTH** Parathyroid hormone

**RT-qPCR** Reverse transcription quantitative polymerase chain reaction

RANKL Receptor activator of NFkB ligand

**RNA** Ribonucleic acid

ROS Reactive oxygen species
RXR Retinoid X receptor

**Secalciferol** 24,25(OH)<sub>2</sub>D<sub>3</sub> or 24,25-dihydroxyvitamin D<sub>3</sub>

**SEM** Standard error of the mean

**SOX9** Gene encoding human SRY (Sex-Determining Region Y)-box 9 Protein

**SPR** Surface plasmon resonance

**TBS** Tris-buffered saline

TLC Thin layer chromatography

**TF** Transcription factor

TGF-β Transforming growth factor beta TNF  $\alpha$  Tumor necrosis factor alpha

**VDR** Vitamin D receptor

WT Wild-Type

# List of Figures

Figure 1	Stages of fracture repair	19
Figure 2	The two forms of vitamin D.	22
Figure 3	Vitamin D pathway	23
Figure 4	Catabolic breakdown of 1,25(OH) <sub>2</sub> D <sub>3</sub> by CYP24A1	27
Figure 5	Ceramide synthesis	36
Figure 6	Production of lactosylceramide	37
Figure 7	Ceramide structure	37
Figure 8	Anabolic modifications of ceramide	38
Figure 9	Lactosylceramide structure	39
Figure 10	Lactosylceramide pathways	40
Figure 11	Overlap-extension PCR.	46
Figure 12	FAM57B protein isoform sequences.	56
Figure 13	FAM57B2 WT and mutant schematic	57
Figure 14	Protein expression of WT and mutant FAM57B2	58
Figure 15	TLC results of lipid enzymatic assay with WT and mutant FAM57B2	59
Figure 16	Localization of FAM57B2 to the ER	61
Figure 17	FAM57B2 WT and mutant immunofluorescence	62
Figure 18	Predictions of FAM57B2 topology	64
Figure 19	Immunofluorescence of HA-tagged FAM57B2 protein loop	65
Figure 20	Immunofluorescence of HA-tagged FAM57B2 N terminus	65
Figure 21	Fam57b2-overexpression enhances chondrogenesis markers	67

Figure 22	24,25(OH) <sub>2</sub> D <sub>3</sub> increases expression of early chondrogenesis marker <i>Col2a1</i>	68
Figure 23	LacCer potentiates ITS effect on the expression of Col10a1	69
Figure 24	LacCer has a negative effect on differentiation of ATDC5 cells with Ascorbic Acid	70
Figure 25	LacCer dosage-dependently decreases proliferation of ATDC5	71
Figure 26	LacCer has no effect on caspase-3 activity	71
Figure 27	Decrease in adhesion to fibronectin upon LacCer incubation	72
Figure 28	No effect of LacCer on migration properties of ATDC5 cells	73
Figure 29	LacCer incubation doesn't lead to ROS accumulation	74
Figure 30	MEK kinase inhibitor treatment on LacCer treated and Fam57b2-overexpressing ATDC cells.	76
Figure 31	Protein topology devised from experimental and predicted data	80
Figure 32	Surface Plasmon Resonance	81
Figure 33	Fam57b2-Intein/Chitin binding domain fusion protein	82
Figure 34	Commercial Protein purification.	83
Figure 35	Transcriptional regulators and signalling pathways	90
List of Table	zs	
Table 1	Primer sequences	55
Table 2	Taqman List	55

## Acknowledgements

First and foremost, I would like to thank my supervisor Dr. René St-Arnaud for the great opportunity to form part of his laboratory for my Master's research project. I am very grateful for Dr. St-Arnaud's support, words of encouragement, guidance and mentorship throughout these past two years. It was definitely a memorable experience and a strong base for my future scientific endeavours. I would also like to thank my committee members, Dr. Pierre Moffatt and Dr. Monzur Murshed, who provided me with constructive advice, feedback, suggestions and ideas throughout my project.

I'd also like to thank past and present lab colleagues for their constant advise and guidance on numerous situations. Particularly, I'd like to thank Dr. Martin Pellicelli and Dr. Corine Martineau for guiding and mentoring me at the beginning of my project. I'd like to thank Ms. Hadla Hariri and Dr. William Addison for their invaluable friendship and scientific advice. I'd also like to thank members of the Murshed and Moffatt laboratories for their camaraderie, advice and friendship. Additionally, thank you to Mr. Mark Lepik for his assistance with figures.

I'd like to extend my gratitude to the McGill University Department of Human Genetics for the assistance and the opportunities granted to me to present my research numerous times and awards given, the staff of Shriner's Hospital for Children, the National Institutes of Health and the National Council of Science and Technology of Mexico for funding provided.

Lastly, gratitude cannot be put into words towards my parents and my sister for their boundless support and encouragement throughout my academic endeavours; and my friends, who always provided moral support and without whom this experience wouldn't have been the same.

## Chapter I: Introduction, Hypothesis and Aims

#### 1. Introduction

In this thesis, a brief introduction to bone physiology, mechanisms of bone and chondrocyte formation and maturation, bone fracture repair and its connection to the Vitamin D pathway will be given. The cloning of *Fam57b2* from fracture repair callus, which set the stage for the studies reported herein, will be presented.

## 1.1 Bone Physiology

Bone is a dense connective tissue of the body that has a variety of functions: provide structural support for the body, serve as an attachment point for ligaments and tendons to permit locomotion, protect internal organs, contain the bone marrow and provide an adequate setting for hematopoiesis, storage of minerals, growth factors and cytokines and help regulate acid-base balance [1]. The skeleton has also recently been shown to play an endocrine role through the hormone osteocalcin [2], although this is beyond the scope of this Introduction.

According to its structure, bone can be classified into compact/cortical and cancellous/trabecular. Cortical bone forms the outer layer of bones, it is hard, metabolically less active, it surrounds the bone marrow and it makes up 80% of the human skeleton [1]. In humans, it is organized into osteons, concentric layers of bone matrix that contain osteocytes which communicate between each other through small canals formed around a vascular center [1, 3]. However, in mice, a commonly used model in research laboratories for the study of bone and its pathologies, cortical bone doesn't contain osteons but rather contains circumferential lamellae (thin sheets or plates of bone matrix) added on the periosteal surface that are rarely remodelled [3]. Meanwhile, trabecular bone is less dense, but more flexible. It has a honeycomb-like network structure, it is highly vascular, it contains the bone marrow and it makes up 20% of the skeleton.

It is organized into trabeculae or packets, thin rods and plates of bone that are arranged towards the areas that support the most stress [1].

In bone, osteoblasts are the cells in charge of secreting bone matrix proteins such as type I collagen, osteocalcin, osteonectin, decorin and biglycan. The organic bone matrix mineralizes when calcium becomes immobilized in the proteoglycan matrix and phosphate is released due to alkaline phosphatase activity, forming hydroxyapatite crystals [4]. As osteoblasts secrete matrix, they can become entrapped within it and differentiate, becoming osteocytes. They develop long processes to communicate amongst each other and they reduce protein production. One of their most vital roles is to act as mechanosensors, detecting pressure and load and communicating this information to other cells to help bone adapt. Their spatial arrangement supports their function as osteocytes comprise 90-95% of all bone cells. On the other hand, osteoclasts are the multinucleated bone resorbing cells. Their origin is hematopoietic, rather than mesenchymal like osteoblasts. They differentiate mainly in the presence of macrophage colony-stimulating factor (M-CSF) and receptor activator of NFκB ligand (RANKL) [1, 4]. To resorb bone, osteoclasts secrete hydrogen ions into the resorbing compartment to acidify the environment, making it ideal for secreted tartrate-resistant acid phosphatase, cathepsin K, matrix metalloproteinase 9 and gelatinase to digest the organic matrix and mobilize the mineral [1].

There are four general categories of bones: long, short, flat and irregular [1]. The way these bones form during development differs, although they both involve the transformation of mesenchyme to bone tissue [5]. Flat bones form through intramembranous bone formation, while long bones develop through endochondral ossification and intramembranous formation. Long bones have some defining characteristics such as a hollow shaft made up of cortical bone termed

diaphysis and rounded epiphyses made up of trabecular bone and protected by dense cortical bone found above the growth plates [1].

#### 1.1.1 Intramembranous Ossification

Intramembranous bone formation occurs in the skull, mandible, clavicles and pelvis. It allows the surface of flat bones to grow and thicken [1]. The process starts with mesenchymal stem cells (MSC), which are found throughout an extracellular matrix (ECM) lacking collagen, that condensate and replicate. They become larger and rounder and increase their Golgi apparatus and rough endoplasmic reticulum, becoming osteoprogenitor cells. As this process continues, the cells begin to migrate outward, their morphology becomes more similar to osteoblasts and the expression of transcription factor (TF) RUNX2 is activated to commit them [5, 6]. Osteoblasts are able to secrete ECM containing type I collagen, forming osteoid, which mineralizes and forms rudimentary bone [7]. Differentiated osteoblasts also form bone spicules that fuse together to form bone trabeculae. During the progression of ossification, the woven bone formed by the interconnection of trabeculae will become filled [6]. Woven bone is however weaker and immature as the collagen fibrils are secreted in a rather unorganized manner. For this reason, this bone has to be remodelled in order to produce a mechanically stronger, lamellar bone where collagen fibrils present alternating orientations [1, 6].

#### 1.1.2 Endochondral Ossification

Endochondral ossification is mainly differentiated from intramembranous ossification by the presence of cartilaginous tissue. At early fetal stages, the skeleton is mostly composed of cartilage which will become bone via endochondral ossification [8]. This type of ossification occurs in the vertebral column, pelvis, and limbs [5].

The initial stage of bones that develop through endochondral ossification is the formation of a cartilage model that will develop into bone. Cartilage develops through the condensation of mesenchymal cells, which will differentiate into chondrocytes and secrete ECM components. The mesenchymal cells become committed to the chondrogenic pathway by the induction of the expression of transcription factors PAX1 and SCLERAXIS, and start expressing transcription factor SOX9 during the condensation stages [5]. This cartilage lattice will serve for the formation of primary and secondary ossification centers, which occur when a mixture of cells invades the network. The primary ossification center occurs in the diaphysis or shaft of the bone, while the secondary ossification center occurs at time of birth in the ends or epiphysis of the bone [9]. The growth plate is the cartilage found between these two centers, which will allow for growth to continue and will be fully replaced by bone at around 20 years of age in humans [9, 10]. However, in mice, growth plate remnants remain throughout life, although its thickness decreases after 3 months of life where longitudinal growth largely decreases [3].

The main reason why some bones develop in this manner is to allow longitudinal bone growth in a mechanically stable manner. Cartilage is mainly found in the growth plate and the epiphysis of long bones, and it is arranged on morphologically and functionally distinct areas. The resting chondrocyte zone is found the furthest from the ossification center, extending outwards towards the epiphysis. The zone of proliferation follows, where chondrocytes undergo mitosis, flatten and align into stacks. This is followed by the zone of hypertrophy, where chondrocytes become highly enlarged in size and actively secrete ECM characterized by collagen type II and X, fibronectin and alkaline phosphatase [5, 10]. The ECM becomes mineralized and hypertrophic chondrocytes in this zone die as they can no longer receive nutrients or eliminate waste easily in the zone of calcification. The cavities left by these apoptotic cells are filled with invading blood

vessels, osteoclasts, osteoprogenitors and bone marrow cells. Osteoclasts resorb the cartilage matrix and osteoprogenitors develop into osteoblasts, which secrete ECM that will become mineralized and remodelled in the zone of ossification [10].

As it has been mentioned, the presence or addition of cartilage into the bone tissue allows for growth to occur. This type of growth can be interstitial, which is longitudinal growth that occurs when chondrocytes divide and continue secreting more matrix. Growth can also be appositional, which is the increase in the diameter or thickness by addition of ECM by chondroblasts and osteoblasts [6].

### 1.2 Chondrocyte Physiology and Differentiation

As we grow up, cartilage is present in our long bones, articular surfaces, intervertebral discs, ears, respiratory tract and nose. This tissue is characterized by being avascular, lacking a neural supply, and surviving under low oxygen concentrations. Because of this, its subsistence depends on nutrient diffusion from the outside and glycolysis to produce lactate [11]. A combination of subjection to mechanical forces and environmental factors controls chondrocyte phenotype [8].

Chondrocytes are the vital-most part of cartilage. They are usually found in cavities in their matrix called lacunae. Although they only make up 5-10% of the total volume of cartilage, they are essential in maintaining the ECM [12]. The type of matrix they secrete consists of: proteoglycans like aggrecan, which provides cartilage with the capacity to resist compression by drawing water into the tissue; glycosaminoglycans (GAG), like hyaluronic acid, a major component of cartilage that is involved in cell adhesion, migration, and differentiation; and type II and X collagen fibers, which give cartilage tensile strength [12, 13]. The ECM is 65-80%

composed of water, 15-25% of collagens and 10% by proteoglycans and other non-collagenous proteins [8].

As has been mentioned before, their origin is mesodermal. MSCs can become a variety of cell types; however, a combination of signaling pathways and control of gene expression will determine their commitment and differentiation to the chondrogenic line [13]. The interactions between mesenchyme-epithelium and mesenchyme-ECM direct cells to condense together and begin proliferating and differentiating [12].

There are many signalling pathways that control progression to differentiation. Wnt signalling is one of the earliest determinants of mesenchymal direction because it acts in chondro-osseus progenitor cells, preventing chondrocyte differentiation and favouring osteoblastic development. WNT activation stabilizes  $\beta$ -catenin, which represses Sox9 expression. SOX9 is an important TF that determines the chondrogenic fate as it is expressed early during the condensation of chondrocytes and continues being expressed until proliferation [14]. It binds to the collagen type II enhancer region to upregulate its expression, but its activity is completely shut down in hypertrophic chondrocytes [12].

Indian Hedgehog (IHH) is a secreted growth factor that is expressed by prehypertrophic chondrocytes. It is also able to signal to the proliferating chondrocytes to activate proliferation through the action of GLI family transcription factors. Bone Morphogenetic Proteins (BMP) are also secreted growth factors that can induce proliferation by the action of SMAD transcription factors and are able to induce ectopic endochondral ossification [14]. They have also been shown to upregulate *Sox9* and *Col2a1* expression in MSCs, and *Col10a1* in chondrocytes [12]. Fibroblast Growth Factors (FGF) can activate MAP (mitogen-activated protein) kinases and STAT family TFs. They act by inhibiting proliferation but activating differentiation to increase the amount of

hypertrophic chondrocytes. A key inducer of hypertrophic differentiation is Runx2, which becomes expressed in prehypertrophic and hypertrophic chondrocytes and whose expression is hampered from proliferative cells [14]. Transforming Growth Factor  $\beta$  (TGF-  $\beta$ ) is another factor whose expression is restricted in the proliferative, hypertrophic and mineralizing zones of cartilage. Insulin-like growth factor-1 (IGF) is a peptide hormone that can induce proliferation and differentiation by increasing production of aggrecan and type II collagen [12].

In culture, primary chondrocytes from humans and mice have a round, polygonal morphology. They are considered an excellent model to study normal chondrocyte physiology and mechanisms; however, they have the tendency to "dedifferentiate" when cultured in monolayer and high-density monolayers can maintain the cartilage phenotype until they are subcultured, but only last for a limited number of passages [12]. High-density micromass has proven useful for primary cell culturing as cells retain their shape and density [15]. Immortalized cell lines have also been successfully used to study chondrocyte differentiation. The rat-calvaria isolated RCJ3 cell line resembles growth plate chondrocyte behaviour in vitro; however, being a cell line isolated from calvaria, its use is most accurate when studying intramembranous ossification [12]. Meanwhile, mouse embryo cell line C3H10T1 can differentiate into different mesoderm derived cell types, but can only be kept in culture for a determined number of passages [16]. HCS-2/8 is likewise an excellent human clonal cell line that recapitulates the chondrocyte phenotype, as well as expression of chondrogenesis gene markers and shows a marked response to cytokines, but has been shown to lack expression of cartilage matrix degrading enzymes [17].

On the other hand, the teratocarcinoma pre-chondrogenic stem cell line, ATDC5, has been extensively used to reproduce all the stages of differentiation observed in endochondral ossification by culturing in monolayer, making it the chosen cell line for the studies presented in

this thesis. Initially, these cells proliferate and, when differentiated with insulin, they produce cartilaginous nodules upon condensation and begin secreting aggrecan and type II collagen. This process lasts 7-10 days and is characteristic of early-phase differentiation, after which cells in these nodules become hypertrophic and express collagen type X and increase in alkaline phosphatase activity. This phenotype is reached after 14 days of differentiation and is characteristic of late-phase differentiation. Mineralization can also be observed and studied after 1 month of differentiation [12].

## 1.3 Fracture Repair Stages

Bone fracture repair is a complicated process that requires the interplay of many factors. Initially, after a bone is fractured, an inflammatory response is triggered. In this initial response, endothelial, neuronal and mesenchymal cells are brought into the site of injury [18]. Inflammation occurs as macrophages, neutrophils, lymphocytes and platelets arrive at the site of the injury and release cytokines, reaching its peak response at 24 hours. Subsequently, a hematoma forms as vessels at the site of the injury clot. Mesenchymal cells are attracted to the injury site by TGF-β, IGF and FGFs secreted by macrophages [19, 20]. The bone marrow changes in architecture within hours, blood vessels around the clot decrease and cells reorganize into high and low-density regions [21]. MSCs begin proliferating at around 3 days post-fracture and differentiating into chondrocytes at around 7-21 days post-fracture [19-21]. These chondrocytes secrete ECM to form a cartilaginous "soft callus" that bridges the injury. The "soft callus" is substituted by a "hard callus" formed primarily by osteoblasts in a process reminiscent of endochondral ossification [20]. The osteoblasts come from the high-density regions of cells and begin differentiating within 24 hours of the injury laying down new bone via intramembranous ossification with activity peaking at 7-10 days post-fracture and disappearing at 14 days. Mineralization of the "soft callus" occurs at the interface site of the cartilaginous callus and the woven bone as proteases are excreted by chondrocytes. Spaces created by apoptosis of mature hypertrophic chondrocytes and protease action are filled in by infiltrating blood vessels which carry osteoclastic precursors [1, 21]. The immature woven bone formed by osteoblasts is remodelled through cooperative osteoblast/osteoclast activity to produce bone that closely resembles the original bone's structure [20].

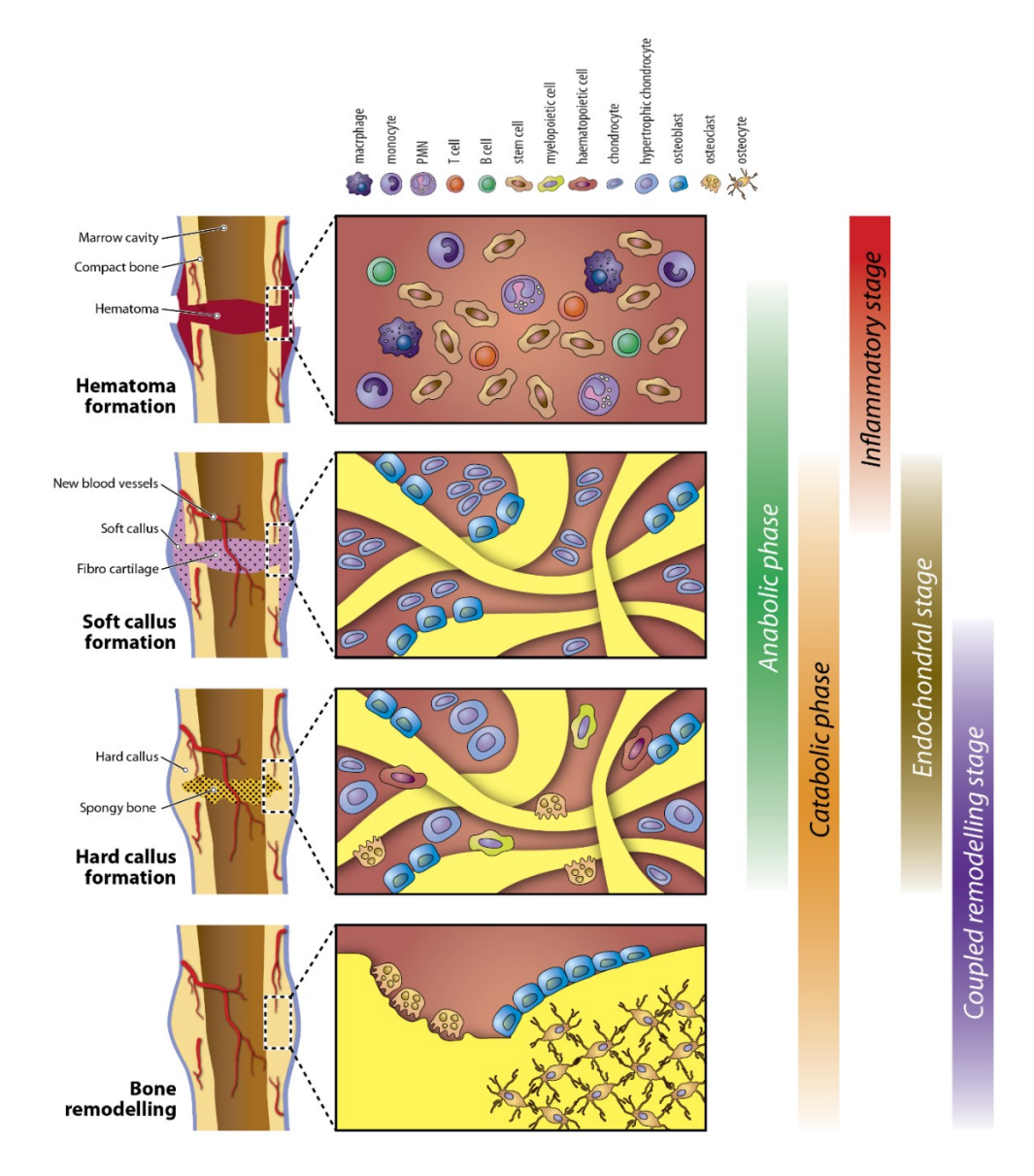


**Fig. 1**. Stages of fracture repair are represented with the key cell types that perform their functions in each phase of healing. Figure adapted from Einhorn and Gerstenfeld (2015) [22], with permission.

The ability with which bones heal depends on a variety of factors: the size and stability of the injury, age and the presence of other health conditions. Small rigid fractures heal directly by intramembranous ossification, while bigger less rigid fractures heal through endochondral and intramembranous ossification steps [18].

Signalling pathways involved in fracture healing involve WNT/β-catenin, Notch, BMP, MAPK (mitogen-activated protein kinase), and PDGF (platelet derived growth factor) among other factors [19]. Wnt signalling controls a variety of cellular functions and covers cell-fate decisions of osteoblasts. Canonical Wnt signalling is increased during fracture healing and promotes osteoblastogenesis; however, if Wnt signalling is activated or inhibited during the early stages of bone healing, this can negatively affect MSC differentiation into osteoblasts [23]. Notch signalling has also been shown to be necessary for MSC differentiation into osteoblasts, where inhibition of this pathway leads to depletion of bone-marrow derived MSCs pool and the possibility of fracture non-union [24-26]. BMP signalling has the ability to activate endochondral ossification and is important for osteogenesis progression [27, 28]. The MAPK pathway has a particularly important role since this pathway is in the crosstalk of other pathways and acts as a transducer of signals from EGF, FGF, and IGF in bone healing [19, 29]. Inflammatory markers such as TNFα (tumor necrosis factor alpha) and NF-κB (nuclear factor kappa-light-chain-enhancer of activated B cells) can also activate the MAPK pathway [19, 30]. This pathway has been shown to have opposing roles in stimulating osteoblast differentiation and inhibiting osteoblast marker gene expression in mature osteoblasts [31]. PDGF signalling is involved in bone healing mainly through the activation of bone marrow-derived MSCs to become osteoblasts and through the attraction of macrophages through chemotaxis [32]. The IGF pathway is involved by inducing osteoblast differentiation, matrix deposition and expression of type I collagen [33]. On the other hand, the FGF pathway is implicated in angiogenesis, wound healing and intramembranous and endochondral signaling in osteoprogenitor cells [34, 35]. It affects osteoblast maturation on a stage-specific manner, and it can lead to higher number of osteocytes in the healing bone [36, 37]. Additionally, it has been shown that when treated in conjunction with BMP2, this can promote bone repair by synergistic action [38].

#### 1.4 Vitamin D

Vitamin D is produced in the body or consumed through the diet in foods such as milk, eggs, salmon, trout, mushrooms, yogurt and others. The importance of its active, hormonal form relies on its capacity to regulate circulating plasma calcium levels to maintain homeostasis [39]. Its discovery in the 1820s as a nutritional supplement lead to the decrease in the incidence of rickets and osteomalacia in the world, two severely debilitating bone diseases in children and adults, respectively. The realization that foods could be supplemented with 7-dehydrocholesterol and irradiated with UV rays in the 1920s lead to the discovery of the endocrine vitamin D pathway and its continuous research on its effect in bone disease, cancer and the immune system [39, 40].

## 1.4.1 Forms and Pathway

There are many metabolites of vitamin D known; however, the best known are cholecalciferol (vitamin D<sub>3</sub>), which is produced in mammalian skin and ergocalciferol (vitamin D<sub>2</sub>), found in plant tissues. The main two differences between these 2 forms rely on the presence of a double bond found between C-22/C-23 and a methyl group bound to C-24 (**Fig. 2**). Although some of the hydroxylating enzymes could use vitamin D<sub>2</sub> as substrate, both metabolites don't follow the same metabolic pathways [39].

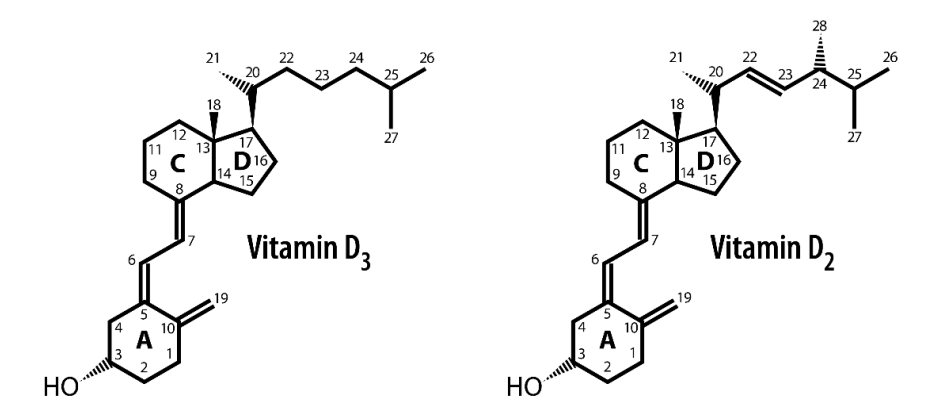


**Fig. 2.** The two forms of Vitamin D: Vitamin D<sub>3</sub> (Cholecalciferol) and Vitamin D<sub>2</sub> (Ergocalciferol). The main difference between each is that ergocalciferol has a double bond at C-22 and a methyl group on C-24.

In mammals, the precursor of vitamin D<sub>3</sub> is 7-dehydrocholesterol, a cholesterol precursor which is found in the skin epidermis. It is photoisomerized by UV rays from the sunlight and cleaved at the B ring to produce vitamin D<sub>3</sub>, also called cholecalciferol. Cholecalciferol is hydroxylated in liver hepatocytes by the high affinity CYP2R1 enzyme (vitamin D<sub>3</sub> 25hydroxylase) or by the lower affinity CYP27A1 enzyme found in liver hepatocytes at the 25<sup>th</sup> carbon to form 25-hydroxyvitamin D<sub>3</sub> (also called calcifediol or 25(OH)D<sub>3</sub>). Calcifediol in this form is released into the bloodstream, where it is bound by vitamin D-binding protein (DBP), an α-globulin that increases its solubility. The production of 25(OH)D<sub>3</sub> in the liver is not highly regulated. Cholecalciferol found in the circulation can readily be converted into 25(OH)D<sub>3</sub> in a concentration-dependent manner, which can be used to measure vitamin D status in patients. DBP-25(OH)D<sub>3</sub> is transported around the body, where upon reaching the kidney proximal tubules is hydroxylated once again at the 1-α position by the CYP27B1 enzyme (25-hydroxyvitamin D<sub>3</sub> 1alpha-hydroxylase) to form 1,25-dihydroxyvitamin D<sub>3</sub> (also called calcitriol or 1,25(OH)<sub>2</sub>D<sub>3</sub>). The action of this enzyme is tightly controlled based on the calcium and phosphorus needs of the body [39].

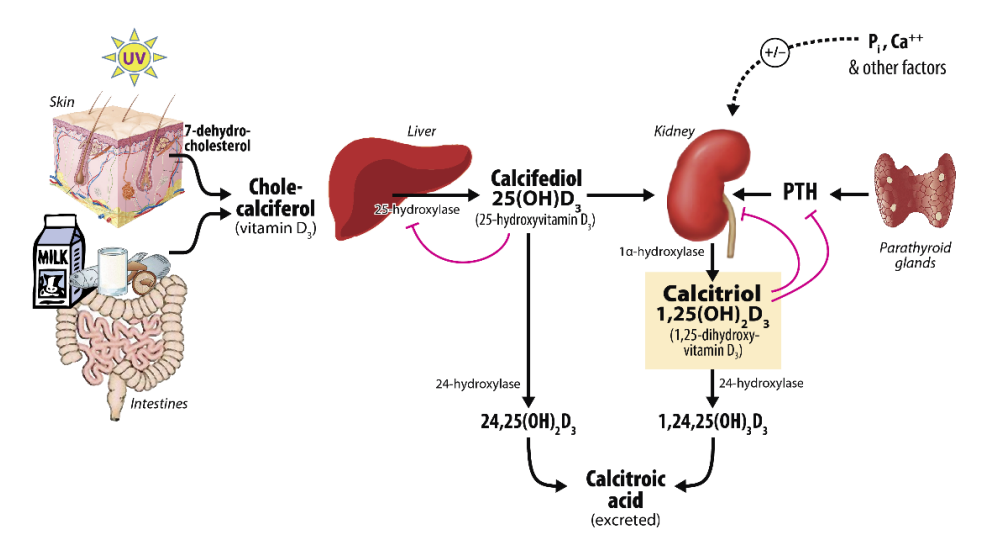


**Fig. 3**. Vitamin D pathway with the key enzymes and metabolites produced. OHase abbreviation stands for "hydroxylase". Figure adapted from Deeb et al. (2007) [41], with permission.

Humans are not capable of overproducing vitamin D from the skin as 7-dehydrocholesterol can also absorb UV rays and convert to inactive photoisomers that are degraded. When 25(OH)D<sub>3</sub> is orally supplemented, its effects can already be seen within 8 to 10 hours. This form of vitamin D is the most abundant and stable in the body. Its normal concentration is within the 20 to 50 ng/mL range. Because 1,25(OH)<sub>2</sub>D<sub>3</sub> is the most active form but not the most stable, its circulating concentrations are lower, ranging form 20 to 65 pg/mL [39].

1,25(OH)<sub>2</sub>D<sub>3</sub> is the active-most form of vitamin D. It acts by diffusing through the cellular membrane and binding to the vitamin D receptor (VDR), a member of the nuclear receptor family of ligand-activated TFs. VDR heterodimerizes with the retinoid-X receptor (RXR), and together they bind the vitamin D-responsive elements of target genes. VDR is found in the parathyroid gland, pancreas, macrophages, skin keratinocytes, mammary glands, reproductive organs, tubular epithelial cells of the kidney, osteoblasts and osteoclast precursors [39].

Mutations in the VDR cause vitamin D-resistant rickets type II, which is characterized by hypocalcaemia, hypophosphatemia, infantile onset and unresponsiveness to 1,25(OH)<sub>2</sub>D<sub>3</sub>, which

leads it to accumulate; on the other hand, 1-alpha-hydroxylase deficiency has the same symptoms with the exception that it is responsive to high levels of 1,25(OH)<sub>2</sub>D<sub>3</sub>, leading it to be named "vitamin D-dependent rickets type I" (VDDR) and being characterized by having very low levels of circulating 1,25(OH)<sub>2</sub>D<sub>3</sub>. However, mutations in the 25-hydroxylases are harder to understand. Compound heterozygotes of *CYP27A1* and *CYP2R1* show decrease in 25(OH)D<sub>3</sub> levels only by 50%, suggesting that other enzymes could be involved in 25-hydroxylation. It is believed that symptoms present themselves when a mutation in any of the genes is present in addition to some calcium stressor [42].

#### 1.4.2 Role in Calcium Homeostasis

Production of 1,25(OH)<sub>2</sub>D<sub>3</sub> by CYP27B1 is controlled by the increase in production of parathyroid hormone (PTH) in response to low circulating calcium and low circulating phosphate. 1,25(OH)<sub>2</sub>D<sub>3</sub> in turn stimulates calcium and phosphorus absorption in the small intestine. In conjunction with PTH, it stimulates RANKL expression in osteoblasts to increase osteoclastogenesis and bone resorption, thus mobilizing calcium from bone, and it increases calcium reabsorption in the distal convoluted tubules of the kidney [40]. Although 25(OH)D<sub>3</sub> is not the natural ligand of the VDR, when it is circulating at high concentrations (1000 ng/mL or greater) such as in vitamin D toxicosis, it can compete with normal concentrations of circulating 1,25(OH)<sub>2</sub>D<sub>3</sub> and induce effects usually attributed to it [39].

In the parathyroid gland, expression of PTH is suppressed to cease *CYP27B1* stimulation [39]. 1,25(OH)<sub>2</sub>D<sub>3</sub> also causes fibroblast growth factor 23 (FGF23) secretion, which stimulates phosphate excretion from the body and decreases *CYP27B1* activity in a negative feedback loop. In osteoblasts, osteocalcin and osteopontin, which are involved in bone remodelling, are

transcriptionally activated; while involucrin is activated in keratinocytes, and carbonic anhydrase in macrophages [40].

One of the genes whose expression is driven by calcitriol is *CYP24A1*, the gene that encodes 1,25-dihydroxyvitamin D<sub>3</sub> 24-hydroxylase, which is in charge of hydroxylating 1,25(OH)<sub>2</sub>D<sub>3</sub> and its precursor 25(OH)D<sub>3</sub> at the 24<sup>th</sup> carbon, producing 1,24,25-trihydroxyvitamin D<sub>3</sub> (1,24,25(OH)<sub>3</sub>D<sub>3</sub>) and 24,25-dihydroxyvitamin D<sub>3</sub> (also called secalciferol or 24,25(OH)<sub>2</sub>D<sub>3</sub>), a metabolite largely believed to be inactive. In particular, the carbons that are found in the side chain are more susceptible to be hydroxylated: C-23, C-24, and C-26. These metabolites can be further processed and converted to calcitroic acid, which is water-soluble and can be excreted from the body [39].

## 1.5 CYP24A1 and 24,25(OH)<sub>2</sub>D<sub>3</sub>

CYP24A1 is a heme-containing, cytochrome P450 enzyme found in the inner membrane of the mitochondria in charge of the stereospecific hydroxylation of the 24<sup>th</sup> carbon of 1,25(OH)<sub>2</sub>D<sub>3</sub> and 25(OH)D<sub>3</sub>. It is classically considered to be a catabolic enzyme, as its expression is induced by 1,25(OH)<sub>2</sub>D<sub>3</sub> to regulate its breakdown in order to avoid hypervitaminosis D [39]. The induction of *Cyp24a1* by 1,25(OH)<sub>2</sub>D<sub>3</sub> was studied *in vitro*, where it was identified that the promoter of this gene contains two VDREs 100bp (base pairs) apart in the non-coding portion, a tandem structure unique to this promoter [43]. More recent studies have indicated that there is a more complex control of *Cyp24a1* expression *in vivo* [44, 45].

Given the fact that 25(OH)D<sub>3</sub> is more abundant in the body and its Michaelis constant (*K*m) is lower than 1,25(OH)<sub>2</sub>D<sub>3</sub>, 24,25(OH)<sub>2</sub>D<sub>3</sub> is the main metabolite produced. In addition, 1,24,25(OH)<sub>3</sub>D<sub>3</sub> is not very stable in the circulation and has a higher affinity to CYP24A1, which causes it to remain bound to the enzyme and become degraded quickly. 24,25(OH)<sub>2</sub>D<sub>3</sub> circulates

in the plasma at a concentration of 2-5 ng/mL, which is 10-fold lower than the circulating 25(OH)D<sub>3</sub> [39].

In order to produce the final degradation product, calcitroic acid, CYP24A1 generates a reaction process in which its substrates are hydroxylated and then oxidized at carbon 24, which is followed by hydroxylation of the 23<sup>rd</sup> carbon and the side chain is cleaved. Calcitroic acid is water soluble and can then become excreted from the body (**Fig. 4**). As it can perform many steps in the degradation of 24,25(OH)<sub>2</sub>D<sub>3</sub>, it is considered to be a multi-catalytic enzyme. Although human CYP24A1 has predominantly C24-oxidation activity, it also has the capacity to express C23-hydroxylation activity, which produces lactone and carboxylic acid as final products. This difference in activity is determined by point-residue differences in the substrate binding and catalytic center of the enzyme [46].

**Fig. 4.** The catabolic breakdown of 1,25(OH)<sub>2</sub>D<sub>3</sub> by CYP24A1 occurs when the substrate is hydroxylated and oxidized at carbon 24, after which it is hydroxylated at carbon 23 and the side chain is cleaved to produce calcitroic acid. Alternatively, CYP24A1 hydroxylates carbon 23 to ultimately degrade it to lactone and carboxylic acid [47]. Reproduced with permission from Schlingmann, K.P., et al. (2011), Copyright Massachusetts Medical Society.

1,25(OH)<sub>2</sub>D<sub>3</sub> induces *Cyp24a1* expression in all target tissues. This induces the 24-oxydation pathway, which leads to catabolic inactivation of 1,25(OH)<sub>2</sub>D<sub>3</sub>, thus maintaining vitamin D homeostasis. In the kidney, CYP24A1 activity is mainly regulated by PTH and 1,25(OH)<sub>2</sub>D<sub>3</sub> concentration [39, 48]. 1,25(OH)<sub>2</sub>D<sub>3</sub> administration increases renal *CYP24A1* mRNA expression, while PTH administration blocks the 1,25(OH)<sub>2</sub>D<sub>3</sub>- mediated increase [49, 50]. However, in the intestine, *CYP24A1* is primarily regulated by 1,25(OH)<sub>2</sub>D<sub>3</sub>, as it lacks a PTH receptor. 1,25(OH)<sub>2</sub>D<sub>3</sub> administration increases intestinal CYP24A1 activity to induce its catabolic breakdown [51], and this response is more acute than the one observed in the kidney [52]. In

osteoblasts, there is a greater induction of CYP24A1 expression in response to  $1,25(OH)_2D_3$  than in the less mature osteoblasts, but expression dampens in differentiated mature cells, reducing  $1,25(OH)_2D_3$  breakdown as osteoblasts mature [53]. In macrophages,  $1,25(OH)_2D_3$  is produced in response to interferon-gamma (IFN $\gamma$ ) by increasing CYP27B1 expression and blunting CYP24A1, which affects the ability of  $1,25(OH)_2D_3$  to regulate itself [54, 55]

In humans, the *CYP24A1* gene is found on chromosome 20 [56]. Mutations in *CYP24A1* lead to Idiopathic Infantile Hypercalcemia, predominantly in infants. Common symptoms include dehydration, failure to thrive, weight loss, fever and vomiting. These patients also present hypervitaminosis D, hypercalcemia, low PTH, nephrocalcinosis and hypercalciuria [47, 57].

## 1.6 Cyp24a1-Gene Deficient Mice

A knockout (KO) mouse model for CYP24A1 was developed in the St-Arnaud lab using embryonic stem cell (ESC) technology, by replacing the heme-binding domain of *Cyp24a1* located on exons 9 and 10 with a PGK-neo (phosphoglycerate kinase promoter driving the neomycin phosphotransferase II gene) selection cassette. The heterozygous progeny from these mice is phenotypically normal and the mutation is transferred with the expected Mendelian ratio. However, 50% of the mutant progeny die at around 3 weeks of age. To understand the cause of this perinatal lethality, macrophage function was analyzed to dismiss impaired response to infection. Lethality was determined to be as a result of hypercalcemia due to high levels of 1,25(OH)<sub>2</sub>D<sub>3</sub>, which cannot easily be cleared from the body, by analyzing the stunted progeny. Pregnant knockout mice also show very high levels of 1,25(OH)<sub>2</sub>D<sub>3</sub> in late stages of pregnancy, which can't be regulated through CYP24A1-mediated catabolism [58, 59]. Additionally, when exogenous 1,25(OH)<sub>2</sub>D<sub>3</sub> was continuously administered, cortical tubular dilation, necrotic debris

and nephrocalcinosis were observed in these mice, showing that excess of 1,25(OH)<sub>2</sub>D<sub>3</sub> causes lethal calcium imbalance [58].

Nonetheless, the surviving half of the progeny is believed to survive by using alternate means of vitamin D regulation. This progeny is normocalcemic and normophosphatemic when fed regular rodent chow. The clearance of 1,25(OH)<sub>2</sub>D<sub>3</sub> in these mice remains impaired, which was observed not only through the absence of 24-hydroxylated metabolites, but also 1,25(OH)<sub>2</sub>D-26,23-lactone, suggesting that vitamin D is regulated by hindering synthesis of 1,25(OH)<sub>2</sub>D<sub>3</sub>, rather than through catabolism [58, 60]. The surviving pups present lower baseline circulating levels of 1,25(OH)<sub>2</sub>D<sub>3</sub> than their WT counterparts, indicating that they may might be downregulating production of 1,25(OH)<sub>2</sub>D<sub>3</sub>, which allows the pups to survive without significant deterioration of their mineral homeostasis [58].

When mice are produced from the mating to *Cyp24a1* knockout mothers (rather than through the mating of heterozygotes), the progeny present abnormally high 1,25(OH)<sub>2</sub>D<sub>3</sub> levels, accumulation of osteoid and deficient mineralization of bones that develop through intramembranous ossification. Particularly, the mandible of *Cyp24a1* KO is sensitive to the mutation and presents a highly reduced amount of bone. Exogenous 24,25(OH)<sub>2</sub>D<sub>3</sub>, administered to attempt to rescue the deficient mineralization phenotype during pregnancy resulted in no successful rescue of the bone abnormalities. The phenotype was then showed to be due to increased 1,25(OH)<sub>2</sub>D<sub>3</sub> concentration during development, by performing a cross to VDR-ablated mice and observing the rescue of the phenotype [58]. However, it also appears that although the need for 24,25(OH)<sub>2</sub>D<sub>3</sub> is not crucial as long bones still develop, 24,25(OH)<sub>2</sub>D<sub>3</sub> still plays a role in chondrogenesis as seen by the incomplete formation of Meckel's cartilage [61].

However, in the opposite case, where *CYP24A1* is constitutively expressed in transgenic rats, albuminuria, hyperlipidemia, reduced circulating 25(OH)D<sub>3</sub> and 24,25(OH)<sub>2</sub>D<sub>3</sub>, low bone mineral density and normal circulating 1,25(OH)<sub>2</sub>D<sub>3</sub> is observed after 8 weeks, rather than the expected hypocalcemia, hyperparathyroidism, growth retardation and rickets. The alteration of renal function is believed to be responsible for most of the phenotype, but it is not fully understood. These experiments show that 1,25(OH)<sub>2</sub>D<sub>3</sub> might have other functions in vitamin D metabolism regulation [62, 63].

It has been shown that more immature chondrocytes in the resting zone of the growth plate respond to 24,25(OH)<sub>2</sub>D<sub>3</sub>, while more mature hypertrophic chondrocytes are more responsive to 1,25(OH)<sub>2</sub>D<sub>3</sub>, meaning that 24,25(OH)<sub>2</sub>D<sub>3</sub> induces the cells to differentiate and change maturation state [64]. This change was suggested by Boyan (2010) and Schwartz (1998), argumenting that this differential response happens because each cell type has a different response in regulating plasma membrane and matrix vesicle enzyme activity, Ca<sup>2+</sup> flux, phospholipid metabolism as well as non-genomic regulation [65, 66]. Other than the specific binding effect of 24,25(OH)<sub>2</sub>D<sub>3</sub> in immature chondrocytes, it has also been observed that it enhances proteoglycan synthesis [67]. It is relevant to notice that results from these studies are specific to the unique system of chondrocytes isolated from the costochondral growth plate and are not easily reproducible.

In order to understand the mechanism though which 24,25(OH)<sub>2</sub>D<sub>3</sub> works, Schwartz et al. (1988) observed that cells in the resting cartilage zone had increased levels of alkaline phosphatase due to increased matrix vesicle enzyme activity and decreased levels of phospholipase A2 (PLA<sub>2</sub>) [68]. Being treated with 24,25(OH)<sub>2</sub>D<sub>3</sub> for 24 hours elicited decrease in proliferation, while treatment for more than 36 hours caused a phenotypic change towards hypertrophic chondrocytes which switched their sensitivity from 24,25(OH)<sub>2</sub>D<sub>3</sub> to 1,25(OH)<sub>2</sub>D<sub>3</sub>. Additionally, Swain et al.

(1993) observed that levels of arachidonic acid, which is found downstream from PLA<sub>2</sub>, also decreased. He observed a differentiation-stage specific change in the fluidity of the lipid membrane when treating resting chondrocytes with 24,25(OH)<sub>2</sub>D<sub>3</sub> [69]. 24,25(OH)<sub>2</sub>D<sub>3</sub> was also shown to regulate prostaglandin production by reducing it in resting zone chondrocytes to levels similar to those found in growth zone cultures [70]. However, it is important to notice that in *Cyp24a1* KO mice, chondrocyte phenotype was not affected [58]. These results led to conclude that chondrocytes regulate their phospholipid metabolism rapidly in response to 24,25(OH)<sub>2</sub>D<sub>3</sub>.

Meanwhile, Sylvia et al. (1993) noticed that, upon treatment with 24,25(OH)<sub>2</sub>D<sub>3</sub>, resting chondrocytes had a time and dose-dependent increase in the activity of protein kinase C (PKC) isoform α, suggesting that it was the mediator of the signal transduction pathway controlling the response. She also showed that this effect was specific to the R enantiomer of 24,25(OH)<sub>2</sub>D<sub>3</sub>, while 24S,25(OH)<sub>2</sub>D<sub>3</sub> had no effect at all [71]. It was later observed that PKC and PLA<sub>2</sub> activity inversely correlate, but their actions converge at MAP kinase, which acts at the gene transcription level to cause the cellular phenotypic responses seen [66].

The studies showing an effect of 24,25(OH)<sub>2</sub>D<sub>3</sub> in chondrocytes during growth and fracture repair suggested that the metabolite might act through a receptor which is different from the VDR. Seo et al. (1996) showed the accumulation of tritium-labelled 1,25(OH)<sub>2</sub>D<sub>3</sub>, and 24,25(OH)<sub>2</sub>D<sub>3</sub> in growth plate cartilage [72]. However, when looking at growth late chondrocytes from *Cyp24A1* KO mice, no disruption of the growth plate cells could be seen [58]. Seo et al. (1996) also showed specific binding of tritium-labelled 24,25(OH)<sub>2</sub>D<sub>3</sub> to the membrane fractions of cells found in the fracture callus of chicks [72]. In two separate studies, Seo et al. (1997) showed that 24,25(OH)<sub>2</sub>D<sub>3</sub> may be important when fractured bones are healing, as circulating levels of this hormone and CYP24A1 enzymatic activity increase in chicks by day 10 post-fracture and return to baseline by

day 15 [73, 74]. Conversely, it has been observed that when bones heal, 24,25(OH)<sub>2</sub>D<sub>3</sub> injected with 1,25(OH)<sub>2</sub>D<sub>3</sub> into the fracture callus causes bones to heal faster than with 1,25(OH)<sub>2</sub>D<sub>3</sub> alone [75].

Seo et al. (1997) also showed that when feeding 24,25(OH)<sub>2</sub>D<sub>3</sub> and other vitamin D<sub>3</sub> metabolites to chicks after bone fracture, the strength of the bones after their repair was increased. They suggested that 24,25(OH)<sub>2</sub>D<sub>3</sub> might be necessary at the specific stage of differentiation to chondrocytes in the fracture callus in rats [74]. Lidor et al. (1987), on the other hand, showed that 24,25(OH)<sub>2</sub>D<sub>3</sub> had an effect in rescuing rachitic cartilage and enhancing healing of fracture through local injection [76]. 24,25(OH)<sub>2</sub>D<sub>3</sub> might be acting through a signal transduction response different from common steroid nuclear receptor and determined that the callus membrane contained the putative binding protein/receptor with high and specific affinity to 24,25(OH)<sub>2</sub>D<sub>3</sub>, and not the 24S,25(OH)<sub>2</sub>D<sub>3</sub> epimer [72].

The *Cyp24a1* KO mice generated in St-Arnaud lab were used to observe the effect that 24,25(OH)<sub>2</sub>D<sub>3</sub> has in fracture repair [58]. It could be observed that callus formation and healing of stabilized, transverse mid-diaphyseal fractures of the tibia of *Cyp24a1* KO mice was significantly delayed compared to control littermates. Bone volume, force necessary to break the bone and percentage of mineralized tissue at day 14 post-osteotomy was reduced and couldn't be corrected with 1,25(OH)<sub>2</sub>D<sub>3</sub>. However, when these mice were given daily injections of 24,25(OH)<sub>2</sub>D<sub>3</sub>, this rescued the histological appearance, biomechanical properties and static histomorphometric index (BV/TV) (Martineau 2017, submitted).

#### 1.7 FAM57B

Although studies mentioned above had tried to elucidate the mechanism through which 24,25(OH)<sub>2</sub>D<sub>3</sub> regulates healing in the fracture callus, none of these studies have been able to

identify exactly how this process occurs. In an effort to identify the putative binding protein/receptor for 24,25(OH)<sub>2</sub>D<sub>3</sub>, we used *Cyp24a1* deficient mouse as a mammalian model. We hypothesized that in fracture calluses of *Cyp24a1* KO mice, the putative receptor would be upregulated to compensate for the little amount of circulating 24,25(OH)<sub>2</sub>D<sub>3</sub>. In order to identify the gene expressing the putative receptor, we performed a cDNA microarray looking for an unknown, transmembrane gene overexpressed in the fracture calluses at day 14 post-operation of *Cyp24a1* KO and WT mice. With this technique, we identified 4 genes with no characterized function, from which only *Family with sequence similarity 57, member B (Fam57b)* (1500016O10Rik) was predicted to code for a transmembrane protein.

The *FAM57B* gene is highly conserved between species. In mice, it produces 3 isoforms through differential promoter usage, where variants 1 and 2 are 275 amino acids long and vary amongst each other in their first 50 aminoacids in the N-terminus, while variant 3 is a truncated isoform of 225 aminoacids lacking 50 aminoacids on the N-terminus [77]. The first and second isoforms, *Fam57b1* and *Fam57b2*, are predicted to have 6 transmembrane alpha helical domains, while *Fam57b3* is predicted to have 5 [77]. However, only *Fam57b1* localizes to the Golgi apparatus, while *Fam57b2* and *Fam57b3* localize to the Endoplasmic Reticulum (ER) (OMIM entry 615175). As detected through RT-qPCR, *Fam57b1* is most highly expressed in the brain and kidney, while *Fam57b3* is mostly highly expressed in testis. However, the second isoform, *Fam57b2*, is most highly expressed in the cartilage and skin. Additionally, the *FAM57B* gene was found to increase in expression in patients with fractures that heal normally compared to patients that present non-union fractures (GEO, Gene Expression Omnibus, GDS369; accessible at www.ncbi.nlm.nih.gov/sites/GDSbrowser?acc=GDS369), which supports its possible role in fracture repair.

All isoforms of *Fam57b* contain a Tram-Lag1-CLN8 (TLC) domain, which is associated with acyl-coA-dependent ceramide synthesis. This poorly characterized domain is 200 residues long and contains an Arginine residue conserved in all families and 2 consecutive Histidine residues related to catalysis and substrate binding. The main functions that have been attributed to this domain are synthesizing ceramide moieties from sphingosine bases and fatty acyl-CoA and activating lipid synthesis. However, it is also believed that the TLC domain could serve to protect proteins from proteolysis, act as lipid sensors and be involved in lipid transport [77, 78].

Currently, there exists one publication related to FAM57B2. In this study, Yamashita-Sugahara et al. (2013) have shown that Fam57b is a transcriptional target of Peroxisome Proliferator-activated Receptor y (PPARy), a member of the nuclear receptor family of transcription factors and known master regulator of adipocyte differentiation. They showed that all isoforms of Fam57b are upregulated during adipogenic differentiation in ST2 cells and 3T3-L1, downregulated when PPARγ is silenced with siPPARγ and that Fam57b has PPARγ response elements near the promoter region, showing that Fam57b2 is a target of PPARy. However, when Fam57b is overexpressed, PPARy expression decreases, suggesting negative feedback. When Fam57b2 is overexpressed in ST2 cells, it increases the ceramide content in the cells, which inhibits adipogenesis when expressed at high levels, acting as a negative regulator of adipogenesis. Particularly, levels of ceramides C16-, C18- and C20- were increased when overexpressing Fam57b2. Additionally, when knocking down Fam57b with siRNA and using a ceramide synthase inhibitor to account for the compensatory activity of other ceramide synthases, there was an decrease in total ceramide level produced [77]. The findings from this paper don't negate a positive role of FAM57B2 in fracture healing, since it has been demonstrated that there is a delay in fracture

repair and lower biomechanical properties when the adipose tissue amount in the callus increases [79].

Our laboratory tested the binding of each of these isoforms to 24,25(OH)<sub>2</sub>D<sub>3</sub> through the use of cellular dielectric spectroscopy by stably transfecting COS-7 cells with an expression vector for each variant. We identified that only *Fam57b2* was able to bind to 24,25(OH)<sub>2</sub>D<sub>3</sub> with high specificity, while it didn't bind to other vitamin D metabolites, steroids, or the 24S,25(OH)<sub>2</sub>D<sub>3</sub> epimer [80, 81]. We also performed radioactive ligand binding analysis, in which it was likewise observed that *Fam57b*-overexpressing cells (Riken clone 1500016O10) bound [<sup>3</sup>H]-24,25(OH)<sub>2</sub>D<sub>3</sub> in a saturable manner, with excess unlabeled 24,25(OH)<sub>2</sub>D<sub>3</sub> outcompeting binding of the tritiated ligand, while 1,25(OH)<sub>2</sub>D<sub>3</sub> and 25(OH)D<sub>3</sub> had much lower affinity (Martineau 2017, submitted).

To study the role of Fam57b2 in chondrocyte cells, a tissue found in the fracture callus, and one of the tissues where Fam57b2 is most highly expressed, St-Arnaud lab developed an antibody to the N-terminal region of the FAM57B2 protein and observed that expression of 35 kDa FAM57B2 protein was induced in differentiating pre-chondrogenic ATDC5 cells starting at around day 7. To study the role Fam57b has in fracture repair, our laboratory developed a mouse strain in which the Fam57b gene was specifically inactivated in tissues expressing the Collagen Type II (Col2a1) gene to inactivate the gene in chondrocytes. This was done by targeting the most conserved exon 6 through Cre-Lox recombination, removing the floxed region and introducing a frameshift to produce a null allele. Mice deficient for FAM57B2 in chondrocytes exhibit the same delay in fracture repair than Cyp24a1-deficient mice, showing a significant decrease in callus volume, mineralized callus, and relative bone volume in female mice at 18 days post-osteotomy.

To find a link to the specific interaction with 24,25(OH)<sub>2</sub>D<sub>3</sub>, an enzymatic assay was developed centered around the idea that the protein contains a domain related to acyl-CoA dependent ceramide synthesis by using sphingosine as substrate for the reaction (Fig. 5).

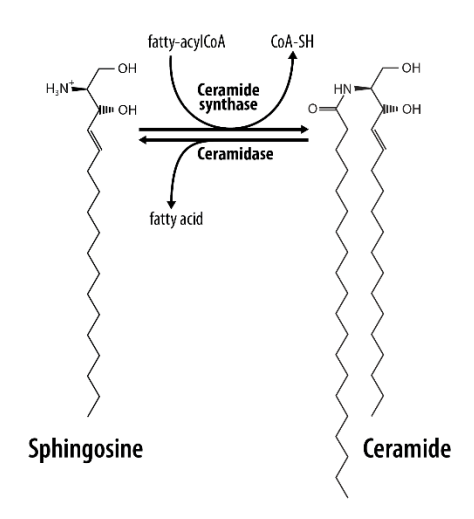


**Fig. 5**. Ceramide synthesis reaction involving a sphingosine substrate and fattyacyl CoA.

Our lab has identified that under incubation of cell extracts overexpressing recombinant FAM57B2 with a sphingosine substrate and fatty acyl-coA in the presence and absence of 24,25- $(OH)_2D_3$ , there is formation of lactosylceramide (LacCer) (D-galactosyl-1,4-beta-D-glucosylceramide OR ( $\beta$ -D-galactosyl-(1-4)- $\beta$ -D-glucosyl-(1-1')-ceramide (Gal $\beta$ 1-4Glc $\beta$ 1Cer)) (**Fig. 6**) [82, 83]. In trying to conciliate our lab's findings with Yamashita-Sugahara et al., we hypothesized that FAM57B2 is a lactosylceramide synthase that is allosterically regulated by  $24,25(OH)_2D_3$  [77]. An allosteric enzyme is one where an effector binds at a separate site than the enzymatic active site, modifying the protein's conformation, substrate specificity and activity [82, 83].

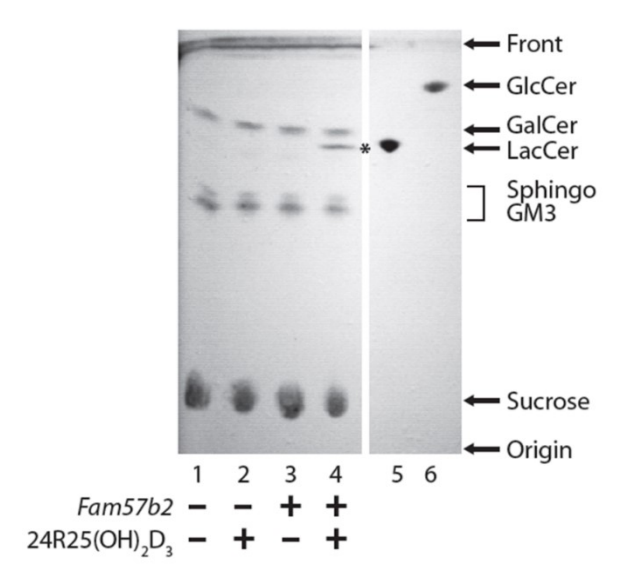


**Fig. 6**. Production of lactosylceramide. TLC plate showing specific production of lactosylceramide in cells overexpressing *Fam57b2* in presence of 24,25(OH)<sub>2</sub>D<sub>3</sub>. Image courtesy of Dr. Corine Martineau.

#### 1.8 Ceramides

Ceramides are waxy lipids classified as sphingolipids because they are composed of a sphingosine and a fatty acid joined by an amide bond (**Fig. 7**) [84].

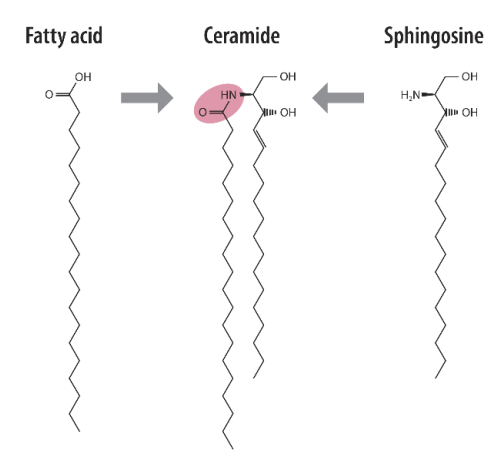


**Fig.** 7. Ceramide structure. Ceramide is composed by a sphingosine and a fatty acid joined together through an amide bond, indicated in pink.

Sphingolipids are mainly produced in the ER and transported to the cellular membrane and other cellular compartments. Ceramide synthesis can occur through a *de novo* pathway through

the condensation of serine and palmitoyl-CoA, sphingomyelin hydrolysis and reacylation of sphingosine [85]. Most anabolic modifications occur in the C1 hydroxyl group, where saccharides and phosphate groups can become attached. However, when ceramide is catabolised, it is usually cleaved at the amide bond [86].

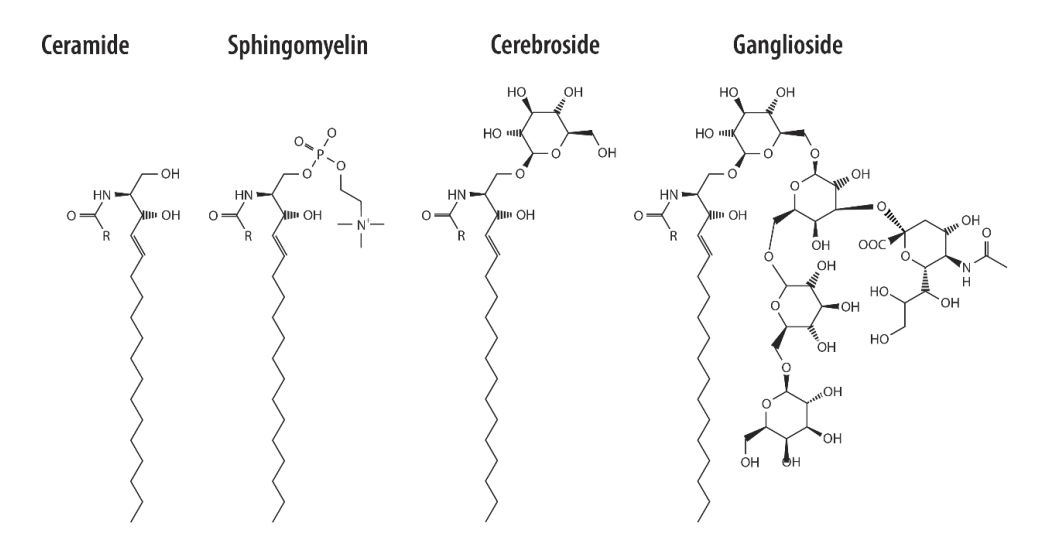


**Fig. 8**. Anabolic modifications of ceramide. Ceramide can be modified at the C1 hydroxyl group, where phosphate groups, sugars and more complex molecules can be attached to created more complex glycosphingolipids.

Ceramides are a family of molecules that share the same headgroup but can differ between each other in the length or hydroxylation of the acyl chain, in the length, hydroxylation or saturation of the sphingoid base, and relative abundance in different tissues [85, 87]. In mammals, C18 sphingosine is the most common chain length found, although C20 long molecules can be found in the brain [88]. These variations give each molecule specificity for different substrates and cellular functions. The enzymes that produce them can also localize to different organelles to provide specific activity and separate regulatory mechanisms [87].

Ceramide and sphingosine have been shown to be involved in apoptosis, growth arrest, senescence and differentiation processes. They do so by functioning as effector molecules to modulate downstream proteins or by modifying membrane architecture and function. It has been

shown that altering ceramide levels, either supressing generation or increasing production lead to disease onset [89]. An important function that ceramides have are to act as an air-liquid barrier in the stratum corneum of the skin, where they make up 30-40% of the lipids, to avoid the drying of tissues in response to air exposure [88].

Ceramides can mostly be found at cell membranes, as they are a component of sphingomyelin, which is a major component of the cell membrane. They can accumulate in certain regions of the cell membrane to facilitate receptor oligomerization and affect cell signalling, stabilize the cell membrane, modify membrane permeability by interacting with ion channels and acting as second messengers by interacting with kinases and phosphatases in the cell [85].

#### 1.8.1 Lactosylceramide

Glycosphingolipids such as lactosylceramide are important components of the cellular membrane. It is presumed that the carbohydrate moiety of these molecules oversees the primary biochemical function, while the ceramide portion is in charge of determining the appropriate place of the lipid in the cellular membrane and providing hydrogen bonding capacity.

#### Lactosylceramide

Fig. 9. Lactosylceramide structure. Lactosylceramide is composed of a carbohydrate moiety and a ceramide moiety.

Lactosylceramide is particularly important because it is the branch point that links the ceramide, globoside and ganglioside pathways together (**Fig. 10**) [90]. It is the major precursor for the synthesis of more complex glycosphingolipids [91].

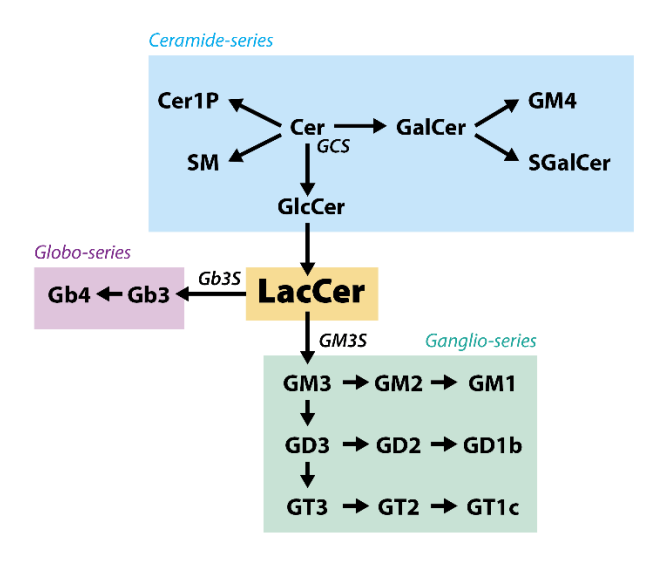


**Fig. 10.** Lactosylceramide is the branchpoint between the ceramide pathway and the more complex glycosphingolipids such as globosides and gangliosides. Figure taken from D'angelo, G., et al. (2013) [92], with permission.

It is believed to be produced in response to pro-inflammatory factors, and its production has been shown to affect pathways involved in differentiation, migration, proliferation, cell adhesion and angiogenesis. Some glycosphingolipids are concentrated in specific regions of the membrane forming lipid rafts, and they can function as receptors or modify the activity of other membrane receptors [90, 91]. Saturated glycosphingolipids, such as LacCer have higher transition temperatures and provide a more ordered and less fluid capacity. LacCer and cholesterol in the plasma membrane interact via hydrogen bonds and hydrophobic van der Waal's interactions. These regions highly differ from phospholipids, which have low melting temperatures, are unsaturated and result in more loose, disordered membranes [88].

LacCer is involved in signal transductions pathways affecting cell proliferation [93], adhesion [94, 95], apoptosis [96], angiogenesis [97] and differentiation [98]. The specific role LacCer has in bone has not been characterized yet. It has been shown that LacCer is involved in osteoclastogenesis *in vitro*, where an inhibitor of glucosylceramide synthase, D-PDMP, inhibited osteoclast formation and IκB and ERK1/2 phosphorylation, which was rescued by LacCer treatment. It has also been shown in several studies that lactosylceramide can be produced in response to inflammation, which will activate oxygen sensitive signalling pathways [88, 90].

LacCer has been shown to be involved in TNF-α signalling to produce intercellular cell adhesion molecules ICAM-1 and activate nuclear factor kB through signalling through reactive oxygen species (ROS) in human endothelial cells [94, 99]. It was also shown to act through ROS in human vascular smooth muscle cells to induce proliferation [100]. Its involvement in apoptosis has also been described. In colon cancer cells, LacCer inhibits apoptosis though increased BCL-2 and decreased caspase activity [101]. In human aortic smooth muscle cells, LacCer has been shown to stimulate Ras-GTP loading, Raf, MEK and ERK kinases and c-fos expression [93]. In a separate study, Mishra et al. (2014) showed that ROS production in cardiomyocytes occurred upstream of the MAPK pathway, leading to activation of ERK1/2 signalling to promote hypertrophy. It was also shown that LacCer can recruit PKC and activate PLA<sub>2</sub> in human neutrophils [102].

## Hypothesis

The original purpose of this project is to characterize FAM57B2, the effector through which 24,25(OH)<sub>2</sub>D<sub>3</sub> is believed to promote its effects on bone healing. Data accumulated from the studies performed in the last couple of years on FAM57B2 and its isoforms have lead us to believe that FAM57B2 is the only isoform of *Fam57b* that contains a specific binding site for 24,25(OH)<sub>2</sub>D<sub>3</sub>. The nature and specificity of action of the protein suggests allosteric enzyme regulation, leading us to hypothesize that FAM57B2 is a lactosylceramide synthase that is allosterically regulated by 24,25(OH)<sub>2</sub>D<sub>3</sub> to produce lactosylceramide, which acts as a second messenger to transduce the 24,25(OH)<sub>2</sub>D<sub>3</sub> signal.

#### Aims

- To identify the specific binding pocket for 24,25(OH)<sub>2</sub>D<sub>3</sub> in the FAM57B2 protein.
- Determine the potential topology and localization of FAM57B2 in the membrane.
- Identify the putative role of FAM57B2 and lactosylceramide in chondrocyte differentiation or activity.
- Identify the signalling pathway through which FAM57B2 and lactosylceramide regulate chondrogenic function.

## Chapter II: Materials and Methods

## 2.1 Cell lines, Antibodies, and Reagents

HEK293 (human embryonic kidney cells) were cultured in Dulbecco's modified Eagle's medium (DMEM) (#11995065, Life Technologies) with 10% Fetal Bovine Serum (#10438018) and 1% Penicillin-Streptomycin (#15140122), all purchased from Gibco, Life Technologies (Burlington, Ontario, Canada). The ATDC5 prechondrogenic teratocarcinoma cells (Atsumi, Miwa, Kimata, & Ikawa, 1990) were cultured in Dulbecco's modified Eagle's medium: Nutrient Mixture F12 (1:1) (DMEM: F12, #11330032) supplemented with 5% Fetal Bovine Serum (#10438018) and 1% Penicillin-Streptomycin (#15140122), from Life Technologies. Both cell lines were grown in a humidified atmosphere at 37 °C with 5% CO<sub>2</sub> and 95% O<sub>2</sub>.

Insulin-Transferrin-Sodium Selenite used for differentiation was purchased from Sigma Aldrich (#I1884). For differentiation experiments using (+)-Sodium L-ascorbate (#A4034, Sigma), ATDC5 cells were cultured in MEM-Alpha medium (#12561056, Life Technologies) supplemented with Sodium Selenite (#S5261) and Transferrin (#T8158), which were purchased from Sigma. For reactive oxygen species experiments, DMEM: F12 without phenol red was used (#21041025, Life Technologies). Charcoal-stripped FBS (#A3382101), CYQUANT<sup>TM</sup> NF Cell Proliferation Assay Kit and Caspase-3 Colorimetric Protease Assay Kit (#KHZ0021) were purchased from Life Technologies (#C35006). Collagen I from rat tail (#C7661), Collagen II from chicken sternal cartilage (#C9301), Fibronectin from bovine plasma (#F4759), Hydrogen peroxide solution (#216763) and 2',7'-Dichlorodihydrofluorescein diacetate (DCFDA) (#D6883) were purchased from Sigma Aldrich. Trizol reagent was obtained from Invitrogen Inc. (#15596026, Carlsbad, USA).

For the enzymatic assay, Bovine Serum Albumin (#A7030) was purchased from Sigma Aldrich, while Sphingosine d18:1 (D-erythro-sphingosine, #860490) and 18:0 Coenzyme

A (stearoyl Coenzyme A ammonium salt, #870718) were purchased from Avanti Polar Lipids, Inc. (Alabaster, Alabama). Avanti Polar Lipids products were dissolved in Chloroform:Methanol:Water (80:20:2 ratio), sonicated for 10 seconds at 30%, aliquoted into glass tubes and dried under nitrogen gas. Working solutions of CoA were resuspended in water, while sphingosine was resuspended in 100% ethanol.

(24R)-24,25-Dihydroxyvitamin D<sub>3</sub> (#17943) was purchased from Sigma Aldrich (#A7030) for the enzymatic assay and Secalciferol or 24R,25(OH)<sub>2</sub>D<sub>3</sub> was purchased from MedChem Express (New Jersey, USA). Working solutions of 24R,25(OH)<sub>2</sub>D<sub>3</sub> obtained from either company were resuspended in 95% ethanol.

Anti-FLAG M2 is a mouse monoclonal antibody (mAb) and was obtained from Sigma Aldrich (#3165). Anti OctA or Anti- FLAG are a rabbit polyclonal Ab obtained from Santa Cruz Biotechnology (sc-807-G). Anti-HA (Hemagglutinin) (#C29F4) is a rabbit Ab and was purchased from Cell Signalling (#3724). Anti-Calregulin (T-19) and (C-17) are goat polyclonal Abs from Santa Cruz Biotechnology (sc-7431) and (sc-6467), respectively. Digitonin (#300410) was purchased from Millipore Ltd. (Billerica, Massachusetts). Secondary antibodies Alexa Fluor 488 goat anti-mouse (#A11001), Alexa Fluor 594 goat anti-rabbit (#A11012) and Alexa Fluor 594 donkey anti-goat (#A11058) were obtained from Life Technologies. Taqman probes, ordered from Life Technologies, are listed in Table 2.

Lactosyl C18 ceramide (D-lactosyl-ß-1,1' N-stearoyl-D-*erythro*-sphingosine) was purchased from Avanti Polar Lipids (#860598P). 5mg of powder were resuspended in 5mL Chloroform:Methanol (85:15 ratio), sonicated for 30 seconds at 30%, aliquoted into glass tubes and dried under nitrogen gas. Working solutions were resuspended in DMSO (dimethyl sulfoxide).

## 2.2 Plasmids, Vector Cloning and Mutagenesis

The full length *Fam57b2* cDNA with FLAG epitope on the C-terminus was inserted into the pLVX-IRES-Puro HIV-1-based, lentiviral expression vector from Clontech (#632183) to yield the pLVX-Fam57b2-FLAG plasmid for transfection and infection assays using the primer set B shown in Table 1 using Phusion® High-Fidelity PCR Kit (#E0553L) from New England Biolabs (Ipswich, MA).

Expression vectors for the 10 different FAM57B2 mutant proteins were obtained by mutating the initial 50 residues located on the N-terminus side of the protein. Five aminoacid substitutions to Alanine were done at a time by overlap extension PCR (OE-PCR) (**Fig. 11**), as described in Ho *et al.* (2016) in greater detail [103].

OE-PCR was also used to insert HA (hemagglutinin) tags inside the coding sequence of Fam57b2 to study the topology and localization of the protein. The OE-PCR technique works through three total PCR reactions: two primary and one secondary reaction. In the primary reactions, performed in separate tubes with separate primer sets, the target gene is amplified with one primer that hybridizes at one end of the target gene and one primer that hybridizes at the site of mutagenesis on either DNA strand (generating fragments AB and CD). This second primer, contains a ~22bp sequence complementary to the target gene, a 15bp overhang containing the mutated mismatched base sequence followed by a 3bp complementary sequence. The product created in these two primary PCR reactions is migrated on a gel and purified. Subsequently, the secondary PCR reaction is performed, where the products of the primary reactions contain an overlap that allows one strand of each fragment to act as a primer on the other (AB+CD) through denaturation and annealing. This reaction is further favoured by adding the original gene flanking primers (primers 'a' and 'd') onto the PCR mix.

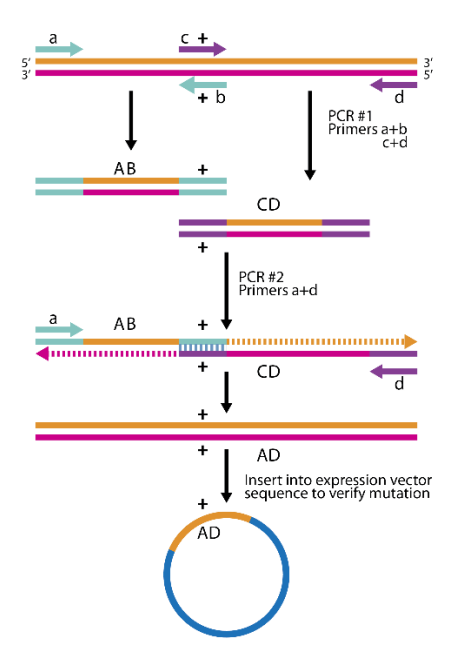


**Fig. 11.** Overlap-extension PCR (OE-PCR). Mutagenesis is performed through 2 PCR reactions by annealing primers containing the desired mutation. The PCR products containing overlapping sequences are used to prime each other for a third PCR reaction, where the mutant product is fused together and cloned into an expression vector. The mutation is indicated by '+'.

Table 1 contains the sequences of all primers used for cloning and mutagenesis, where primer set A is the forward (fwd) and reverse (rev) primers that flank the gene (primers 'a' and 'd' in the analogy above), and primer sets C-O are the primers used for mutagenesis or HA tag insertion (primers 'b' and 'c' in the analogy above). The DNA fragments were digested with restriction enzymes, ligated, and cloned in Top10 bacteria (Life Technologies, #C404010).

# 2.3 Transfection of HEK293 and Infection of ATDC5 cells with Target DNA

HEK293 cells were plated and grown for 16 hours prior to transfection in 6 well plates at a concentration of 2 x 10<sup>5</sup> cells/well. On the day of transfection, pLVX and pLVX-Fam57b2 were transfected in duplicates (2 wells/condition). Per condition, a mix of 2 μg of vector DNA with 200 μL of Opti-MEM was prepared. In a separate tube, 20 μL of lipofectamine with 180 μL Opti-MEM per condition were prepared. The lipofectamine mix was added to each vector DNA

preparation and incubated for 45 min. During the incubation time, the media in the cells was substituted with Opti-MEM. After the incubation time, 1.2 mL of Opti-MEM were added to each DNA-lipofectamine mix and 800 μL of each mix is added to the cells in duplicate. The cells were incubated for 4 hours, after which the medium was removed and changed to fresh DMEM growing medium (2 ml in each well for 6 well-plate). This protocol was followed for all *Fam57b2* mutants and HA-tagged *Fam57b2*.

For transfections, proteins were extracted 24 hours after transfection. For stable transfections, cells were placed under selective medium (puromycin at a concentration of 1.5 µg/mL) for 3 days after which the cells were passaged and plated for extraction in 10 cm plates.

To create virus for ATDC5 infection, HEK293 cells were plated on 10 cm plates at a concentration of 1 x 10<sup>6</sup> cells per condition the day before transfection. For each condition, 10 μg of pLVX and pLVX-*Fam57b2* DNA vector and 10 μg of viral packaging vectors psPAX2 and pMD2.G at a ratio of 3:1 were used. On the day of transfection, 10 μg of DNA were incubated with 500 μL of 2x HBS (HEPES Buffered Saline). In a separate tube, 50 μL of 2.5 M CaCl<sub>2</sub> were diluted in 450 μL of distilled water. The HBS/DNA mix was vortexed while CaCl<sub>2</sub> is added drop by drop. The complexes were incubated at room temperature (RT) for 20 minutes and then the mix was added dropwise around the plate. 24 hours after transfection, the media was substituted with DMEM: F12 medium with 5% FBS to collect viral particles. The media was collected and fresh DMEM: F12 medium was added onto each plate. The 2 media collections were pooled and aliquoted into 10 mL working aliquots. ATDC5 cells were infected when they were at a 60-70% confluency. Media was changed the following day into selection media at a concentration of 3.5 μg/mL of puromycin for 3 days, after which cells are passaged and plated.

## 2.4 FAM57B2 Protein Expression

To assess the protein expression of WT FAM57B2 and all the FAM57B2 mutants, cells were extracted with 300 μL from 100 mm plates for stable transfects and 100 μL from 1 well of a 6-well plate for transient transfects with RIPA buffer (50 mM Tris-HCl, pH 7.5, 150 mM NaCl, 1% NP-40, 0.5% sodium deoxycholate, 0.1% SDS) after 2 washes with cold PBS. Cells extracts were sonicated for 10 sec at 30% amplification and centrifuged for 15 min at 10 000 rpm at 4 °C. Supernatants were transferred into a separate tube and protein concentration was measured with the Bradford assay. Forty (40) μg of protein were denatured for 5 minutes at 95 °C with Laemmli buffer (0.0005% Bromophenol blue, 5% beta-mercaptoethanol, 10% glycerol, 2% SDS and 62.5 mM Tris-HCl, pH 6.8). Samples were resolved by SDS-PAGE on a 12% acrylamide gel, blotted onto a PVDF membrane and revealed by immunoblotting with anti-FLAG antibody (1:2000).

## 2.5 Chondrocyte Cell Regulation Assays

#### 2.5.1 Proliferation

To assess proliferation, ATDC5 cells were plated in 96 well plates at a density of 2 000 cells/well the day before treatment. Proliferation was assessed over 24, 48, 72 and 96 hours under increasing concentrations of LacCer (0  $\mu$ M, 10  $\mu$ M and 20  $\mu$ M). The protocol described in CYQUANT<sup>TM</sup> NF Cell Proliferation Assay Kit was followed.

#### 2.5.2 Differentiation

ATDC5 cells were plated on 12 well-plates at a concentration of 50 000 cells/well and were allowed to grow for 5 days. When cells reached confluency, they were induced to differentiate under 4 different conditions: Control medium (DMEM: F12 + 5% FBS), LacCer (10  $\mu$ M), 1x ITS (5  $\mu$ g/mL insulin, 5  $\mu$ g/mL transferrin, 30 mM sodium selenite), and 1x ITS + LacCer. Media was

changed every 2-3 days. Cells were rinsed twice with PBS before extraction with 500  $\mu$ L/well Trizol.

When differentiating ATDC5 cells with ascorbic acid, cells were plated and grown as described previously. However, differentiation was induced at confluency under 4 conditions: Control medium (DMEM: F12 + 5% FBS), Ascorbic Acid (50  $\mu$ g/mL), LacCer (10  $\mu$ M), and Ascorbic acid + LacCer. Media was changed every 2-3 days and cells were extracted as previously described.

When differentiating empty vector infected and *Fam57b2*-infected ATDC5 cells, cells were plated at 50 000 cells/well in 12 well plates. Differentiation was started at confluency by substituting media with DMEM:F12 + 5% FBS + 1x ITS. Treatment with 24,25(OH)<sub>2</sub>D<sub>3</sub> of *Fam57b2*-infected cells was started at confluency, by substituting the media with DMEM: F12 + 5% charcoal-stripped FBS + 1x ITS with 0.1 µM 24,25(OH)<sub>2</sub>D<sub>3</sub> or vehicle. Media was changed every 2-3 days and cells were extracted as previously described.

#### 2.5.3 Adhesion

To assess cellular adhesion, 96 well plates were coated with solutions of collagen I (10  $\mu$ g/cm<sup>2</sup>), collagen II (5  $\mu$ g/cm<sup>2</sup>) or fibronectin (5  $\mu$ g/cm<sup>2</sup>) for 2 hours, after which the solution was pipetted out and allowed to air dry. On the day of the experiment, 2% BSA/PBS was used to block for 2 hours at 100  $\mu$ L / well at room temperature (RT). Thirty (30) minutes before trypsinizing, ATDC5 cells were incubated with 0  $\mu$ M, 5  $\mu$ M, 10  $\mu$ M or 20  $\mu$ M LacCer. Cells were trypsinized for 5 minutes and the enzyme was neutralized with DMEM-F12 with 5% FBS. Cells were spun down at 9 000 rpm for 5 minutes and rinsed twice in serum free medium. After resuspending, cells were diluted to 4 x 10<sup>5</sup>cells/ml in serum free medium with increasing concentrations of LacCer. A 100  $\mu$ L cell suspension was added into each well in triplicate (40 000 cells/well). Cells were

placed in the incubator for 2 hours. After the incubation,  $100~\mu L$  of fresh serum free media were added to the cells carefully down the side of each well. The plate was inverted gently onto an absorbent paper and the wash solution was removed. This procedure was repeated twice checking that wells containing solely BSA have no or few cells. Wells were then fixed with  $100~\mu L$  of 50% methanol for 10 minutes at RT, which was after substituted with  $100~\mu L$  of freshly filtered (0.2  $\mu$ m) 0.5% crystal violet in 20% methanol/PBS. Cells were stained for 20 min at RT on a shaker. The plate was then inverted gently onto an absorbent paper. The plated was then washed by immersion in a plastic tray containing tap water. The procedure was repeated twice more, after which the remaining solution was pulled off from each well with a pipette. The plate was allowed to dry for 5-10 min at RT. Fifty (50)  $\mu$ L of 1% SDS was added to the wells and it was allowed to solubilize for 1 hour under dark, after which the optical density (OD) was measured at wavelength 595 nm.

# 2.5.4 Cell Migration

To assess cellular migration, the protocol from Liang et al. (2007) was followed [104]. ATDC5 cells were plated at a density of 100 000 cells per well in a 12-well plate. Cells were allowed to grow until they were 90-100% confluent. The cell monolayer was scraped in a straight line with a P200 pipette tip. The debris was removed by rinsing once with PBS and then it was replaced with the appropriate treatment media. ATDC5 cells were incubated with increasing concentrations of LacCer (0 μM, 10 μM, 20 μM) with 0.5% FBS or 2% FBS. Different amounts of FBS were used to avoid cellular death and to increase the likelihood that the cellular activity was due to migration rather than cellular proliferation. After 16 and 20 hours of incubation at 37 °C, cellular migration was measured with EVOS<sup>TM</sup> XL Core Imaging System. The change on the

scratched area was calculated by subtracting the area of the scratch after recovery from the total initial scratched area by using Adobe Photoshop® CC.

## 2.5.5 Apoptosis

To assess apoptosis, the protocol found in the Caspase-3 Colorimetric Protease Assay Kit was followed. ATDC5 cells were plated at a density of 20 000 cells/well in a 24 well plate. Cells were treated with increasing concentrations of LacCer (0  $\mu$ M, 10  $\mu$ M, 20  $\mu$ M) for 72 and 96 hours.

## 2.5.6 Reactive Oxygen Species

To assess production of Reactive Oxygen Species (ROS), DCFDA resuspended in 100% ethanol was used. ATDC5 cells were plated in a 96 well plate at a cellular density of 25 000 cells/well, with one row of cells left without cells for negative controls the day before the experiment. Cells were rinsed once with PBS and incubated with 10  $\mu$ M DCFDA diluted in phenol red free DMEM: F12 in the dark for 45 minutes. Cells were then washed once with PBS and incubated at 37 °C for different amounts of time with increasing concentrations of LacCer (10  $\mu$ M, 20  $\mu$ M and 50  $\mu$ M) in phenol red free DMEM: F12 for a time course experiment. DMSO treatments for 30 minutes, 3 hours, 5 hours and 8 hours were used as vehicle controls. Samples were assayed in duplicates. Cells were kept under dark at all times until the end of the incubation time and the fluorescence intensity was measured at Excitation/Emission (Ex/Em) = 485/535 nm with a gain of 45.

#### 2.6 Immunofluorescence

Transfected HEK293 cells were plated on glass sterilized coverslips in 12-well plates at a density of 1.6 x 10<sup>5</sup> cells/well. Following 24 hours, the cells were washed in PBS twice then fixed in 4% paraformaldehyde (PFA) for 20 min at room temperature. Wells were rinsed gently 3 times

with PBS, followed by blocking with 5% BSA in PBS for 1 hour. Following this, cells were permeabilized with 0.3% Triton X-100 in PBS for 1 hour or with 0.005% Digitonin in PBS with 120mM sucrose for 5 minutes. Wells were washed 3 times with PBS which was followed by immunodetection with the primary antibodies mouse anti-FLAG (1:2000), rabbit anti-HA (1:1600), mouse anti-HA (1:500), goat anti-OctA (1:250), and goat anti-calregulin 7431/6467 (1:250) antibodies respectively in PBS + 1% BSA mix overnight at 4 °C. The following day, the cells were washed 3 times with PBS. Then, the secondary antibodies Alexa Fluor 594 goat anti-rabbit, Alexa Fluor 488 goat anti-mouse, and Alexa Fluor 594 donkey anti-goat at 1:1000 were diluted in PBS + 1% BSA and added for 1 hour at room temperature on the shaker; covered by aluminium foil. This was followed by 3 washes in PBS after which coverslips were mounted on slides with Prolong® Gold antifade reagent with DAPI (Life Technologies). Immunofluorescence images were obtained using a Leica DMR fluorescence microscope (Leica Microsystems, Wetzlar, Germany) connected to a digital DP70 camera (Olympus, Center Valley, PA).

# 2.7 Enzymatic Assay and Thin Layer Chromatography

In order to test the enzymatic activity of FAM57B2, a protocol derived from Yamashita-Sugahara et al. (2013) was followed. HEK293 cells were transiently or stably transfected with pLVX and pLVX-*Fam57b2* [77]. Cells were allowed to grow until they reached confluence in a 100 mm petri dish, after which they were rinsed twice with cold PBS. Cells were extracted using 300 μL of a HEPES homogenization buffer (20 mM HEPES-KOH, pH 7.4, 25 mM KCL, 250 mM sucrose, 2 mM MgCl<sub>2</sub>, 1 mM protease inhibitor cocktail, 1 mM phenylmethylsulphonyl fluoride (PMSF)). Cell lysates were sonicated for 1 minute at 30% intensity 10s/10s on/off on ice and protein concentration was assessed using the Bradford method. Fifty (50) μg of each whole cellular lysate in 50 μL HEPES buffer were incubated with 200 μL of reaction mix (15 μM sphingosine,

20 μM BSA and 50 μM C18-CoA in homogenization buffer). Each reaction was incubated in the presence of ethanol 95% vehicle, 10 µM 24,25(OH)<sub>2</sub>D<sub>3</sub> or 1 µM 1,25(OH)<sub>2</sub>D<sub>3</sub> for 30 min at a 37 °C water bath. The reaction was stopped by adding chloroform: methanol to reach a ratio of 2:1:0.8 to extract the lipids using the Folch partitioning method [105]. The vials are shaken vigorously for 1 hour and then centrifuged at 500 rpm for 3 minutes. The heterogeneous solution was split into an upper aqueous phase containing water and methanol, while the lower phase contained lipids in chloroform and methanol. The upper phase was discarded and the lower phase was dried under nitrogen gas. The dried lipids were then resuspended in 60 µL of chloroform:methanol (2:1) and spotted on a 20x20 cm silica plate for Thin Layer Chromatography (TLC). The spots were lightly marked 2 cm from the bottom of the plate. The mobile phase of the TLC consisted of 150 mL of Chloroform: Methanol: (0.2% w/v) Calc<sub>2</sub> (60:35:8) [106, 107]. When the mobile phase saturated the chamber, the silica plate spotted with all the samples and standards was placed vertically inside the chamber with the spots at the bottom of the plate. The chamber was sealed with vacuum grease and the mobile phase was allowed to migrate upwards via capillary action for around 1.5 hours under the chemical hood until the mobile phase migrated 2 cm from the top of the plate. To visualize the lipids, a developing solution consisting on 3% copper acetate in H<sub>3</sub>PO<sub>4</sub> 8% (aqueous) was sprayed evenly on the plate and then the plate was heated in a mini-oven until charred lipids showed on the plate.

# 2.8 Real-Time RT-PCR (RT-qPCR)

RNA from ATDC5 cells was extracted with TRIzol (Invitrogen) by following the manufacturer's instructions. One microgram of RNA was reverse transcribed into cDNA using the High Capacity cDNA Reverse Transcription Kit (#4368813) from Applied Biosystems according to the manufacturer's protocol. Real-time PCR amplification was performed using the TaqMan<sup>TM</sup>

Fast Advanced Master Mix (#4444557, Applied Biosystems) on the QuantStudio<sup>TM</sup> 7 Flex Real-Time PCR System (Applied Biosystems) and specific Assay-On-Demand TaqMan assays for *Col2a1, Col10a1, Ihh* and *Fam57b2*. Relative quantification of mRNA was performed according to the comparative cycle threshold (CT) method (number of cycles required for the fluorescent signal to cross a threshold and exceed background level) [108] with *B2 microglobin* (*B2m*) or *phosphoglycerate kinase 1* (*Pgk1*) mRNA levels as an endogenous controls. Samples were assayed in triplicates.

#### 2.9 Statistical Analysis

For the RT-qPCR results, Two-way Anova was performed using GraphPad Prism 6 version on the 2<sup>-ddCt</sup>. For migration assays, Two-way Anova was performed using GraphPad Prism 6. Proliferation and ROS were performed using a One-way Anova on GraphPad Prism 6. Adhesion assays were performed with a Student's t-test. A probability value (p-value) of 0.05 or less was considered statistically significant.

The values are reported as mean fold induction standard error of the mean (SEM), The asterisk (\*) indicates whether there is a significant statistical increase or decrease compared to the mean of a specific condition: (\*) p < 0.05, (\*\*) p < 0.01, (\*\*\*) p < 0.001. The post-hoc test used in both assays was Tukey.

## 2.10 Tables

 Table 1: Primer sequences

Symbol	Gene Name	Forward Primer: Seq 5' - 3'	Reverse Primer: Seq 5' – 3'
A	pLVX-Puro-IRES	CTCGTTTAGTGAACCGTCAGAT	ACACCGGCCTTATTCCAAG
В	Fam57b2-FLAG	GGGCTAGCATGGCCCTGCTCTTCCTG	GAGGATCCTTACTTATCGTCGTCATCC
			TTGTAATCGTCCTGGGTCTGACAAGGA
			GAGG
С	Fam57b2 L(3-5)A	AGCATGGCCGCGCCCCTGCTGGGGTGTGT	CAGGGCGGCCGCGCCATGCTAGTCTC
		CTTCTT	GAGGAATTCAC
D	Fam57b2 L(6-10)A	TTCGCGGCGCAGCTGCATTCTTCCCACTGTG	GAATGCAGCTGCCGCCGCAAGAGCA
		CTTTGTGG	GGGCCATGCTAGTC
E	Fam57b2 F(11-15)A	GTCGCCGCCGCAGCGGCCTTTGTGGTATTACG	AAACGGCGGCGTCGCCGGGACACACC
		CTGGGGC	CCAGCAGGAAGAGC
F	Fam57b2 F(16-20)A	TGCGCUGCGGCAGCAGCGTGGGGGCTGCAGA	CCACGCTGCTGCCGCAGCGCACAGTGG
		ATCGAACCA	GAAGAAGACACAC
G	Fam57b2 W(21-25)A	CGCGCGGCGGCGGCCTCGAACCAGCTTA	ATTGGCCGCCGCGGCCGCTAATACCAC
		CGGATGGAGAG	AAAGCACAGTGGG
Н	Fam57b2 R(26-30)A	AATGCAGCCGCCGCAGCGATGGAGAGGCAAG	CATCGCTGCGGCGGCTGCATTCTGCAG
		AGGCTGTCT	CCCCCAGCGTAAT
I	Fam57b2 M(31-35)A	CGGGCGGCGGCAGCGGCTGTCTTGGTGG	AGCCGCTGCCGCCGCCGTAAGCT
		CATCCAAGT	GGTTCGATTCTGC
J	Fam57b2 A(36-40)A	GAGGCTGCCGCGGCGCATCCAAGTTGGTGT	GGATGCCGCCGCGGCAGCCTCTTGCCT
		CCTCTGTCC	CTCCATCCGTAAG
K	Fam57b2 S(41-45)A	GCAGCCGCGGCGCCTCTGTCCAAGCCA	AGAGGCCGCCGCGCGGCTGCCACCA
		TCATGGCCT	AGACAGCCTCTT
L	Fam57b2 S(46-50)A	TCCGCCGCCGCAGCCGCCATGGCCTCCACAGC	CATGGCGGCTGCGGCGGACACCA
		TGGCTACA	ACTTGGATGCCACC
M	HA-Fam57b2-FLAG	ATCTCGAGATGTACCCATACGATGTTCCAGAT	GAGGATCCTTACTTATCGTCGTCATCC
		TACGCTGCCCTGCTCTTCCTGCT	TTGTAATCGTCCTGGGTCTGACAAGGA
			GAGG
N	Fam57b2-HA-25	TATCCATATGATGTTCCAGATTATGCTCGAAC	AGCATAATCTGGAACATCATATGGATA
		CAGCTTACGGATGGAG	ATTCTGCAGCCCCCAGCGTAATA
0	Fam57b2-HA-30	TATCCATATGATGTTCCAGATTATGCTATGGA	AGCATAATCTGGAACATCATATGGATA
		GAGGCAAGAGGCTG	CCGTAAGCTGGTTCGATTCTGC

Table 2: TaqMan list

Gene Name	RefSeq <sup>1</sup>	Catalog # <sup>2</sup>
Col2a1	NM_031163.3	Mm00491889_m1
Col10a1	NM_009925.4	Mm00487041_m1
Ihh	NM_010544.2	Mm00439613_m1
Fam57b2	NM_026884.1	Mm01276192_m1
Pgkl	NM_008828.3	Mm00435617_m1
B2M	NM_008084.2	4352932E

Reference Sequence that provides a comprehensive and well-annotated reference for genome annotation, gene identification and characterization from the National Center of Biotechnology Information (NCBI) 109. Information, N.C.f.B.

55

<sup>&</sup>lt;sup>2</sup> Catalog number used to identify product in ThermoFisher Scientific Database.

#### Chapter III: Results

#### 3.1 FAM57B2 WT and Mutant Protein Outline

In order to study FAM57B2 and determine the specific amino acid sequence required for 24,25(OH)<sub>2</sub>D<sub>3</sub> binding, a *Fam57b2* vector construct was built through the use of restriction enzyme digestion, ligation and PCR. Because the diverging portion between all 3 isoforms of the FAM57B protein is only found in the initial 50 amino acids on the N-terminus of the protein (**Fig.** 12), we focused on this section of the protein to perform mutagenesis.

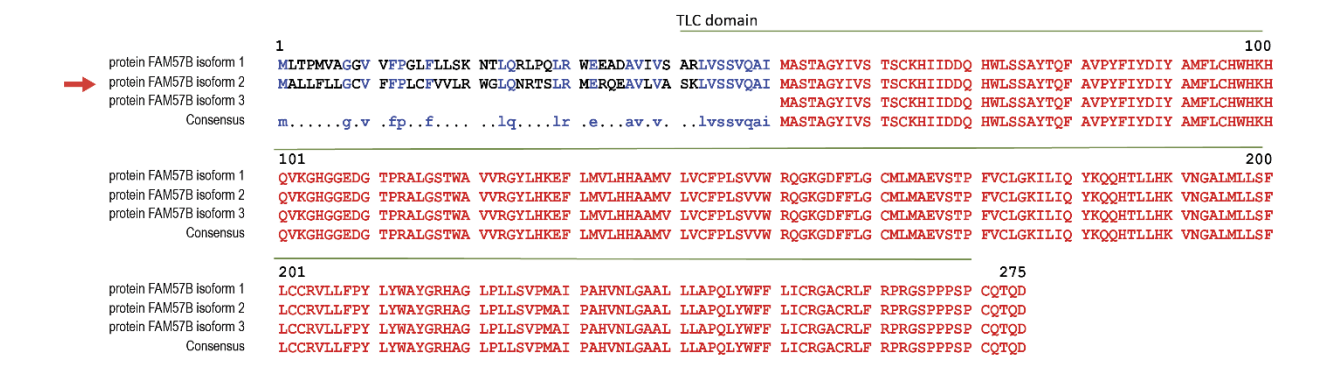


**Fig. 12**: The difference in the homology of the 3 isoforms of FAM57B relies in the initial 50 amino acids at the N-terminus. All isoforms contain a TLC domain, a domain associated to acyl-CoA-dependent ceramide synthesis. FAM57B2, the protein of interest is marked with a red arrow.

Mutagenesis was performed by Alanine Scanning of 5 consecutive amino acids at a time using OE-PCR. A set of 10 mutants covering the initial 50 residues located on the N-terminus side of the protein was created for which a schematic is shown in **Fig. 13**.

isoform 2 AA	MALLFLLGCVFFPLCFVVLRWGLQNRTSLRMERQEAVLVASKLVSSVQA MASTAGYIVSTSCKHIIDDQHWLSSAYTQFAVPYFIYDIYAMFLCHWHKH QVKGHGGEDGTPRALGSTWAVVRGYLHKEFLMVLHHAAMVLVCFPLSVVWRQGKGDFFLGCMLMAEVSTPFVCLGKILIQYKQQHTLLHKVNGALML SFLCCRVLLFPYLYWAYGRHAGLPLLSVPMAIPAHVNLGAALLLAPQLYWFFLICRGACRLFRPRGSPPPSPCQTQD
WT FAM57B2	MALLFLLGCVFFPLCFVVLRWGLQNRTSLRMERQEAVLVASKLVSSVQAI
Mut. 1: L(3-5)A	MAAAALLGCVFFPLCFVVLRWGLQNRTSLRMERQEAVLVASKLVSSVQAI
Mut. 2: L(6-10)A	MALLF <mark>AAAAA</mark> FFPLCFVVLRWGLQNRTSLRMERQEAVLVASKLVSSVQAI
Mut. 3: F(11-15)A	MALLFLLGCVAAAAAFVVLRWGLQNRTSLRMERQEAVLVASKLVSSVQAI
Mut. 4: F(16-20)A	MALLFLLGCVFFPLCAAAAAWGLQNRTSLRMERQEAVLVASKLVSSVQAI
Mut. 5: W(21-25)A	MALLFLLGCVFFPLCFVVLRAAAAARTSLRMERQEAVLVASKLVSSVQAI
Mut. 6: R(26-30)A	MALLFLLGCVFFPLCFVVLRWGLQNAAAAAMERQEAVLVASKLVSSVQAI
Mut. 7: M(31-35)A	MALLFLLGCVFFPLCFVVLRWGLQNRTSLRAAAAAAAVLVASKLVSSVQAI
Mut. 8: A(36-40)A	MALLFLLGCVFFPLCFVVLRWGLQNRTSLRMERQEAAAAASKLVSSVQAI
Mut. 9: S(41-45)A	MALLFLLGCVFFPLCFVVLRWGLQNRTSLRMERQEAVLVAAAAAASVQAI
Mut. 10: S(46-50)A	MALLFLLGCVFFPLCFVVLRWGLQNRTSLRMERQEAVLVASKLVSAAAAA

**Fig. 13**: Schematic of the WT FAM57B2 protein sequence and 10 mutants generated by Alanine Scanning.

## 3.2 FAM57B2 Protein Expression

In order to confirm FAM57B2 protein expression, a FLAG epitope was introduced on the C-terminus of *Fam57b2*. As it can be seen in **Fig. 14**, transfection to generate stable cell lines in HEK 293 cells allowed to immunodetect a 31 kDa sized band using anti-FLAG antibody in cell extracts of WT FAM57B2 and 8 of the mutants, while no signal was detected in the negative control empty vector. Mutants 2 and 3 show detection of a very faint band in stable cell extracts. Stable transfection of these mutants was repeated to confirm poor expression (**Fig. 14A**). To ensure that all mutant proteins are capable of being expressed, the vector constructs were transfected transiently into HEK293 cells and blotted against the FLAG epitope. Expression of all constructs was observed in this case (**Fig. 14B**). As WT FAM57B2 and 8 of its mutant proteins can be detected in transient and stable transfections, these proteins are stable enough and can be easily studied. However, mutant 2 and mutant 3 can only be detected transiently and not stably, which

could be due to the fact that the protein is degraded or is not stable enough. Repeating the stable transfection allowed us to determine that the site of integration of the gene into the cell's genome was not the reason for its poor expression because it likely integrated into a random site in each experiment.

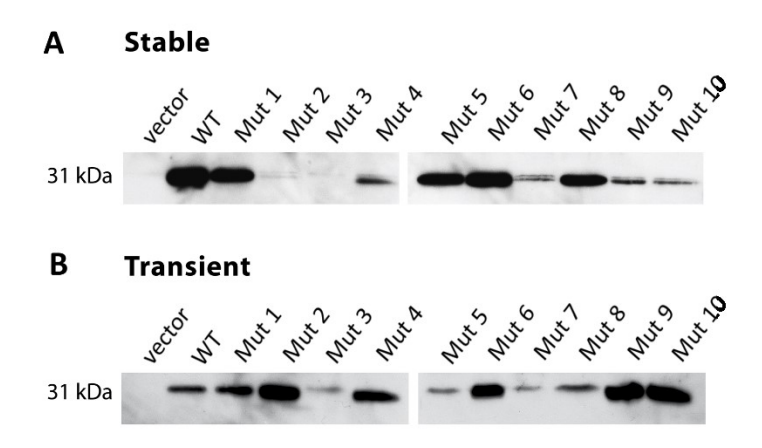


**Fig. 14**: Protein expression confirmation by Western blot of WT and mutant FAM57B2 in HEK293 cells through stable and transient transfection. **A.** WT FAM57B2 and all mutants except mutant 2 and mutant 3 were successfully expressed via stable transfection; however, **B.** All mutants were able to be immunodetected when expressed transiently. Empty vector was used as a negative control.

# 3.3 24,25(OH)<sub>2</sub>D<sub>3</sub>-dependent Production of Lactosylceramide

To confirm the 24,25(OH)<sub>2</sub>D<sub>3</sub>-dependent production of lactosylceramide by FAM57B2, the enzymatic assay described in **Fig. 6** was performed with the WT and mutant FAM57B2 constructs. The standard assay was first performed in the presence of 1,25(OH)<sub>2</sub>D<sub>3</sub> or 24,25(OH)<sub>2</sub>D<sub>3</sub> to show specificity towards the 24,25(OH)<sub>2</sub>D<sub>3</sub> metabolite (**Fig. 15A**). In order to track the uptake of sphingosine, fluorescent NBD-sphingosine was used as substrate in the presence of 1,25(OH)<sub>2</sub>D<sub>3</sub> or 24,25(OH)<sub>2</sub>D<sub>3</sub>, which showed that NBD-sphingosine was not being uptaken by the enzyme (**Fig. 15B**). To determine if the reaction's success was dependent on concentrations of substrates, varying amounts of Fatty Acyl-CoA and sphingosine were provided

to transfected cells in the presence of 24,25(OH)<sub>2</sub>D<sub>3</sub> (positive condition) (**Fig. 15C**). It was subsequently attempted to vary the viscosity of the reaction buffer and to attempt the reaction in the presence of additional ions using NBD-sphingosine (**Fig. 15D**). The classical assay was also performed with the mutant versions of the protein in the presence of 24,25(OH)<sub>2</sub>D<sub>3</sub> (**Fig. 15E**). In all the assays, the results did not show production of LacCer in *Fam57b2*-overexpressing cells.

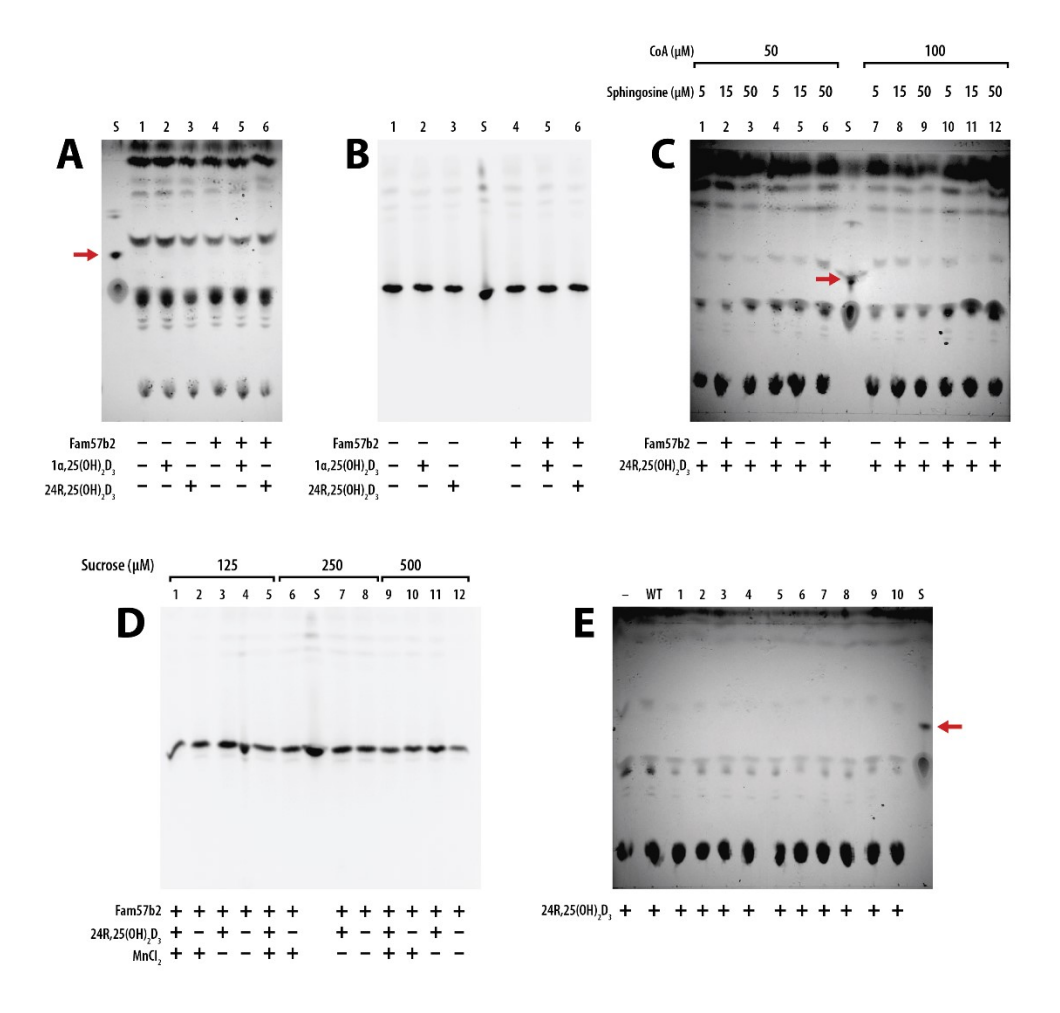


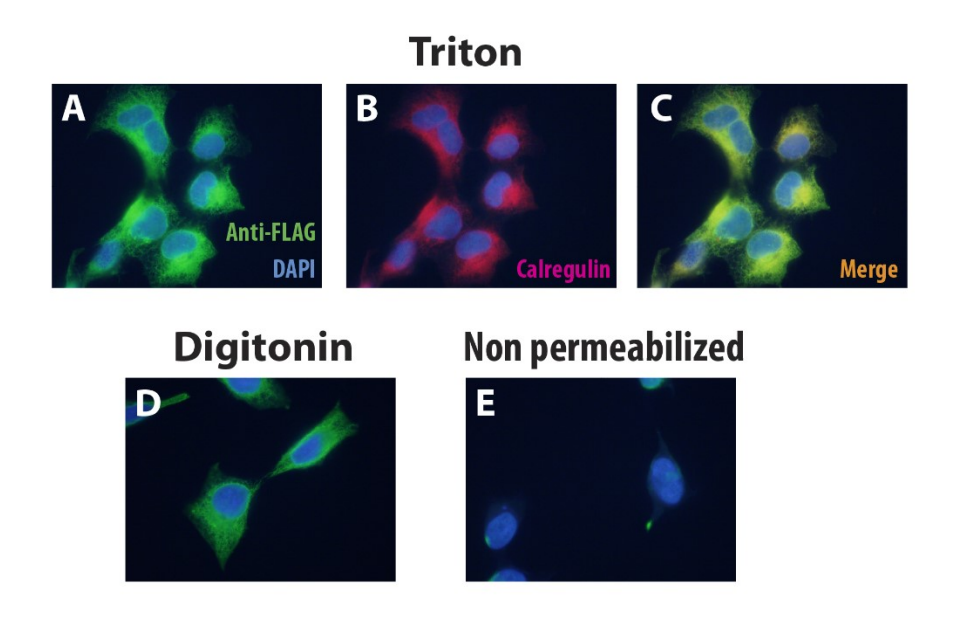
**Fig. 15**: Thin Layer Chromatography (TLC) results of lipid enzymatic assay with WT and mutant Fam57b2-overexpressing HEK293 cells didn't show 24,25(OH)<sub>2</sub>D<sub>3</sub>-dependent production of LacCer. **A.** Standard assay. **B.** Assay performed with fluorescent NBD-sphingosine. **C.** Assay varying the concentrations of Fatty Acyl-CoA and sphingosine. **D.** Assay performed varying the viscosity of the reaction buffer in the presence and absence of extra ions. **E.** Assay performed with WT and mutant forms of FAM57B2. A red arrow points at the LacCer standard.

Many parameters come into play when studying the enzymology of a relatively unknown protein. We believe that variables such as the level of expression of the protein, state of the cells, presence of interfering substances, stability of substrates and products, incubation time, saturation of the reaction; and technical parameters such as lipid migration by TLC in a new facility, could have come into play when studying this reaction. Production of LacCer in response to 24,25(OH)<sub>2</sub>D<sub>3</sub> in *Fam57b2*-overexpressing cells has been shown in previous data, but optimization of the parameters still has to be done. The structure-function analysis so far was not successful due to the challenging nature of this assay. Alternate strategies have been identified and are presented in the Discussion. To gain further insight of the structure-function relationships of the FAM57B2 protein, we constructed a new series of mutants that examined the subcellular localization and topology of FAM57B2.

## 3.4 Cellular Localization and Topology of FAM57B2

To confirm the localization of FAM57B2 to the ER, an anti-Calregulin antibody was used in conjunction with anti-FLAG antibody in C-terminus FLAG-tagged FAM57B2 transiently transfected HEK293 cells. Experiments were likewise performed in chondrogenic ATDC5 cells, yielding similar results (data not shown). Permeabilization via digitonin allows detection of epitopes found on the cytosolic compartment as it only permeabilizes the plasma membrane, while triton permeabilization allows detection of epitopes found anywhere as it permeabilizes all membranes. This permits discrimination between intraorganellar localization of the FLAG tag as opposed to extraorganellar. It can be observed that anti-FLAG (**Fig. 16A**) and anti-Calregulin, a luminal ER marker, (**Fig. 16B**) fluorescence images co-localize (**Fig. 16C**), indicating that FAM57B2 is found in the ER. Only anti-FLAG can be detected in digitonin permeabilized cells (**Fig. 16D**), confirming that digitonin permeabilization is specific to the plasma membrane, as anti-

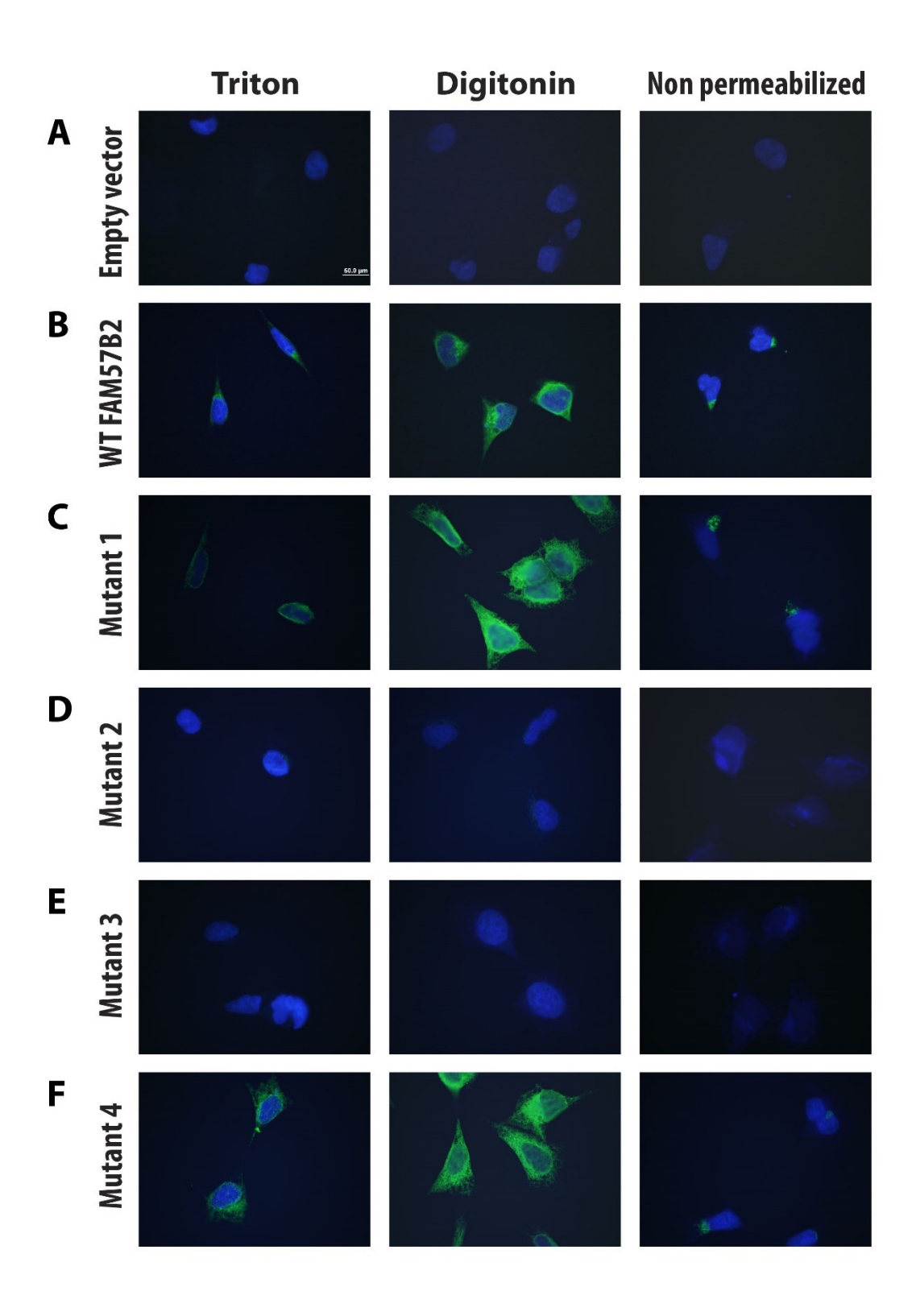
Calregulin can not be detected when only the plasma membrane is permeabilized. These results indicate that FAM57B2 is localized in the ER and its C-terminus is facing the cytosolic compartment.



**Fig. 16:** Immunofluorescence results of C-terminus FLAG-tagged FAM57B2. Immunodetection of triton permeabilized cells with anti-FLAG and anti-calregulin antibody (a luminal ER maker) shows that they both co-localize.

To confirm the expression of C-terminus FLAG-tagged WT and mutants of FAM57B2 in HEK293 cells, immunofluorescence studies were performed on transiently transfected cells using an anti-FLAG antibody. The FLAG tag was detected in both triton and digitonin permeabilized cells. Results indicate that in triton and digitonin permeabilized cells, WT FAM57B2 protein can be detected (**Fig. 17B**), as compared to empty vector transfected cells (**Fig. 17A**). Mutant 1 and mutants 4-10 (**Fig. 17 C, F-L**) can also be detected in both triton and digitonin permeabilization, indicating that these mutants are expressed and their C-terminus faces the cytosolic compartment. However, mutants 2 and 3 (**Fig. 17D and E**) can not be detected or are very poorly detected with

either permeabilization method. These mutants, which comprise of amino acids 6-15 are predicted to form part of a transmembrane domain of the protein.



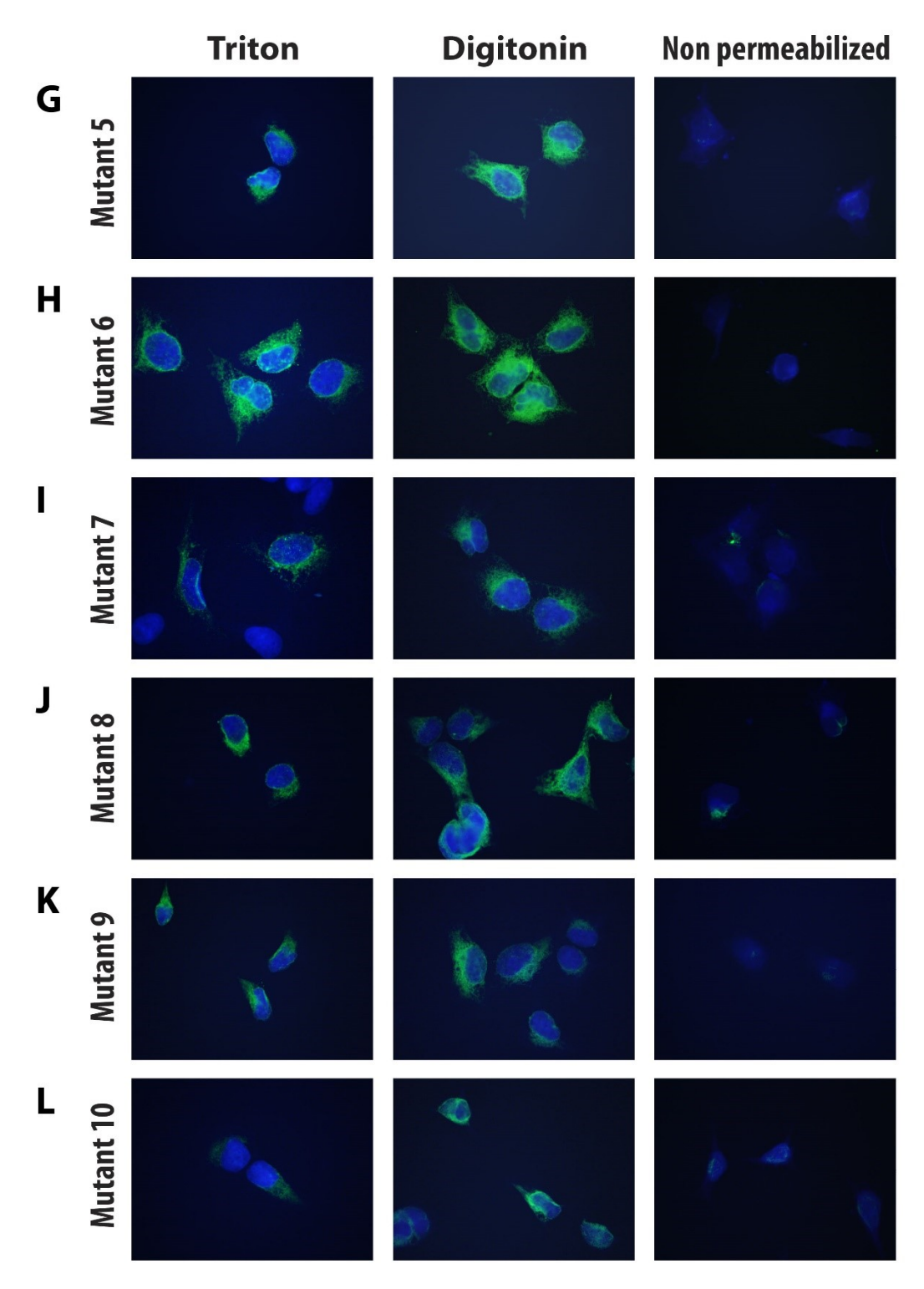


**Fig. 17:** Immunofluorescence results of C-terminus FLAG-tagged WT and mutant FAM57B2 after transient transfection. All constructs were able to be immunodetected and visualized in HEK293 cells except mutant 2 and mutant 3, suggesting that these mutant proteins are unstable and become degraded.

To analyze the topology of the FAM57B2 within the membrane, several topological and signal prediction softwares were used. TOPCONS [110, 111] and TMHMM [112] server predictions were compounded to observe overlapping predictions (**Fig. 18A**) and are shown in a schematic (**Fig. 18B**).

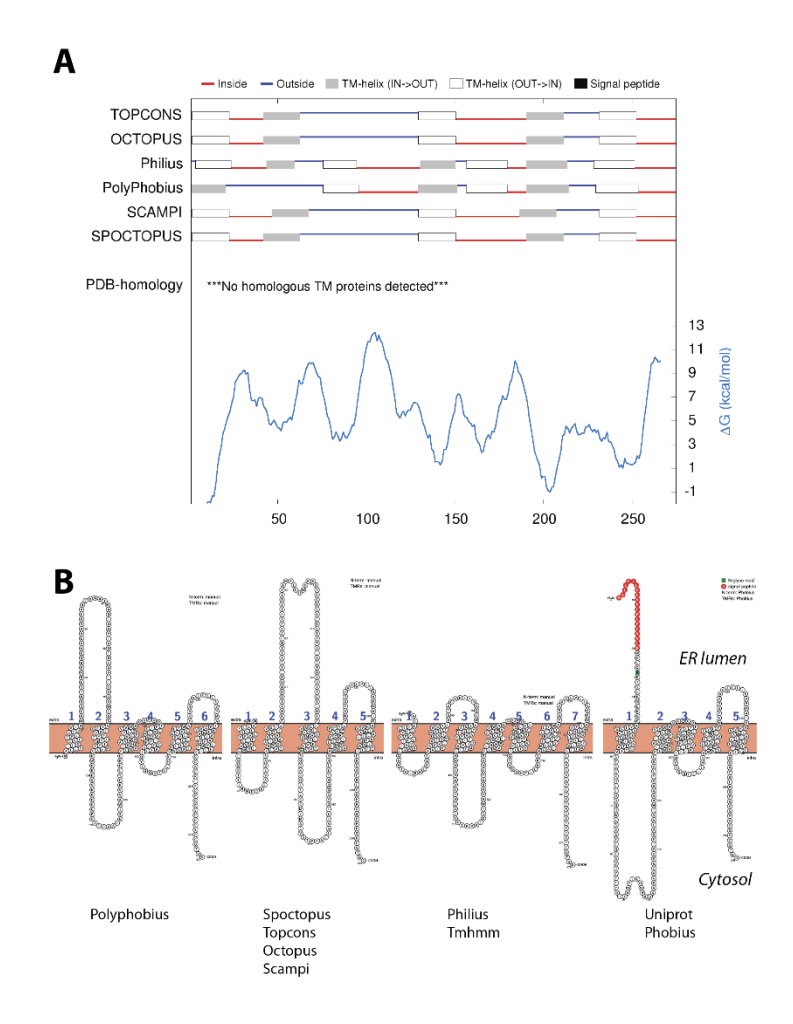


**Fig. 18**. Predictions of FAM57B2 topology within the membrane illustrated with Protter visualization program [113].

On this basis, to be able to discriminate and identify the most accurate prediction, with a specific focus on the N-terminal initial 50 amino acids, two HA tags were inserted into a protein loop at amino acid position 25 (AA25) and amino acid position 30 (AA30). An HA tag was also introduced into the N-terminus to observe its localization within the cell. Immunodetection of

digitonin permeabilized (**Fig. 19B**) and triton permeabilized (**Fig. 19A**) cells looks similar, meaning that the HA tags located at AA25 and AA30 are both facing the cytosolic side and are not intraorganellar. When looking at the IF of N-terminus HA-tagged FAM57B2, similar signals are observed, which we interpret to mean that the N-terminus of FAM57B2 faces the cytosolic space (**Fig. 20**).

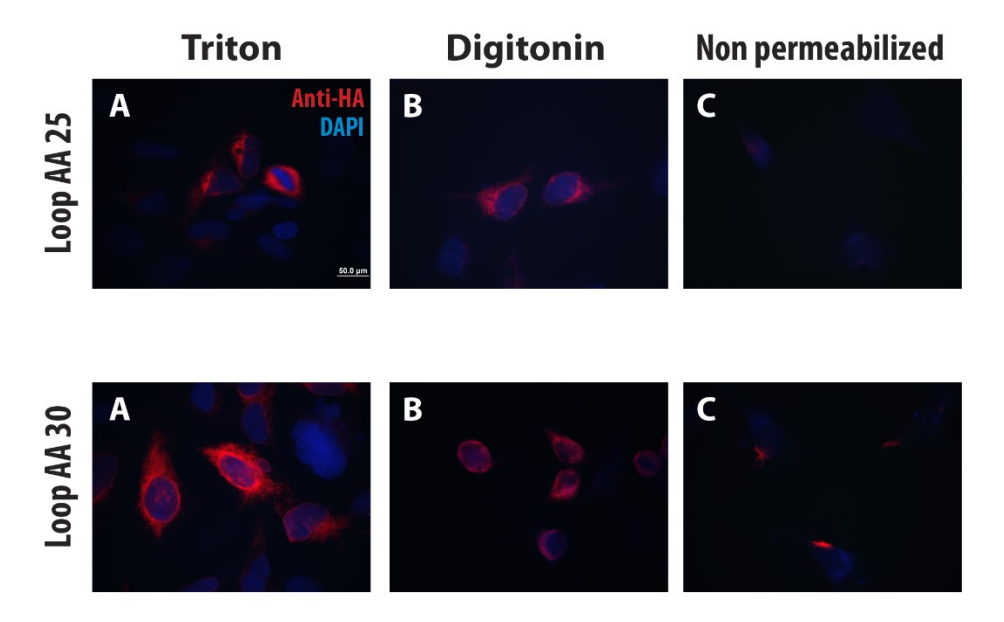


**Fig. 19:** Immunofluorescence results of HA-tagged FAM57B2 protein loop based on topological prediction. Immunodetection of digitonin permeabilized and triton permeabilized cells looks similar, meaning that the HA tags located at AA25 and AA30 are both facing the cytosolic side and are not intraorganellar.

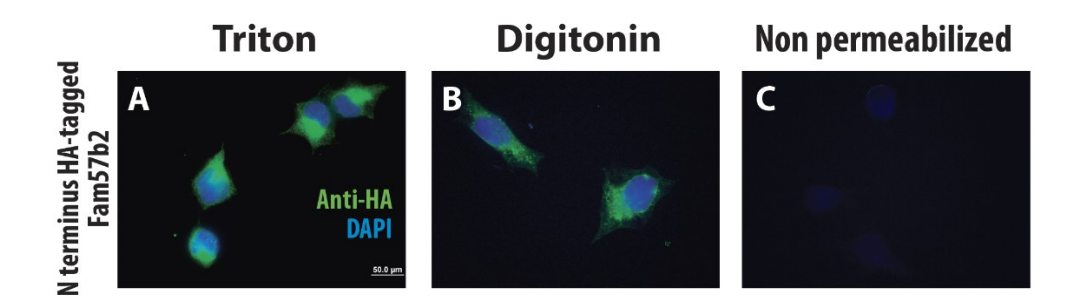


**Fig. 20:** Immunofluorescence results of N-terminus HA-tagged FAM57B2. Immunodetection of digitonin permeabilized (which only permeabilizes the cell membrane) and triton permeabilized (which permeabilizes all membranes) cells yields similar signals, which we interpret to mean that the N-terminus of Fam57b2 faces the cytosolic space.

Altogether, these results indicate that FAM57B2 localizes to the ER, where both termini face the cytosolic compartment of the cell, as well as amino acid positions 25 and 30. FAM57B2 mutated in amino acids 6-15 is undetected via immunofluorescence with anti-FLAG antibody as a protein that is either unstable or degraded seems to be produced. These results suggest an alternate protein topology that will be presented in the Discussion.

## 3.5 Fam57b2-overexpression in ATDC5 Cells

Because *Fam57b2* is expressed predominantly in skin and cartilage tissue, and the formation of a chondrocyte formed "soft callus" is a stage of the fracture repair process of bones, a differentiation assay with ATDC5 pre-chondrogenic cells was performed to ascertain the effect *Fam57b2* overexpression has in the cellular phenotype.

ATDC5 cells were infected with a *Fam57b2* overexpression vector and differentiated with ITS (insulin-transferrin-selenium) differentiating medium for 14 days. We measured a significant increase in the expression of both chondrogenic differentiation markers *Col2a1* and *Col10a1* in *Fam57b2*-overexpressing cells compared to the empty vector infected cells (**Fig. 21A**). Alcian blue staining shows a marked increase in the staining of glycosaminoglycans and chondrocyte nodules at D14 (**Fig. 21B**).

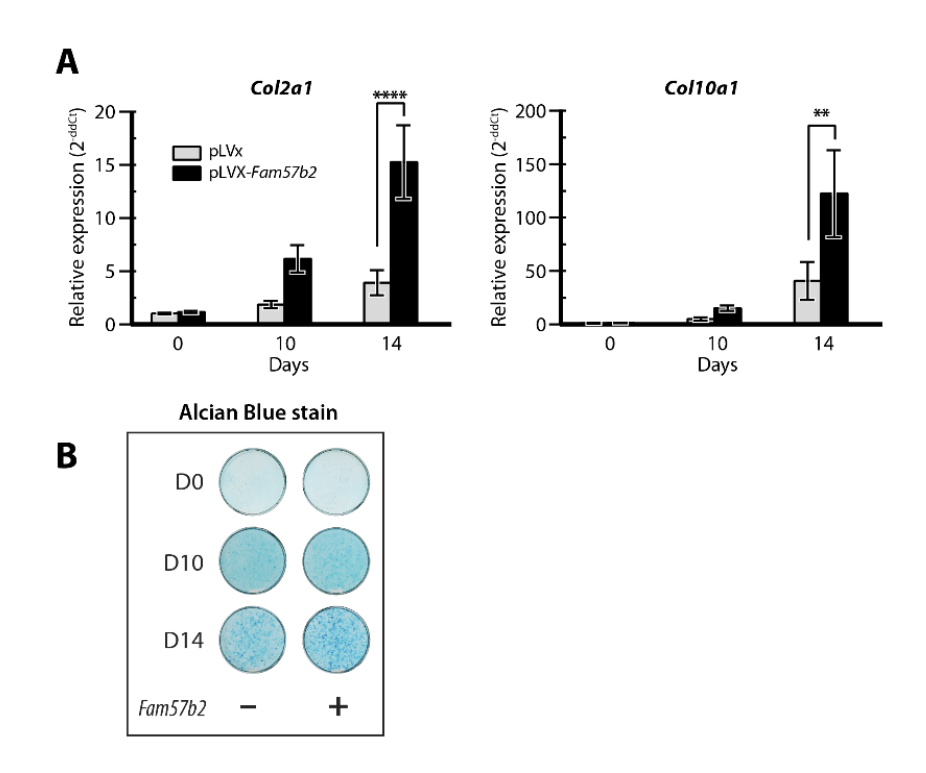


**Fig. 21:** Fam57b2-overexpression enhances expression of Col2a1 and Col10a1 differentiation markers in ATDC5 cells. **A.** Cells were differentiated for 10 and 14 days and chondrogenesis markers Col2a1 and Col10a1 and were used to assess successful differentiation via RT-qPCR. **B.** Alcian blue staining of glycosaminoglycans in differentiated empty vector and Fam57b2-overexpressing ATDC5 cells at D10 and D14.

# 3.6 Fam57b2-overexpression in ATDC5 Cells and 24,25(OH)<sub>2</sub>D<sub>3</sub> Effect on ATDC5 Differentiation

To assess if there is an effect of 24,25(OH)<sub>2</sub>D<sub>3</sub> treatment on differentiation of *Fam57b2*-overexpressing ATDC5 cells, cells were differentiated for 10 and 14 days in charcoal-stripped, vitamin D-depleted ITS differentiating medium. There was a significant increase in the expression of *Col2a1* marker at D10, which indicates that 24,25(OH)<sub>2</sub>D<sub>3</sub> treatment positively influences early stage differentiation of chondrocytes (**Fig. 22A**). Alcian blue staining of glycosaminoglycans in differentiated empty vector and *Fam57b2*-overexpressing ATDC5 cells upon 24,25(OH)<sub>2</sub>D<sub>3</sub> treatment at D10 and D14 was successful (**Fig. 22B**).

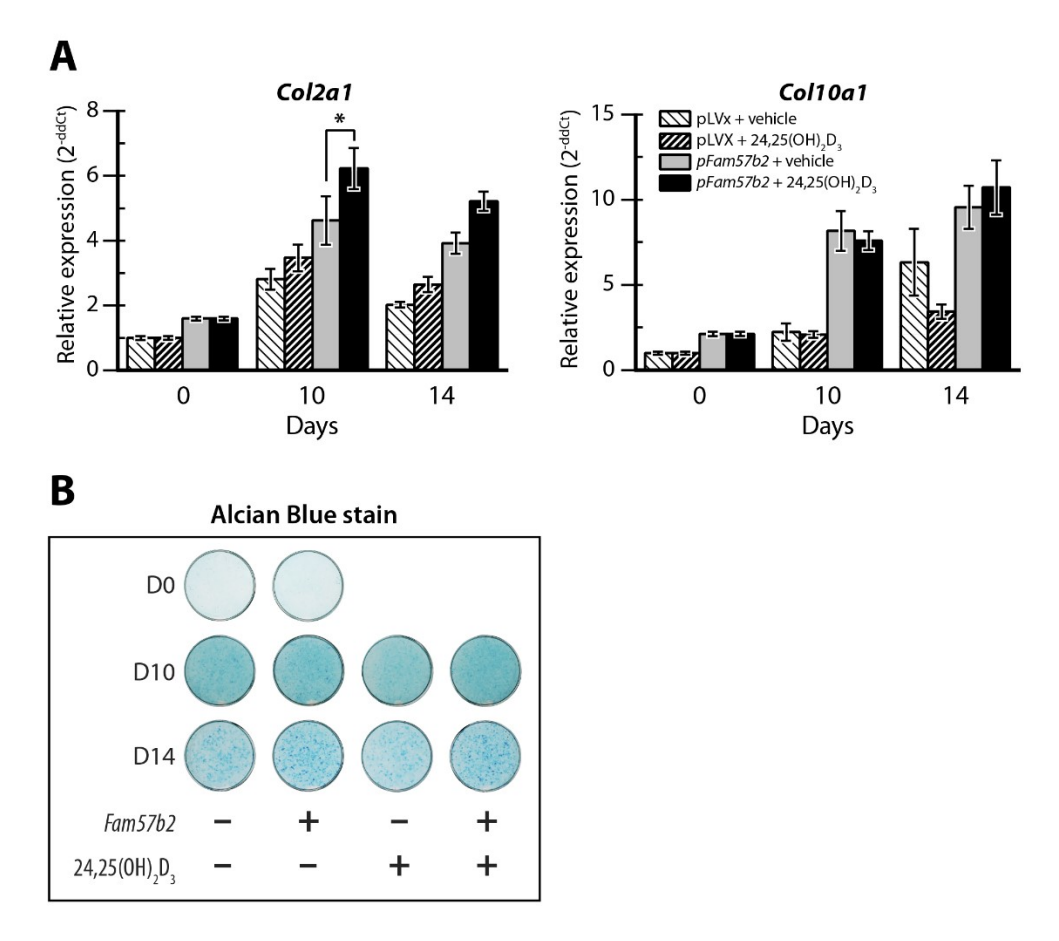


**Fig. 22:** 24,25(OH)<sub>2</sub>D<sub>3</sub> increases expression of *Col2a1* marker in differentiating *Fam57b2*-overexpressing cells. **A.** Cells were differentiated for 10 and 14 days with and without 24,25(OH)<sub>2</sub>D<sub>3</sub> treatment and chondrogenesis markers *Col2a1* and *Col10a1* and were used to assess successful differentiation via RT-qPCR. The experiment was performed 3 times and a representative result is shown here. **B.** Alcian blue staining of glycosaminoglycans in differentiated empty vector and *Fam57b2*-overexpressing ATDC5 cells with and without 24,25(OH)<sub>2</sub>D<sub>3</sub> treatment.

# 3.7 Lactosylceramide Effect on Cell Differentiation, Proliferation, Adhesion, Migration and Apoptosis

As we have shown, LacCer is produced upon incubation of FAM57B2 with 24,25(OH)<sub>2</sub>D<sub>3</sub>. In order to determine what effect LacCer has on cellular functions of chondrocytes, assays with ATDC5 pre-chondrogenic cells were performed. In order to identify if LacCer plays a role in chondrogenesis, ATDC5 cells were differentiated with LacCer alone, differentiation-inducing ITS, and combined treatment of LacCer with ITS. A time course of day 3, day 7, day 10 and day

14 showed that LacCer alone didn't increase the expression of early stage chondrogenic differentiation gene marker *Col2a1*, or late stage markers *Col10a1* and *Ihh*. However, LacCer was able to potentiate the effect that ITS has on the expression of the hypertrophic chondrocyte marker *Col10a1* at D10 and D14 of differentiation (**Fig. 23A**). Alcian blue staining was used to reveal staining of glycosaminoglycans at D14, and an increase in the staining of ITS + LacCer compared to ITS treated cells was observed (**Fig. 23B**). These results show that LacCer plays a role in chondrocyte differentiation, where it enhances differentiation of chondrocytes under induction of differentiation with insulin.

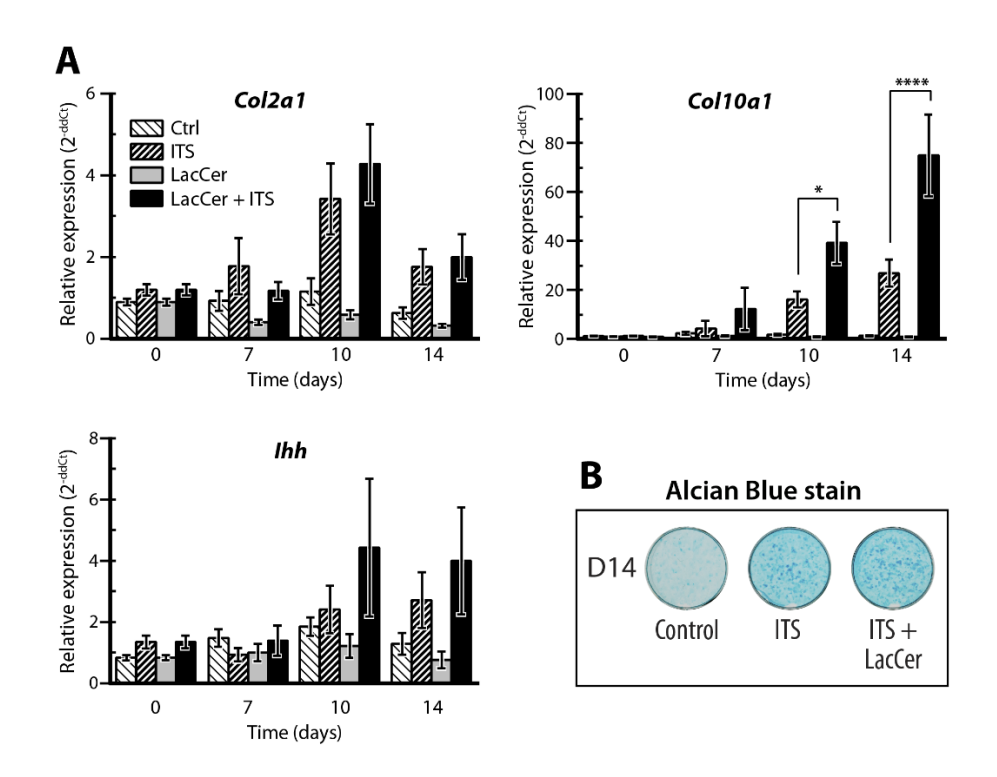


**Fig. 23:** LacCer potentiates the effect Insulin-Transferrin-Selenium (ITS) has in the expression of *Col10a1* differentiation marker in ATDC5 cells. **A.** Cells were differentiated for 7, 10 and 14 days and chondrogenesis markers *Col2a1*, *Col10a1* and *Ihh* were used to assess differentiation via RT-qPCR. **B.** Alcian blue staining of glycosaminoglycans in differentiated ATDC5 cells at D14.

In order to understand if the potentiation of differentiation was specific to induction with insulin, differentiation was performed with Ascorbic Acid and LacCer compound treatment, where

it was observed that LacCer was not able to potentiate the effect produced by ascorbic acid on the expression of chondrogenic markers, but rather seemed to have a negative effect on them (**Fig. 24**), suggesting that the mechanism of induction of differentiation is affected in different ways by this lipid. This likely happens as insulin induces differentiation through its receptor while ascorbic acid does so by acting as a cofactor involved in chondrogenesis.

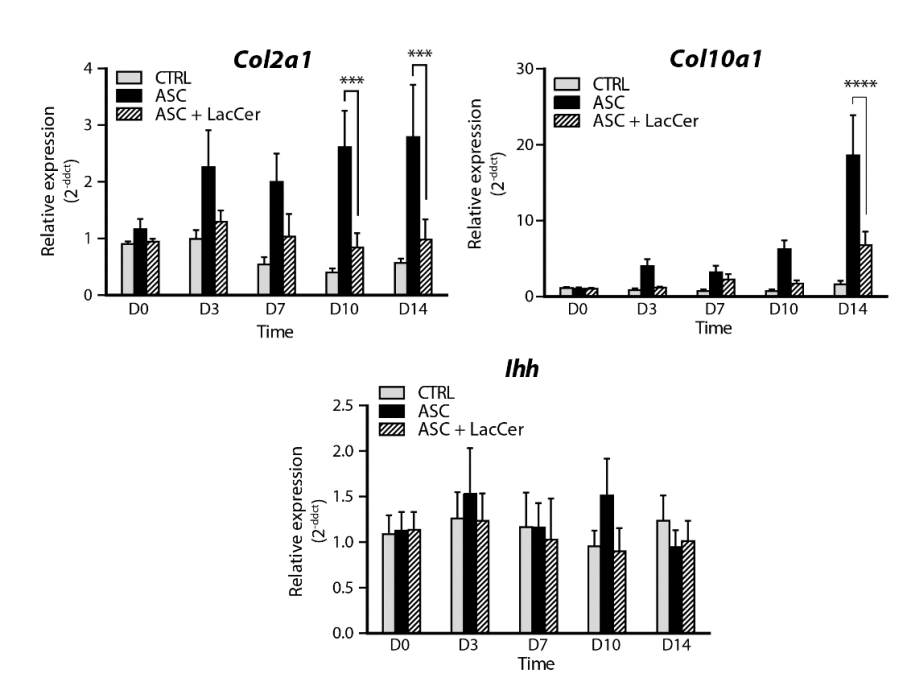


Fig. 24: LacCer has a negative effect on differentiation of ATDC5 cells with ascorbic acid.

LacCer has been shown to act as a mitogenic agent to affect proliferation of aortic smooth muscle cells [93]. To determine if proliferation of chondrocytes is affected by LacCer, a proliferation assay was performed with fluorescently labelled nucleoside analog EdU (5-ethynyl-2'-deoxyuridine). At 72 hours, there can already be observed a downwards trend in proliferation upon LacCer treatment, and upon 96 hours, there's a marked dosage-dependent decrease in proliferation of ATDC5 cells upon incubation with LacCer (Fig. 25). This leads us to conclude that LacCer reduces proliferation of chondrocytes upon prolonged incubation with it.

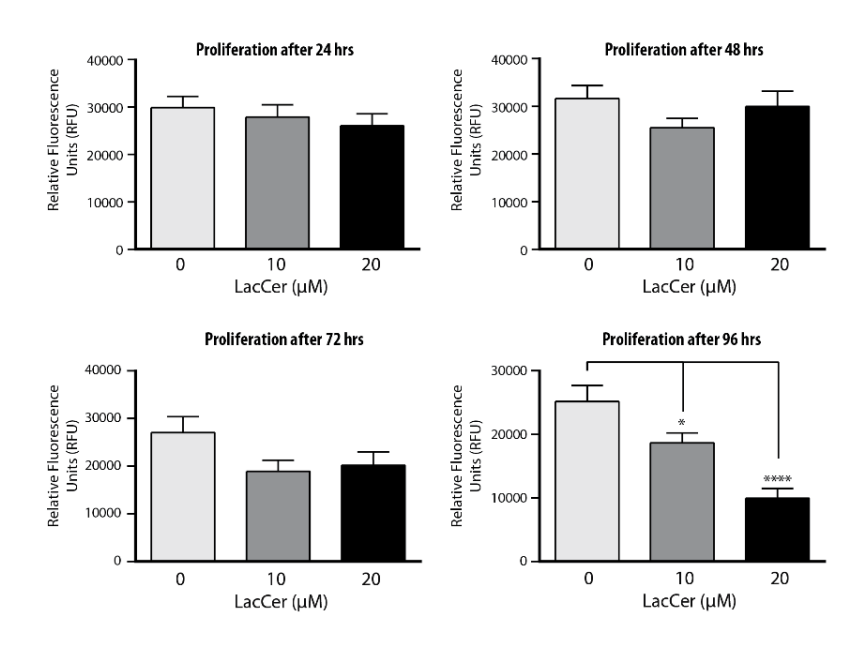


Fig. 25: LacCer dosage-dependently decreases proliferation of ATDC5 cells.

To assay if the decrease in proliferation of ATDC5 cells after exposure to LacCer for 96 hours was due to apoptosis of these cells, a colorimetric Caspase 3-activity assay was performed. No increase in Caspase-3 activity was observed upon treatment with LacCer for 72 and 96 hrs (**Fig. 26**). Therefore, we conclude that although there is a decrease in proliferation of ATDC5 cells upon incubation with LacCer, this doesn't happen due to the programmed cell death but rather through some other mechanism.

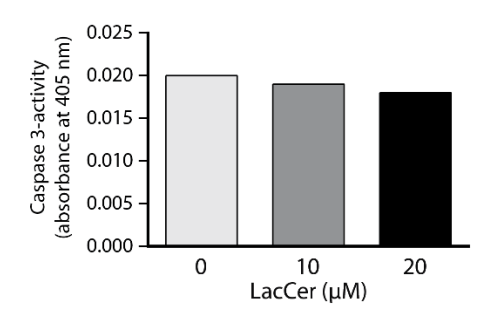
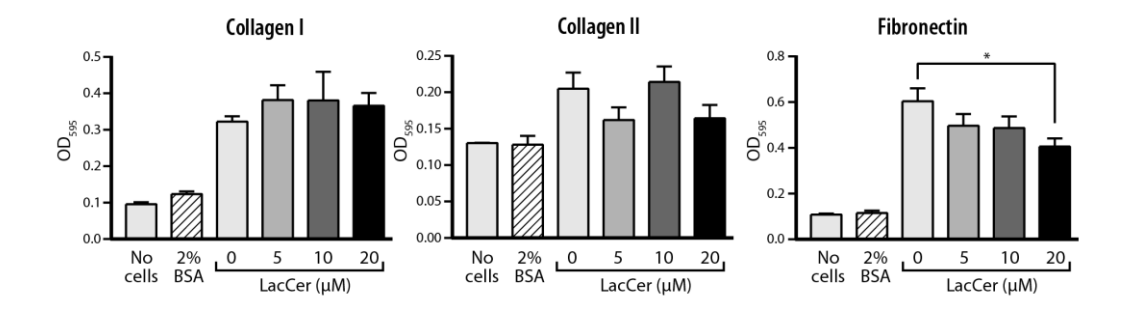


Fig. 26: LacCer has no effect on Caspase-3 activity to induce apoptosis of ATDC5 cells.

LacCer was shown to modulate adhesion of neutrophils and monocytes to endothelial cells in other studies [94, 95]. To assay if the cell adhesion capabilities of ATDC5 cells were affected after LacCer treatment, 96-well plates coated with different substrata such as collagen I, collagen II and fibronectin. Substrata were used to mimic the biological context in which chondrocyte cells may be found, where collagen I is found predominantly in bone tissue, while collagen II is found in cartilage tissue and fribronectin is one of the earliest ECM proteins synthetized by osteoblasts [114], expecting to see increased adhesion to ECM proteins found in the callus during bone fracture repair. Preincubation with increasing concentrations of LacCer, followed by trypsinisation and treatment with LacCer showed that LacCer doesn't seem to increase the adherence capacity of ATDC5 cells under any concentration in Collagen I and II substrata; nonetheless, results showed that 20 µM treatment with LacCer significantly decreases the capacity of ATDC5 cells to attach to a Fibronectin substratum (Fig. 27). These data lead us to conclude that LacCer influences proteins and mechanisms required in adhesion of chondrocytes to the ECM, particularly to fibronectin, reducing adhesion; while no conclusions can be made from attachment to collagen fibers as cells didn't seem to attach well to these substrata.



**Fig. 27**: Adhesion assay performed on Collagen I, II and Fibronectin substrata showing that there is a negative trend in the ability of ATDC5 cells to adhere to fibronectin with increasing concentrations of LacCer. 2% BSA was used as a negative control.

To study if LacCer has an effect on migration properties of ATDC5 cells, a scratch assay was used. ATDC5 cells were grown in a monolayer to 90-100% confluency, and then this monolayer was "scratched". Incubation of cells with LacCer for 16-20 hrs showed no effect on the amount of migration to the wounded area (Fig. 28). Varying concentrations of serum, ranging from 2% to 0.5% FBS, were used to ensure that the effects observed were likely due to migration, rather than cell proliferation. We can conclude with high certainty that chondrocytes' abilities to migrate to a wounded area are not influenced by LacCer. Although this assay yielded negative results, a more sophisticated approach could we used to compliment these results, such as transwell migration assay.

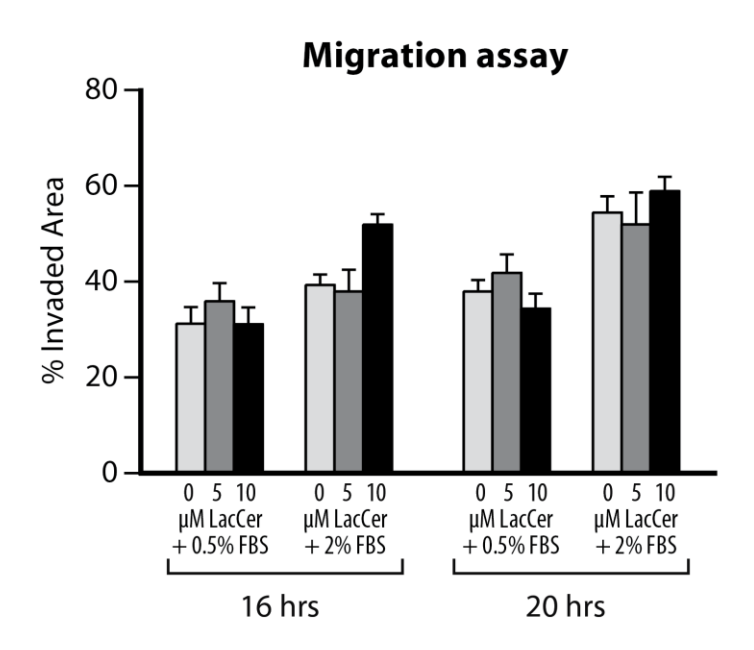


Fig. 28: No effect of LacCer on the percent invasion into a wounded area.

## 3.8 Signal Transduction

Several studies have shown that treatment with LacCer leads to the production of Reactive Oxygen Species (ROS) after treatment in fibroblasts and cardiomyocytes [91, 115, 116]. In turn, ROS production has been shown to affect proteins upstream of MAPK p42/44 [91, 115, 117]. In

addition, ROS production has been proved to induce chondrocyte hypertrophy in ATDC5 cells [117, 118]. To assay if exposure to LacCer promoted an increase of ROS production in chondrogenic cells, ATDC5 cells were incubated with a fluorescent permeable probe for ROS, DCFDA (2',7'-dichlorofluorescin diacetate), in phenol red free DMEM:F12 and exposed to increasing concentrations of LacCer (10 μM, 20 μM and 50 μM). A time course experiment, ranging from 5 min to 8 hrs showed that there is no effect of LacCer on ROS production in these cells (Fig. 29). A positive signal can be detected after 8 hours of treatment with LacCer, but this effect is also found in the DMSO vehicle condition, indicating that the effect is not specific to LacCer. Cells exposed to H<sub>2</sub>O<sub>2</sub> were used as a positive control. These results lead us to conclude that LacCer doesn't lead to accumulation of ROS in chondrocytes after treatment with this ceramide, and DMSO is able to induce detection of ROS after long time treatment.

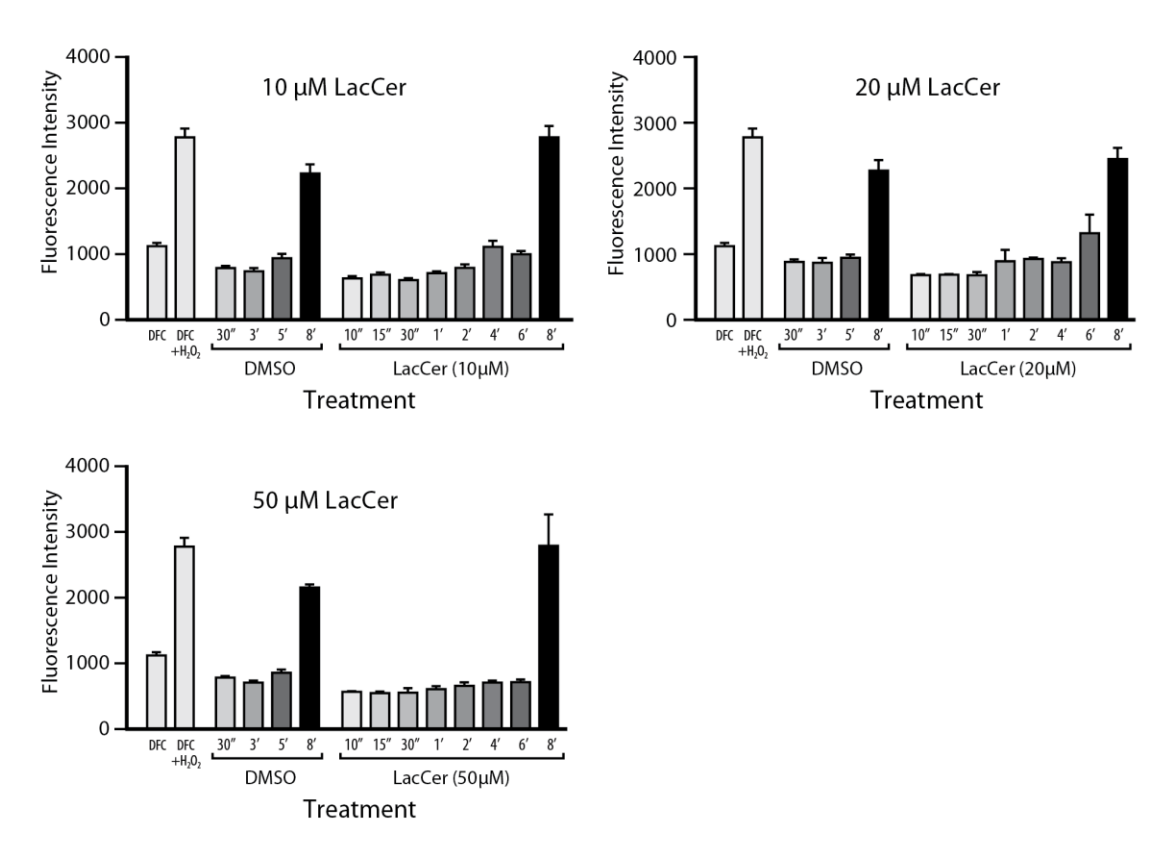
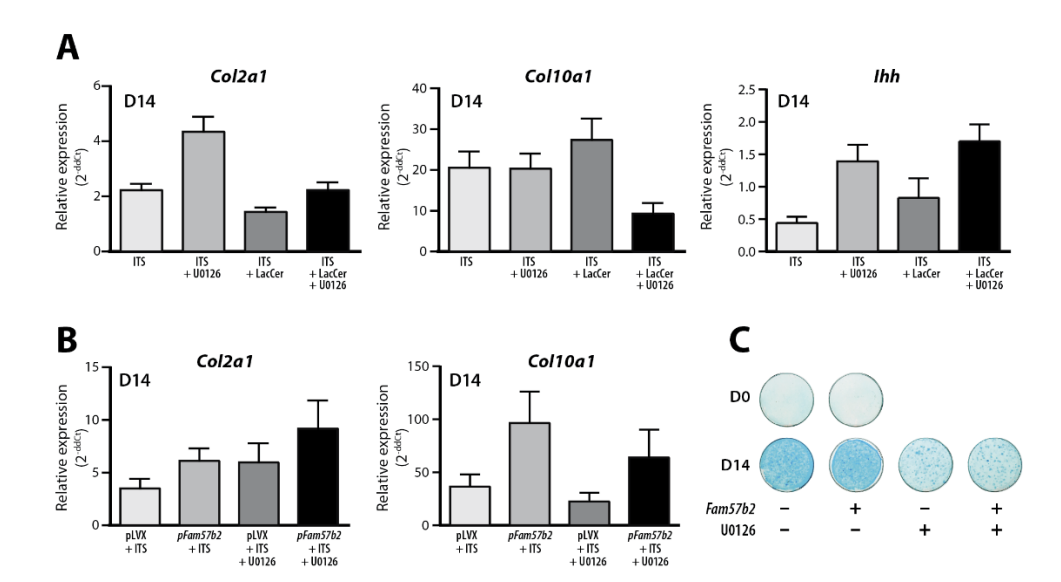


Fig. 29: Increasing concentrations of LacCer have no effect on the accumulation of oxygen radicals in ATDC5 cells.

It has been shown by several authors [119-121] that the signaling pathway mainly affected by insulin binding in ATDC5 cells is the MAPK p42/44 signaling pathway. Specifically, a difference can be observed at the level of Erk phosphorylation (P-Erk), where it is greatly increased in insulin-treated differentiating cells. It has also been observed that LacCer influences MAPK p42/44 in aortic smooth muscle cells [93] and osteoclasts [122]. Therefore, the MAPK p42/44 pathway was assessed with a MEK (MAPK/ERK Kinase) kinase inhibitor to observe if the potentiation of differentiation by LacCer and the enhancement of chondrogenesis were due to this pathway's activation. To assess if the MAPK pathway is involved in the potentiation of differentiation by LacCer observed in ATDC5 cells, MEK kinase inhibitor U0126 was administered during differentiation with ITS for 14 days (Fig. 30A). Although initially results seemed to indicate the involvement of this pathway in the differentiation, several repetitions indicated that results were highly variable. Consequently, the inhibitor was instead administered to Fam57b2-overexpressing cells differentiated until day 14 with ITS to observe if MAPK p42/44 pathway involvement could be observed more clearly in this case (Fig. 30B). Unfortunately, results were likewise highly variable and hard to conclude something from. However, Alcian blue staining showed decreased staining of glycosaminoglycans in cells treated with the inhibitor (Fig. **30C**), indicating that MEK inhibition does affect chondrogenesis.



**Fig. 30:** MEK kinase inhibitor U0126 treatment to assess the MAPK pathway involvement on ATDC5 differentiation under LacCer treatment and *Fam57b2*-overexpression **A.** ATDC5 cells were differentiated for 14 days with ITS or ITS+LacCer with and without U0126 treatment and chondrogenesis markers *Col2a1*, *Col10a1* and *Ihh* were assessed via RT-qPCR. **B.** *Fam57b2*-overexpressing ATDC5 cells were differentiated with ITS with and without U0126 inhibitor treatment. **C.** Alcian blue staining of glycosaminoglycans in differentiated empty vector and *Fam57b2*-overexpressing ATDC5 cells at D14.

## Chapter IV: Discussion

Understanding the role that 24,25(OH)<sub>2</sub>D<sub>3</sub> plays in in bone health has been a topic of great interest and continuous debate. Initially, it was believed that 24,25(OH)<sub>2</sub>D<sub>3</sub> was solely a degradation product from Vitamin D catabolism [123, 124], but further research has suggested that it plays a role in chondrocyte health and fracture healing in chicks [74]. Compound data from the literature showing the increase of CYP24A1 expression and its product during fracture healing in chicken [73], as well as <sup>3</sup>[H] 24,25(OH)<sub>2</sub>D<sub>3</sub> accumulation in the callus on membrane fractions [75] and its binding response in resting cartilage chondrocytes [68] hints at a role in bone fracture repair, which was studied in deeper detail in our laboratory.

We set out to examine the role of 24,25(OH)<sub>2</sub>D<sub>3</sub> in a mammalian fracture healing. To do this, our laboratory developed a *Cyp24a1*-deficient mouse strain [58], from which *Fam57b* was cloned. This mouse strain presents a lethal hypercalcemia phenotype in half of the progeny while the surviving half doesn't present any phenotype other than a delay in fracture repair, characterized by lower callus volume and decreased mineralization in the callus. The fact that half of the progeny from this mouse strain die from excess of 1,25(OH)<sub>2</sub>D<sub>3</sub> that can't be cleared form the body and not due to the lack of 24,25(OH)<sub>2</sub>D<sub>3</sub>, indicated that 24,25(OH)<sub>2</sub>D<sub>3</sub> is not vital for mouse survival. Exogenous administration of 24,25(OH)<sub>2</sub>D<sub>3</sub> during fracture healing of these mice lead to the rescue of the reduced biomechanical properties of the callus. This data suggests that 24,25(OH)<sub>2</sub>D<sub>3</sub> acts to optimize fracture repair of bones but is not an essential metabolite without which fracture repair will not occur.

Several researchers have been on the quest to identify a specific receptor for 24,25(OH)<sub>2</sub>D<sub>3</sub>; however, its characterization has not been possible thus far. We used the *Cyp24a1* KO mouse strain to identify *Fam57b* as a gene upregulated in the fracture callus of these mice, which we hypothesize to mean that it is upregulated to compensate for low circulating 24,25(OH)<sub>2</sub>D<sub>3</sub>.

FAM57B2 has been partially characterized in our laboratory, where it has been observed that it is a membrane protein that binds  $24,25(OH)_2D_3$  in a specific and saturable manner. This isoform is also mostly expressed in the skin and in cartilage, which is not surprising, as ceramides form part of the stratum corneum, the layer of the epidermis that serves as a barrier layer against water loss. However, its expression in cartilage hints at a possible function in chondrocyte regulation. Only one paper has described the function of Fam57b2 so far, showing that it decreases adipocyte differentiation through the production of ceramides, therefore regulating adipogenesis [77].

During the course of this project, we have been able to express and detect WT FAM57B2 through the attachment of a FLAG tag to the C-terminus of the protein. WT FAM57B2 could successfully be immunodetected via western blot and immunofluorescence in transient and stable cell transfections, indicating that the protein is stable and well expressed in mammalian cells. We then set to create 10 mutants for FAM57B2 to identify its binding site for 24,25(OH)<sub>2</sub>D<sub>3</sub>. We hypothesize this binding site must be found within the first 50 amino acids in the N-terminus, because this portion is the only one that differs between the 3 isoforms and only isoform 2 was shown to bind specifically to 24,25(OH)<sub>2</sub>D<sub>3</sub> through radioactive binding assays. Stable transfection of the created mutants showed that all but two mutants could be expressed and detected; nonetheless, through transient transfection we could observe that all mutant forms of FAM57B2 can be detected via western blot.

When attempting to localize FAM57B2 and its mutant forms, IF following transient transfection didn't allow to detect the same two mutants that could not be detected in the stable FAM57B2 mutant cell lines. These mutants (Mutant 2 and Mutant 3 of **Fig. 13**), which comprise of amino acids 6-15 were predicted to form part of a transmembrane domain of the protein. Probably, we were unable to detect these mutants because a change in the amino acid composition

of these amino acids affected its stability within the membrane and caused the proteins to become degraded. The main topological prediction softwares used, TMHMM and TOPCONS, allowed us to obtain an approximation of the conformation of FAM57B2 within the membrane and predict the probability that certain residues will form part of the binding site for 24,25(OH)<sub>2</sub>D<sub>3</sub> or will be structurally important for stability in the membrane. TMHMM works by calculating the probability that a residue sits inside, outside or in the helix along with all other possible scenarios through the model; while TOPCONS compiles predictions from several transmembrane topology and signal peptide servers and creates a consensus prediction with as high as 83% accuracy [110, 111]. Experimentally, we were able to confirm that FAM57B2 localizes to the Endoplasmic Reticulum, that both termini of this protein are cytosolic, and that amino acids at position 25 and 30 also face the cytosol. We have observed that the experimental results are conflicting with the prediction models, where none of the models fully agrees with the results obtained. In addition, we interpret the inability to express and visualize mutants 2 and 3 as a gain of instability when these amino acids are mutated, possibly because these residues are an important transmembrane region and they may contain a signal sequence for ER localization. On this basis, a new topological prediction was created using Protter (Fig. 31).

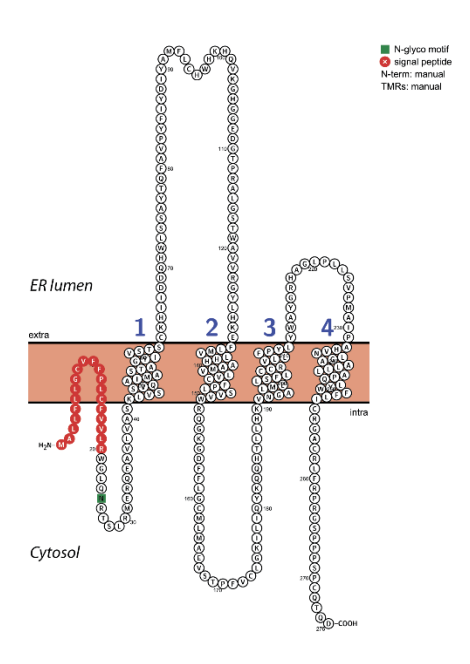


**Fig. 31**. Protein prediction devised from experimental and predicted data illustrated with Protter visualization program. [113]

Due to the inability to test the functionality of the WT and mutant *Fam57b2* constructs via enzymatic assay followed by TLC, we decided to follow other strategies to determine the site of binding to 24,25(OH)<sub>2</sub>D<sub>3</sub> in FAM57B2. We set to purify the FAM57B2 protein in order to perform Surface Plasmon Resonance (SPR), a technology that works via immobilization of a ligand on the surface of a dextran coated chip. Polarized light gets passed through a prism, which hits an electrically conducting surface at the opposing surface of the chip (**Fig. 32A**). Plasmons or electron charge density waves are generated, which reduce the intensity of reflected light and change the reflection angle in proportion to the mass on the sensor surface when an analyte binds to the ligand (**Fig. 32B**). The changes in association and dissociation of the analyte to the ligand can be measured and a curve can be created (**Fig. 32C**) [125].

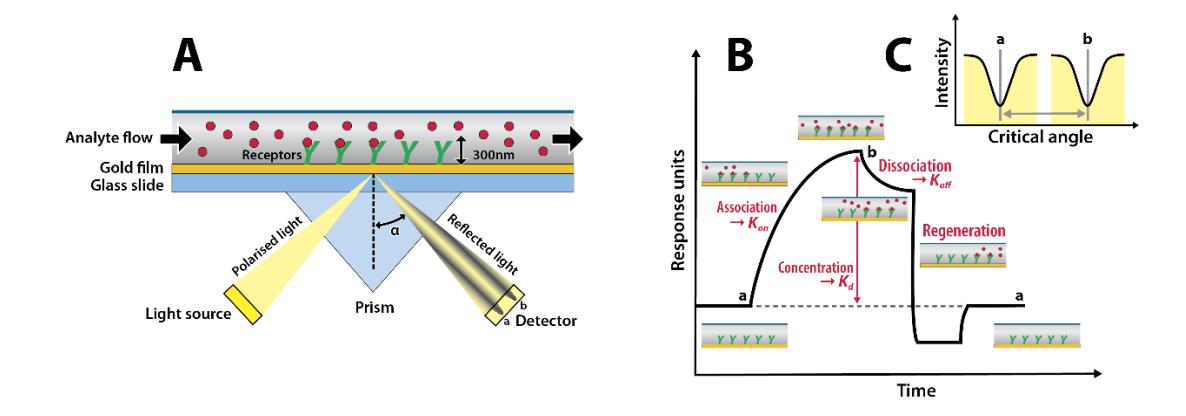


**Fig. 32:** Surface Plasmon Resonance is a technique where a light source is passed through a prism, reflecting on the backside of a gold sensor chip where the FAM57B2 protein is immobilized, and into a detector. An interaction can be detected when there's a change in the reflectivity of the light (**C**) due to a binding interaction (**A**) and an association/dissociation curve (**B**) can be made to quantify it. Figure taken from Patching, S.G. (2014) [126], with permission.

Initially, protein purification by creating a FAM57B2-Intein/Chitin binding domain fusion protein was attempted. Proteins were extracted from membrane and cytosolic extracts to increase the likelihood of purifying sufficient quantities of fusion protein and increase the specificity of purification. Proteins were denatured at 46 °C to avoid membrane protein aggregation and at 100 °C. The products of the purification were migrated on and SDS-PAGE and stained with Coomasie blue (Fig. 33A) and Silver Stain (Fig. 33B). Results showed that although the protein can be detected via Western blot using Anti-FLAG antibody (Fig. 33A), the protein purified in the cytosolic fraction does not seem to have been purified in great quantities as observed by the lack of a thick band at ~31 kDa and it also seems to have been purified with other non-specific proteins, which makes it a poor tool for SPR binding studies. The membrane fractions could not be detected via either kind of gel stain and are not sufficient to perform SPR either.

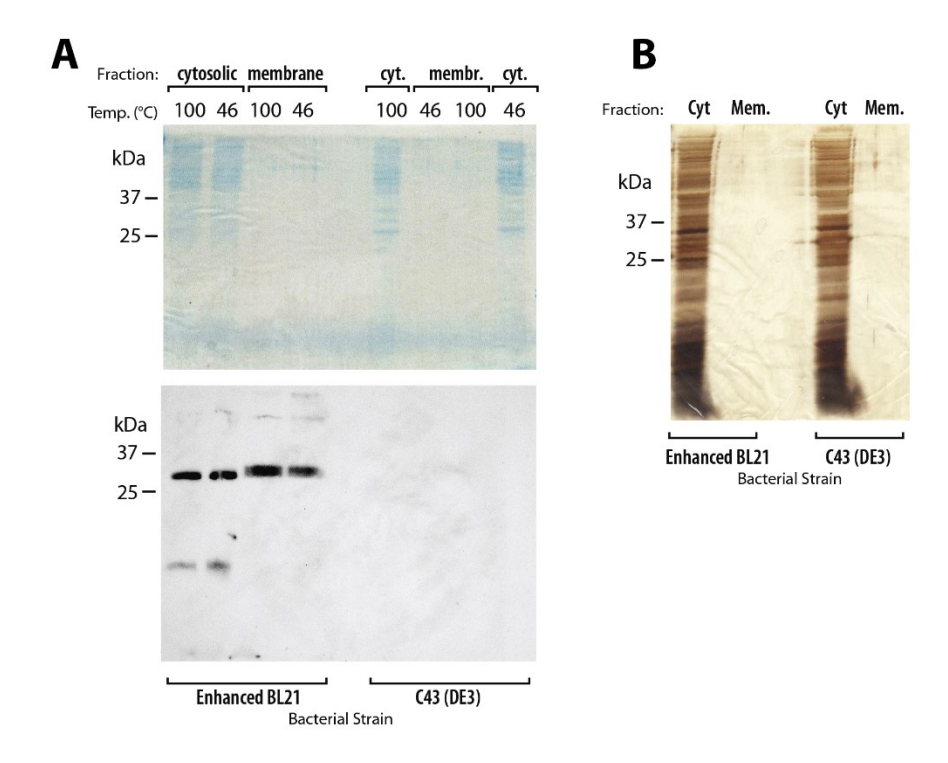


**Fig. 33:** Fam57b2-Intein/Chitin binding domain fusion protein. **A.** Coomasie blue stain and Western blot and **B.** Silver Stain of fusion protein from cytosolic and membrane extracts expressed in Enhanced BL21 and C43 bacteria.

We therefore attempted commercial purification using other tags proven to be successful for purification of membrane proteins: Trx and GST affinity tags (**Fig. 34A**). Results from fusion protein affinity purifications with these tags showed that, although extracts can be detected via Western Blot, elution of the purified product was unsuccessful using either tag (**Fig. 34B**).

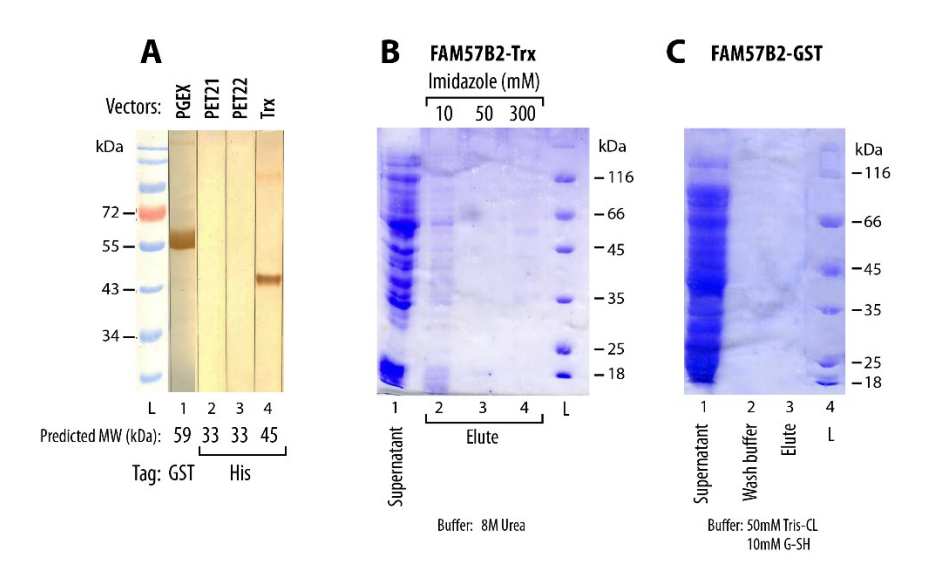


**Fig. 34:** FAM57B2-Trx and FAM57B2-GST fusion proteins. **A.** Western blot of FAM57B2-Trx and FAM57B2-GST detected with anti-His and anti-GST antibodies. **B.** Coomasie blue stain of supernatant and elute of FAM57B2-Trx and **C.** FAM57B2-GST fusion proteins.

FAM57B2 is a protein that is difficult to purify since it contains ~5 transmembrane regions. Being an integral membrane protein, it requires high concentrations of detergents to extract and solubilize the protein from its natural environment. Membrane proteins also often tend to form aggregates when they are being purified or may require cholesterol-disrupting chemicals like nystatin or filipin to be solubilized more efficiently [127]. Given the fact that bacteria were used to express the fusion proteins, it is possible that forced expression of membrane proteins oversaturated the transport capacity of the bacteria leading the proteins to be accumulated in inclusion bodies (aggregates of partially folded over-expressed proteins). Another possible reason why purification in bacteria was unsuccessful is that some bacteria lack some of the post-translational modification machinery that is commonly found in more complex organisms, and these post-translational modifications might be necessary for the protein's stability [128, 129]. Protein purification would likely be more successful in an insect or mammalian system, but likely more complicated.

On the other hand, uncovering the mode of interaction of 24,25(OH)<sub>2</sub>D<sub>3</sub> with FAM57B2 was a major step into hypothesizing what the protein does and how it influences bone fracture repair. Our lab was able to produce an enzymatic assay showing 24,25(OH)<sub>2</sub>D<sub>3</sub>-dependent production of lactosylceramide upon incubation of *Fam57b2*-overexpressing HEK293 cell extracts in a HEPES-sucrose buffer with a sphingosine and a C18 fatty-acyl CoA substrate (**Fig.** 6). This assay could further be used to clearly and visually demonstrate the production of the desired product in all the FAM57B2 mutants in which binding is non-affected and the lack of a product when 24,25(OH)<sub>2</sub>D<sub>3</sub> binding has been impaired. The assay was performed and troubleshooted, but the exact conditions for optimal enzymatic activity are yet to be fully established. We have observed that a pH close to 7.6 and KCl salt addition to the buffer are favourable to the reaction. We will perform the enzymatic assay on cell extracts of FAM57B2 mutants to identify the residues necessary for interaction once the assay is well established.

Identifying LacCer as the product of FAM57B2 upon interaction with 24,25(OH)<sub>2</sub>D<sub>3</sub>, has allowed us to study its role as a signalling molecule to regulate chondrocyte activity in fracture repair. LacCer was shown to have an effect in several regulatory functions of chondrocytes through assays performed in pre-chondrogenic ATDC5 cells. Although LacCer didn't affect the migration properties of chondrocytes to a wounded area, we were able to observe reduced adhesion of ATDC5 to a fibronectin substratum and the inability of these cells to attach to Collagen I and II substrata under LacCer incubation. Albeit production of fibronectin to produce ECM rapidly after injury by neutrophils and macrophages is very important during fracture repair, as stated by Bastian et al. (2016), our results suggest that chondrocytes don't promote further chondrogenic cellular adhesion in the stage in which production of LacCer has become initiated in the callus [130].

LacCer supplementation was shown to decrease chondrocyte proliferation dosedependently upon incubation for 96 hours. We confirmed that the reduction in proliferation didn't occur due to induction of apoptosis upon LacCer treatment, but that it must be occurring though an independent mechanism. LacCer was also shown to potentiate differentiation under insulin induction. Because a switch in the regulatory mechanisms of the cell has to happen, cells must stop proliferating in order to begin and maintain differentiation [131]. This is in concordance with the results obtained in the assays performed. As LacCer has been shown to be a vital component of lipid rafts, it is possible that upon its production in the chondrocyte cells, it recruits other proteins, receptors and signal transductors that lead to the phenotypes observed. We sought to identify if potentiation of differentiation by LacCer was specific to induction with insulin or if the same effect would be observed in chondrocytes differentiated with ascorbic acid. We observed that this was not the case, which we believe is due to the fact that ascorbic acid is an essential cofactor for prolyl lysyl hydroxylase, a key enzyme in collagen biosynthesis that hydroxylates lysyl residues in the collagen triple helix or the telopeptides of collagen and is also capable of glycosylating hydroxylysines, while differentiation with insulin happens through its own receptor [132].

We also assessed differentiation in Fam57b2-overexpressing ATDC5 cells, to see if a similar effect would be observed as with LacCer treatment. Fam57b2-overexpressing ATDC5 cells present a significant increase in the expression of chondrogenic markers, Col2a1 and Col10a1, indicating that Fam57b2 overexpression increases chondrogenesis. When these cells are treated with 24,25(OH)<sub>2</sub> D<sub>3</sub>, there is a further increment in the expression of Col2a1, indicating that the treatment positively influences early stage differentiation of Fam57b2-overexpressing ATDC5 cells. This data correlates with the effect that the product compound, LacCer, has on these cells during differentiation with insulin. This mechanism of action of 24,25(OH)<sub>2</sub> D<sub>3</sub> is further

supported by the genetic model where *Fam57b* was deleted specifically in chondrocytes of mice and a similar callus formation defect phenotype was observed as in *Cyp24a1* KO mice, which can rescued be with LacCer treatment; while in *Cyp24a1* KO mice, the phenotype was rescued with either exogenous LacCer or 24,25(OH)<sub>2</sub> D<sub>3</sub> treatment, demonstrating a common pathway [Martineau, submitted]. Given the fact that we have been able to observe an effect of treatment with 24,25(OH)<sub>2</sub> D<sub>3</sub> on *Fam57b2*-overexpressing ATDC5 cells suggestive of an interaction, it would be interesting to study the effect that 24,25(OH)<sub>2</sub> D<sub>3</sub> treatment has on mutant *Fam57b2* constructs, by creating stable cell lines of all the mutant constructs and assaying the differentiation phenotype under 24,25(OH)<sub>2</sub> D<sub>3</sub> treatment to identify under which mutant the effect is lost.

Based on several studies to identify signal transductors of differentiation of ATDC5 cells, we identified the MAPK p42/44 signaling pathway as the pathway mainly affected by differentiation inducers [119-121]. In other cell types, LacCer was shown to likewise influence this pathway [93, 122]. We assessed this pathway by using MEK kinase inhibitor, U0126, to observe if the potentiation of differentiation by LacCer and the enhancement of chondrogenesis were due to this pathway's activation. Initially, levels of expression of chondrogenic markers analyzed by RT-qPCR were increased in the LacCer + ITS condition and supressed upon addition of the inhibitor, but we were unable to reliably replicate these results. We assessed phosphorylation of p42/44 after treatment during differentiation, but unfortunately results were also inconclusive. We also attempted to assess the involvement of the MAPK p42/44 pathway in the enhanced chondrogenesis phenotype observed upon Fam57b2-overexpression. The inhibitor was administered and chondrogenesis markers were assayed, but unfortunately results were likewise highly variable. However, alcian blue staining showed decreased staining of glycosaminoglycans in cells treated with the inhibitor, indicating that MEK inhibition does affect chondrogenesis.

Alternatively, the literature has also indicated that LacCer can induce production of ROS in certain cell types [91, 115, 116] and alter proteins upstream of MAPK p42/44 [91, 115, 117]. On the other hand, studies in ATDC5 cells have shown that ROS production can induce chondrocyte hypertrophy [117, 118]. We sought an alternative way to demonstrate involvement of MAPK p42/44 by assaying production of ROS time and concentration dependently. We observed that in this system, LacCer is unable to influence ROS production in ATDC5 cells. Consequently, other pathways shown to be involved in chondrocyte regulation should be screened after LacCer treatment or *Fam57b2* overexpression to identify the transduction players responsible for the observed effects.

## Chapter V: Conclusions and Future Directions

By identifying the role that 24,25(OH)<sub>2</sub>D<sub>3</sub> plays in fracture repair, we have a better understanding of the Vitamin D metabolic pathway and the implications that our findings have in the treatment of bone fractures. Together with *in vivo* studies performed in mice, we have uncovered potential clinical applications in the therapeutic management of fractures through the supplementation of 24,25(OH)<sub>2</sub>D<sub>3</sub> or lactosylceramide to help accelerate the fracture healing in patients prone to long bone fractures, especially because of the risk of infection after surgery [133]. In addition, in Canada, roughly 32% of the population does not have sufficient levels of vitamin D in their system, which increases to 40% in the winter [134]. With the knowledge gathered, it can be inferred that 25(OH)<sub>2</sub>D supplementation, which is already recommended to people that live in countries with low sun exposure, pregnant breastfeeding and menopausal women, older people and dark-skinned people, can be indirectly beneficial in bone healing, as it will be eventually converted in the body to 24,25(OH)<sub>2</sub>D<sub>3</sub>.

Overall, we have increased the understanding of how 24,25(OH)<sub>2</sub>D<sub>3</sub> or lactosylceramide act in the bone and how their supplementation has the potential to become new therapeutic agents to help speed up and optimize the fracture repair process. We believe that the findings presented here are of great relevance and novelty and have contributed to expanding the fields of vitamin D and fracture repair, particularly on the function of 24,25(OH)<sub>2</sub>D<sub>3</sub> and FAM57B2.

In the future, we will follow other strategies to determine the site of binding to 24,25(OH)<sub>2</sub>D<sub>3</sub> in FAM57B2. To complete this objective of the project, radiolabeling of 24,25(OH)<sub>2</sub>D<sub>3</sub> and performing saturation or competitive binding analysis can be performed as an alternative. Additionally, more efforts can be invested into attempting to purify FAM57B2 to perform SPR, as this technique is widely used to study protein interaction with small molecules and for drug screening. Perhaps synthesizing specifically the 50 amino acid portion belonging to

the differing portion between FAM57B isoforms and testing this peptide for binding will be a more preferable approach to follow.

Another possible method worth attempting, would be to reconstitute a micelle to simulate biological membrane conditions around the immunoprecipitated protein followed by 24,25(OH)<sub>2</sub>D<sub>3</sub> treatment before incubation. Given the fact that we have been able to observe an effect of treatment with 24,25(OH)<sub>2</sub>D<sub>3</sub> on *Fam57b2*-overexpressing ATDC5 cells suggestive of an interaction, it seems worthwhile to study the effect that 24,25(OH)<sub>2</sub>D<sub>3</sub> treatment has on mutant *Fam57b2* constructs, by creating stable cell lines of all the mutant constructs and assaying the differentiation phenotype under 24,25(OH)<sub>2</sub>D<sub>3</sub> treatment to identify under which mutant the effect is lost.

We were unable to clearly demonstrate the involvement of ROS or the MAPK pathway in the signal transduction that leads to the phenotypes observed in the ATDC5 cells. It has however also been stated in the literature that upon treatment with 24,25(OH)<sub>2</sub>D<sub>3</sub>, resting chondrocytes had a time and dose-dependent increase in the activity of PKC isoform α, suggesting that it was the mediator of the signal transduction pathway controlling the response. It was later observed that PKC and PLA<sub>2</sub> activity inversely correlate. Boyan et al. (2010) also states that inhibition of PLA-2 can enhance PKC activation upon 24,25(OH)<sub>2</sub>D<sub>3</sub> action. The actions of these enzymes converge at MAP kinase, which acts at the gene transcription level to cause the cellular phenotypic responses such as chondrocyte maturation [66, 71]. It has also been shown that LacCer can activate PKC and activate PLA<sub>2</sub> in human neutrophils [102], cardiomyocytes [116] and fibroblasts [91], whose downstream signaling likewise mediates activation of MAPK p42/44 [95]. It is believed that the phenotypic effects are also caused by changes in the phospholipid and fatty acid composition of cells after treatment, causing changes in membrane fluidity, turnover of phospholipids and

activation of kinases [65]. Additionally, it seems worthwhile to also assess signaling through other pathways that have proven to be implicated in chondrocyte regulation (**Fig. 35**).

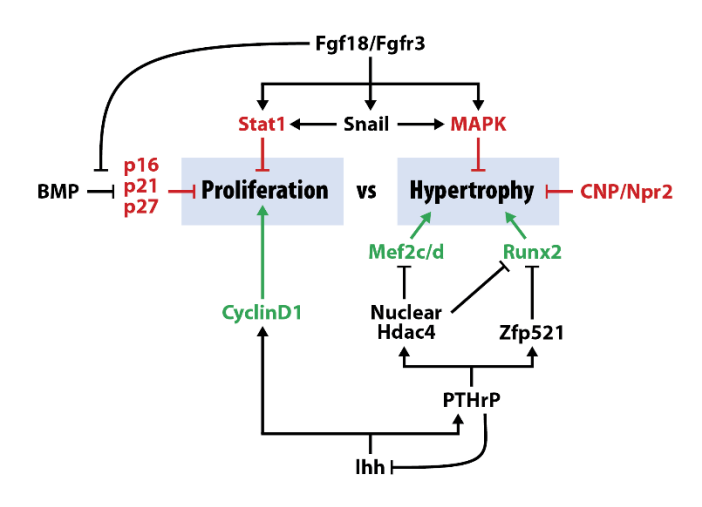


**Fig. 35:** Transcriptional regulators and signaling pathways that regulate chondrocyte proliferation and hypertrophy.

On the other hand, it is of great interest to determine if a local source of 24,25(OH)<sub>2</sub>D<sub>3</sub> is necessary for fracture healing or if the metabolite can be obtained from the circulation. Since the effector FAM57B2 is mostly expressed in chondrocytes, it is possible that *Cyp24a1*-mediated synthesis of 24,25(OH)<sub>2</sub>D<sub>3</sub> in chondrocytes is necessary. For this purpose, a mouse model with cell-type specific inactivation of *Cyp24a1* in chondrocytes will be used to test this hypothesis. Alternatively, it is possible that site-specific production of 24,25(OH)<sub>2</sub>D<sub>3</sub> in osteoblasts and macrophages could be a relevant source of the metabolite which could be acting through a distance and be a physiologically important site of synthesis of 24,25(OH)<sub>2</sub>D<sub>3</sub> for optimal fracture healing. Additionally, since *Fam57b2*'s expression pattern also encompasses skin and ceramides are a type of lipid broadly found in the skin, this is suggestive of an implication of this isoform in cutaneous wound healing.

Overall, *in vitro* studies shown herein in addition to the *in vivo* studies performed in the lab strongly indicate involvement of FAM57B2 and LacCer in chondrocyte regulation. Allosteric regulation of FAM57B2 for the synthesis of LacCer seems specific to 24,25(OH)<sub>2</sub>D<sub>3</sub>. The results gathered from this thesis are consistent with the hypothesis that FAM57B2 is involved in the endochondral stage of fracture healing in bones through its involvement in the increase in differentiation of chondrocytes. The hypothesis is further supported by the observation that ablation of *Fam57b2* in chondrocytes of mice induces impaired fracture healing, which can be rescued through LacCer supplementation. LacCer is likewise suggested to be involved in the endochondral stage of fracture healing by decreasing proliferation and potentiating differentiation of chondrocytes. Better understanding of FAM57B2 structure, mode of interaction with 24,25(OH)<sub>2</sub>D<sub>3</sub> and signalling pathways implicated could yield novel therapeutic targets towards fracture repair.

## Chapter VI: References

- 1. Clarke, B., *Normal bone anatomy and physiology*. Clinical journal of the American Society of Nephrology, 2008. **3**(Supplement 3): p. S131-S139.
- 2. Shao, J., et al., Bone regulates glucose metabolism as an endocrine organ through osteocalcin. International journal of endocrinology, 2015. **2015**.
- 3. Treuting, P.M. and S.M. Dintzis, *Comparative anatomy and histology: a mouse and human atlas (expert consult)*. 2011: Academic Press.
- 4. Florencio-Silva, R., et al., *Biology of bone tissue: structure, function, and factors that influence bone cells.* BioMed research international, 2015. **2015**.
- 5. Gilbert, S.F., *The developmental mechanics of cell specification*. Developmental biology, 6th edition. Sunderland (MA): Sinauer Associates, 2000.
- 6. Percival, C.J. and J.T. Richtsmeier, *Angiogenesis and intramembranous osteogenesis*. Developmental Dynamics, 2013. **242**(8): p. 909-922.
- 7. Brighton, C.T. and R.M. Hunt, *Early histological and ultrastructural changes in medullary fracture callus*. JBJS, 1991. **73**(6): p. 832-847.
- 8. Salter, D.M., Cartilage. Current Orthopaedics, 1998. 12(4): p. 251-257.
- 9. Netter, F.H., et al., *Musculoskeletal System: Anatomy*. Physiology, Metabolic Disorders (Netter Collection of Medical Illustrations, Volume 8, Part 1) Third edition, Saunders, 1987: p. 44-74.
- 10. Mackie, E., et al., *Endochondral ossification: how cartilage is converted into bone in the developing skeleton*. The international journal of biochemistry & cell biology, 2008. **40**(1): p. 46-62.
- 11. Muir, H., The chondrocyte, architect of cartilage. Biomechanics, structure, function and molecular biology of cartilage matrix macromolecules. Bioessays, 1995. **17**(12): p. 1039-1048.
- 12. Lin, Z., et al., *The chondrocyte: biology and clinical application*. Tissue engineering, 2006. **12**(7): p. 1971-1984.
- 13. Dominici, M., T. Hofmann, and E. Horwitz, *Bone marrow mesenchymal cells: Biological properties and clinical applications*. Journal of biological regulators and homeostatic agents, 2000. **15**(1): p. 28-37.
- 14. Wuelling, M. and A. Vortkamp, *Chondrocyte proliferation and differentiation*, in *Cartilage and Bone Development and Its Disorders*. 2011, Karger Publishers. p. 1-11.
- 15. Otero, M., et al., *Human chondrocyte cultures as models of cartilage-specific gene regulation*. Human cell culture protocols, 2012: p. 301-336.
- 16. Pinney, D.F. and C.P. Emerson Jr, 10T1/2 cells: an in vitro model for molecular genetic analysis of mesodermal determination and differentiation. Environmental health perspectives, 1989. **80**: p. 221.
- 17. Saas, J., et al., *Molecular phenotyping of HCS-2/8 cells as an in vitro model of human chondrocytes*. Osteoarthritis and cartilage, 2004. **12**(11): p. 924-934.
- 18. Batoon, L., et al., *Osteomacs and Bone Regeneration*. Current Osteoporosis Reports, 2017. **15**(4): p. 385-395.
- 19. Majidinia, M. and B. Yousefi, *The Roles of Signaling Pathways in Bone Repair and Regeneration*. Journal of Cellular Physiology, 2017.
- 20. Ono, T. and H. Takayanagi, *Osteoimmunology in Bone Fracture Healing*. Current Osteoporosis Reports, 2017. **15**(4): p. 367-375.

- 21. Barnes, G.L., et al., *Growth factor regulation of fracture repair*. Journal of Bone and Mineral Research, 1999. **14**(11): p. 1805-1815.
- 22. Einhorn, T.A. and L.C. Gerstenfeld, *Fracture healing: mechanisms and interventions*. Nature Reviews Rheumatology, 2015. **11**(1): p. 45-54.
- 23. Krishnan, V., H.U. Bryant, and O.A. MacDougald, *Regulation of bone mass by Wnt signaling*. Journal of Clinical Investigation, 2006. **116**(5): p. 1202.
- 24. Zhu, F., M.T. Sweetwyne, and K.D. Hankenson, *PKC*δ *Is Required for Jagged-1 Induction of Human Mesenchymal Stem Cell Osteogenic Differentiation*. Stem Cells, 2013. **31**(6): p. 1181-1192.
- 25. Hilton, M.J., et al., *Notch signaling maintains bone marrow mesenchymal progenitors by suppressing osteoblast differentiation.* Nature medicine, 2008. **14**(3): p. 306.
- Wang, C., et al., *NOTCH signaling in skeletal progenitors is critical for fracture repair.* The Journal of clinical investigation, 2016. **126**(4): p. 1471.
- 27. Gimble, J., et al., *Bone morphogenetic proteins inhibit adipocyte differentiation by bone marrow stromal cells.* Journal of cellular biochemistry, 1995. **58**(3): p. 393-402.
- 28. Carreira, A., et al., Bone morphogenetic proteins: facts, challenges, and future perspectives. Journal of dental research, 2014. 93(4): p. 335-345.
- 29. Daigang, L., et al., LPS-stimulated inflammation inhibits BMP-9-induced osteoblastic differentiation through crosstalk between BMP/MAPK and Smad signaling. Experimental cell research, 2016. **341**(1): p. 54-60.
- 30. Zhou, F.H., et al., *TNF-α Mediates p38 MAP Kinase Activation and Negatively Regulates Bone Formation at the Injured Growth Plate in Rats.* Journal of Bone and Mineral Research, 2006. **21**(7): p. 1075-1088.
- 31. Schindeler, A. and D.G. Little, *Ras-MAPK Signaling in Osteogenic Differentiation: Friend or Foe?* Journal of Bone and Mineral Research, 2006. **21**(9): p. 1331-1338.
- 32. Shah, P., L. Keppler, and J. Rutkowski, *A review of platelet derived growth factor playing pivotal role in bone regeneration*. Journal of Oral Implantology, 2014. **40**(3): p. 330-340.
- 33. Arvidson, K., et al., *Bone regeneration and stem cells*. Journal of cellular and molecular medicine, 2011. **15**(4): p. 718-746.
- 34. Yun, Y.-R., et al., *Fibroblast growth factors: biology, function, and application for tissue regeneration.* Journal of tissue engineering, 2010. **1**(1): p. 218142.
- 35. Ornitz, D.M. and P.J. Marie, FGF signaling pathways in endochondral and intramembranous bone development and human genetic disease. Genes & development, 2002. **16**(12): p. 1446-1465.
- 36. Coutu, D.L. and J. Galipeau, *Roles of FGF signaling in stem cell self-renewal, senescence and aging.* Aging (Albany NY), 2011. **3**(10): p. 920.
- 37. Kawaguchi, H., et al., Stimulation of fracture repair by recombinant human basic fibroblast growth factor in normal and streptozotocin-diabetic rats. Endocrinology, 1994. 135(2): p. 774-781.
- 38. Khorsand, B., et al., Regeneration of bone using nanoplex delivery of FGF-2 and BMP-2 genes in diaphyseal long bone radial defects in a diabetic rabbit model. Journal of Controlled Release, 2017. **248**: p. 53-59.
- 39. Feldman, D., J. Pike, and F. Glorieux, *Vitamin D. 2. 1–2 Elsevier*. 2005, Burlington.
- 40. Plum, L.A. and H.F. DeLuca, *Vitamin D, disease and therapeutic opportunities*. Nature reviews Drug discovery, 2010. **9**(12): p. 941-955.

- 41. Deeb, K.K., D.L. Trump, and C.S. Johnson, *Vitamin D signalling pathways in cancer:* potential for anticancer therapeutics. Nature reviews. Cancer, 2007. **7**(9): p. 684.
- 42. Miller, W.L., Genetic disorders of Vitamin D biosynthesis and degradation. The Journal of steroid biochemistry and molecular biology, 2017. **165**: p. 101-108.
- 43. Kerry, D.M., et al., *Transcriptional synergism between vitamin D-responsive elements in the rat 25-hydroxyvitamin D3 24-hydroxylase (CYP24) promoter.* Journal of Biological Chemistry, 1996. **271**(47): p. 29715-29721.
- 44. Pike, J.W. and M.B. Meyer, Regulation of mouse Cyp24a1 expression via promoter-proximal and downstream-distal enhancers highlights new concepts of 1, 25-dihydroxyvitamin D 3 action. Archives of biochemistry and biophysics, 2012. **523**(1): p. 2-8.
- 45. Kumar, R., et al., *Systematic characterisation of the rat and human CYP24A1 promoter*. Molecular and cellular endocrinology, 2010. **325**(1): p. 46-53.
- 46. Beckman, M.J., et al., *Human 25-hydroxyvitamin D3-24-hydroxylase, a multicatalytic enzyme.* Biochemistry, 1996. **35**(25): p. 8465-8472.
- 47. Schlingmann, K.P., et al., *Mutations in CYP24A1 and idiopathic infantile hypercalcemia*. New England Journal of Medicine, 2011. **365**(5): p. 410-421.
- 48. Horst, R.L., et al., *Impaired 24, 25-dihydroxyvitamin D production in anephric human and pig.* Journal of Clinical Investigation, 1981. **67**(1): p. 274.
- 49. Shinki, T., et al., *Parathyroid hormone inhibits 25-hydroxyvitamin D3-24-hydroxylase mRNA expression stimulated by 1 alpha, 25-dihydroxyvitamin D3 in rat kidney but not in intestine*. Journal of Biological Chemistry, 1992. **267**(19): p. 13757-13762.
- 50. SHIGEMATSU, T., et al., Human parathyroid hormone inhibits renal 24-hydroxylase activity of 25-hydroxyvitamin D3 by a mechanism involving adenosine 3', 5'-monophosphate in rats. Endocrinology, 1986. 118(4): p. 1583-1589.
- 51. Goff, J.P., et al., *Effect of dietary calcium or phosphorus restriction and 1, 25-dihydroxyvitamin D administration on rat intestinal 24-hydroxylase.* Endocrinology, 1992. **131**(1): p. 101-104.
- 52. Henry, H.L., *The 25 (OH) D 3/1α, 25 (OH) 2 D 3-24R-hydroxylase: a catabolic or biosynthetic enzyme?* Steroids, 2001. **66**(3): p. 391-398.
- 53. Nishimura, A., et al., Regulation of messenger ribonucleic acid expression of 1 alpha, 25-dihydroxyvitamin D3-24-hydroxylase in rat osteoblasts. Endocrinology, 1994. **134**(4): p. 1794-1799.
- 54. Dusso, A., et al., γ-Interferon-induced resistance to 1, 25-(OH) 2 D3 in human monocytes and macrophages: a mechanism for the hypercalcemia of various granulomatoses. The Journal of Clinical Endocrinology & Metabolism, 1997. **82**(7): p. 2222-2232.
- 55. Vidal, M., C.V. Ramana, and A.S. Dusso, *Stat1-vitamin D receptor interactions antagonize* 1, 25-dihydroxyvitamin D transcriptional activity and enhance stat1-mediated transcription. Molecular and cellular biology, 2002. **22**(8): p. 2777-2787.
- 56. Hahn, C., et al., Localization of the human vitamin D 24-hydroxylase gene (CYP24) to chromosome 20q13. 2→ q13. 3. Cytogenetic and Genome Research, 1993. 62(4): p. 192-193.
- 57. Hill, F.J. and J.A. Sayer, *Clinical and Biochemical Features of Patients with CYP24A1 Mutations*, in *A Critical Evaluation of Vitamin D-Basic Overview*. 2017, InTech.

- 58. St-Arnaud, R., et al., Deficient mineralization of intramembranous bone in vitamin D-24-hydroxylase-ablated mice is due to elevated 1, 25-dihydroxyvitamin D and not to the absence of 24, 25-dihydroxyvitamin D. Endocrinology, 2000. **141**(7): p. 2658-2666.
- 59. Kovacs, C.S. and H.M. Kronenberg, *Maternal-fetal calcium and bone metabolism during pregnancy, puerperium, and lactation.* Endocrine reviews, 1997. **18**(6): p. 832-872.
- 60. Masuda, S., et al., Altered pharmacokinetics of 1a, 25-dihydroxyvitamin D3 and 25-hydroxyvitamin D3 in the blood and tissues of the 25-hydroxyvitamin D-24-hydroxylase (Cyp24a1) null mouse. Endocrinology, 2005. **146**(2): p. 825-834.
- 61. St-Arnaud, R., A. Arabian, and F. Glorieux, *Abnormal bone development in mice deficient for the vitamin D 24-hydroxylase gene*. Journal of Bone and Mineral Research, 1996. **11**: p. S126.
- 62. Kasuga, H., et al., Characterization of transgenic rats constitutively expressing vitamin D-24-hydroxylase gene. Biochemical and biophysical research communications, 2002. **297**(5): p. 1332-1338.
- 63. Hosogane, N., et al., Mechanisms for the reduction of 24, 25-dihydroxyvitamin D3 levels and bone mass in 24-hydroxylase transgenic rats. The FASEB Journal, 2003. 17(6): p. 737-739.
- 64. Schwartz, Z., et al., *Treatment of resting zone chondrocytes with 24, 25-dihydroxyvitamin D3 [24, 25-(OH) 2D3] induces differentiation into a 1, 25-(OH) 2D3-responsive phenotype characteristic of growth zone chondrocytes.* Endocrinology, 1995. **136**(2): p. 402-411.
- 65. Boyan, B., et al., 24R, 25-Dihydroxyvitamin D3 [24R, 25 (OH) 2 D 3] controls growth plate development by inhibiting apoptosis in the reserve zone and stimulating response to 1α, 25 (OH) 2 D 3 in hypertrophic cells. The Journal of steroid biochemistry and molecular biology, 2010. **121**(1): p. 212-216.
- 66. Schwartz, Z., et al., The synergistic effects of vitamin D metabolites and transforming growth factor-β on costochondral chondrocytes are mediated by increases in protein kinase C activity involving two separate pathways. Endocrinology, 1998. **139**(2): p. 534-545.
- 67. Fine, N., et al., Autoradiographic localization of 24R, 25-dihydroxyvitamin D3 in epiphyseal cartilage. Bone, 1985. **6**(2): p. 99-104.
- 68. Schwartz, Z., et al., Direct effects of 1, 25-dihydroxyvitamin D3 and 24, 25-dihydroxyvitamin D3 on growth zone and resting zone chondrocyte membrane alkaline phosphatase and phospholipase-A2 specific activities. Endocrinology, 1988. 123(6): p. 2878-2884.
- 69. Swain, L., et al., Nongenomic regulation of chondrocyte membrane fluidity by 1, 25-(OH) 2D3 and 24, 25-(OH) 2D3 is dependent on cell maturation. Bone, 1993. 14(4): p. 609-617.
- 70. Schwartz, Z., et al., Regulation of prostaglandin E2 production by vitamin D metabolites in growth zone and resting zone chondrocyte cultures is dependent on cell maturation. Bone, 1992. **13**(5): p. 395-401.
- 71. Sylvia, V., et al., *Maturation-dependent regulation of protein kinase C activity by vitamin D3 metabolites in chondrocyte cultures.* Journal of cellular physiology, 1993. **157**(2): p. 271-278.
- 72. Seo, E.-G., A. Kato, and A.W. Norman, Evidence for a 24R, 25 (OH) 2-Vitamin D3Receptor/Binding Protein in a Membrane Fraction Isolated from a Chick Tibial Fracture-Healing Callus. Biochemical and biophysical research communications, 1996. 225(1): p. 203-208.

- 73. Seo, E.G. and A.W. Norman, *Three-Fold Induction of Renal 25-Hydroxyvitamin D3-24-Hydroxylase Activity and Increased Serum 24, 25-Dihydroxyvitamin D3 Levels Are Correlated with the Healing Process After Chick Tibial Fracture.* Journal of Bone and Mineral Research, 1997. **12**(4): p. 598-606.
- 74. Seo, E.-G., T.A. Einhorn, and A.W. Norman, 24R, 25-dihydroxyvitamin D3: an essential vitamin D3 metabolite for both normal bone integrity and healing of tibial fracture in chicks. Endocrinology, 1997. 138(9): p. 3864-3872.
- 75. Kato, A., et al., Studies on 24R, 25-dihydroxyvitamin D 3: evidence for a nonnuclear membrane receptor in the chick tibial fracture-healing callus. Bone, 1998. **23**(2): p. 141-146.
- 76. Lidor, C., et al., *Healing of rachitic lesions in chicks by 24R, 25-dihydroxycholecalciferol administered locally into bone.* Journal of Bone and Mineral Research, 1987. **2**(2): p. 91-98.
- 77. Yamashita-Sugahara, Y., et al., Fam57b (Family with Sequence Similarity 57, Member B), a Novel Peroxisome Proliferator-activated Receptor γ Target Gene That Regulates Adipogenesis through Ceramide Synthesis. Journal of Biological Chemistry, 2013. **288**(7): p. 4522-4537.
- 78. Winter, E. and C.P. Ponting, *TRAM, LAG1 and CLN8: members of a novel family of lipid-sensing domains?* Trends in biochemical sciences, 2002. **27**(8): p. 381-383.
- 79. Brown, M.L., et al., Delayed fracture healing and increased callus adiposity in a C57BL/6J murine model of obesity-associated type 2 diabetes mellitus. PloS one, 2014. **9**(6): p. e99656.
- 80. Tanaka, Y., et al., Determination of stereochemical configuration of the 24-hydroxyl group of 24, 25-dihydroxyvitamin D3 and its biological importance. Archives of biochemistry and biophysics, 1975. 170: p. 620-626.
- 81. Ishizuka, S., T. Takeshita, and A.W. Norman, *Naturally occurring 24, 25-dihydroxyvitamin D3 is a mixture of both C-24R and C-24S epimers.* Archives of biochemistry and biophysics, 1984. **234**(1): p. 97-104.
- 82. Traut, T.W., Allosteric regulatory enzymes. 2007: Springer Science & Business Media.
- 83. Brown, N.C. and P. Reichard, *Role of effector binding in allosteric control of ribonucleoside diphosphate reductase*. Journal of molecular biology, 1969. **46**(1): p. 39-55.
- 84. Khavandgar, Z. and M. Murshed, *Sphingolipid metabolism and its role in the skeletal tissues*. Cellular and molecular life sciences, 2015. **72**(5): p. 959-969.
- 85. Dinoff, A., N. Herrmann, and K.L. Lanctôt, *Ceramides and depression: A systematic review.* Journal of Affective Disorders, 2017.
- 86. Perry, D.K. and Y.A. Hannun, *The role of ceramide in cell signaling*. Biochimica et Biophysica Acta (BBA)-Molecular and Cell Biology of Lipids, 1998. **1436**(1): p. 233-243.
- 87. Airola, M.V. and Y.A. Hannun, *Sphingolipid metabolism and neutral sphingomyelinases*, in *Sphingolipids: Basic Science and Drug Development*. 2013, Springer. p. 57-76.
- 88. Iwabuchi, K., et al., Role of ceramide from glycosphingolipids and its metabolites in immunological and inflammatory responses in humans. Mediators of inflammation, 2015. **2015**.
- 89. SHARMA, K. and S. Yufang, *The yins and yangs of ceramide*. Cell research, 1999. **9**(1): p. 1-10.
- 90. Christie, W., Oligoglycosylceramides (Non-Acidic). 2014.

- 91. Chatterjee, S. and A. Pandey, *The Yin and Yang of lactosylceramide metabolism: implications in cell function*. Biochimica et Biophysica Acta (BBA)-General Subjects, 2008. **1780**(3): p. 370-382.
- 92. D'angelo, G., et al., Vesicular and non-vesicular transport feed distinct glycosylation pathways in the Golgi. Nature, 2013. **501**(7465): p. 116.
- 93. Bhunia, A.K., et al., *Lactosylceramide stimulates Ras-GTP loading, kinases (MEK, Raf), p44 mitogen-activated protein kinase, and c-fos expression in human aortic smooth muscle cells*. Journal of Biological Chemistry, 1996. **271**(18): p. 10660-10666.
- 94. Bhunia, A.K., et al., *Lactosylceramide mediates tumor necrosis factor-α-induced intercellular adhesion molecule-1 (ICAM-1) expression and the adhesion of neutrophil in human umbilical vein endothelial cells*. Journal of Biological Chemistry, 1998. **273**(51): p. 34349-34357.
- 95. Gong, N., et al., Lactosylceramide recruits PKCα/ε and phospholipase A2 to stimulate PECAM-1 expression in human monocytes and adhesion to endothelial cells. Proceedings of the National Academy of Sciences of the United States of America, 2004. **101**(17): p. 6490-6495.
- 96. Martin, S.F., N. Williams, and S. Chatterjee, *Lactosylceramide is required in apoptosis induced by N-Smase*. Glycoconjugate journal, 2006. **23**(3): p. 147-157.
- 97. Kolmakova, A., et al., *VEGF recruits lactosylceramide to induce endothelial cell adhesion molecule expression and angiogenesis in vitro and in vivo*. Glycoconjugate journal, 2009. **26**(5): p. 547-558.
- 98. Xu, F., et al., *Effect of ceramide on mesenchymal stem cell differentiation toward adipocytes*. Applied biochemistry and biotechnology, 2010. **160**(1): p. 197-212.
- 99. Yeh, L.-H., et al., *Lactosylceramide mediates shear-induced endothelial superoxide production and intercellular adhesion molecule-1 expression.* Journal of vascular research, 2001. **38**(6): p. 551-559.
- 100. Balagopalakrishna, C., et al., *Minimally modified low density lipoproteins induce aortic smooth muscle cell proliferation via the activation of mitogen activated protein kinase.* Molecular and cellular biochemistry, 1997. **170**(1-2): p. 85-89.
- 101. Kakugawa, Y., et al., *Up-regulation of plasma membrane-associated ganglioside sialidase* (Neu3) in human colon cancer and its involvement in apoptosis suppression. Proceedings of the National Academy of Sciences, 2002. **99**(16): p. 10718-10723.
- 102. Arai, T., et al., Lactosylceramide stimulates human neutrophils to upregulate Mac-1, adhere to endothelium, and generate reactive oxygen metabolites in vitro. Circulation research, 1998. **82**(5): p. 540-547.
- 103. Ho, S.N., et al., *Site-directed mutagenesis by overlap extension using the polymerase chain reaction.* Gene, 1989. 77(1): p. 51-59.
- 104. Liang, C.-C., A.Y. Park, and J.-L. Guan, *In vitro scratch assay: a convenient and inexpensive method for analysis of cell migration in vitro*. Nature protocols, 2007. **2**(2): p. 329-333.
- 105. Folch, J., M. Lees, and G. Sloane-Stanley, A simple method for the isolation and purification of total lipids from animal tissues. J biol Chem, 1957. **226**(1): p. 497-509.
- 106. Gammack, D., *Physicochemical properties of ox-brain gangliosides*. Biochemical Journal, 1963. **88**(2): p. 373.

- 107. Zacharias, C., et al., A truncated epoxy-glucosylceramide uncouples glycosphingolipid biosynthesis by decreasing lactosylceramide synthase activity. Journal of Biological Chemistry, 1994. **269**(18): p. 13313-13317.
- 108. Higuchi, R., et al., *Simultaneous amplification and detection of specific DNA sequences*. Nature Biotechnology, 1992. **10**(4): p. 413-417.
- 109. Information, N.C.f.B.
- 110. Tsirigos, K.D., et al., *The TOPCONS web server for consensus prediction of membrane protein topology and signal peptides.* Nucleic acids research, 2015. **43**(W1): p. W401-W407.
- 111. Bernsel, A., et al., *TOPCONS: consensus prediction of membrane protein topology.* Nucleic acids research, 2009. **37**(suppl 2): p. W465-W468.
- 112. *TMHMM Server v. 2.0.*
- 113. Omasits, U., et al., *Protter: interactive protein feature visualization and integration with experimental proteomic data.* Bioinformatics, 2013. **30**(6): p. 884-886.
- 114. Tang, C.-H., et al., Enhancement of fibronectin fibrillogenesis and bone formation by basic fibroblast growth factor via protein kinase C-dependent pathway in rat osteoblasts. Molecular pharmacology, 2004. **66**(3): p. 440-449.
- 115. Mishra, S. and S. Chatterjee, *Lactosylceramide promotes hypertrophy through ROS generation and activation of ERK1/2 in cardiomyocytes*. Glycobiology, 2014. **24**(6): p. 518-531.
- 116. Nakamura, H., et al., Lactosylceramide-induced phosphorylation signaling to group IVA phospholipase A2 via reactive oxygen species in tumor necrosis factor-α-treated cells. Journal of Cellular Biochemistry, 2017.
- 117. Morita, K., et al., Reactive oxygen species induce chondrocyte hypertrophy in endochondral ossification. Journal of Experimental Medicine, 2007. **204**(7): p. 1613-1623.
- 118. Mirza, R., et al.,  $3\beta$ -Hydroxysterol-Delta24 reductase plays an important role in long bone growth by protecting chondrocytes from reactive oxygen species. Journal of bone and mineral metabolism, 2012. **30**(2): p. 144-153.
- 119. Yang, M., et al., *Aloe-Emodin Induces Chondrogenic Differentiation of ATDC5 Cells via MAP Kinases and BMP-2 Signaling Pathways*. Biomolecules & therapeutics, 2016. **24**(4): p. 395.
- 120. Choi, H.J., et al., Stimulation of chondrogenesis in ATDC5 chondroprogenitor cells and hypertrophy in mouse by Genkwadaphnin. European journal of pharmacology, 2011. **655**(1): p. 9-15.
- 121. Phornphutkul, C., K.-Y. Wu, and P.A. Gruppuso, *The role of insulin in chondrogenesis*. Molecular and cellular endocrinology, 2006. **249**(1): p. 107-115.
- 122. Iwamoto, T., et al., *Lactosylceramide is essential for the osteoclastogenesis mediated by macrophage-colony-stimulating factor and receptor activator of nuclear factor-κB ligand.* Journal of Biological Chemistry, 2001. **276**(49): p. 46031-46038.
- 123. Brommage, R., et al., *1-But not 24-hydroxylation of vitamin D is required for skeletal mineralization in rats*. American Journal of Physiology-Endocrinology and Metabolism, 1983. **244**(3): p. E298-E304.
- 124. Ameenuddin, S., et al., 24-hydroxylation of 25-hydroxyvitamin D3: is it required for embryonic development in chicks? Science, 1982. 217(4558): p. 451-452.
- 125. De Jong, L.A., et al., *Receptor–ligand binding assays: technologies and applications*. Journal of Chromatography B, 2005. **829**(1): p. 1-25.

- 126. Patching, S.G., Surface plasmon resonance spectroscopy for characterisation of membrane protein–ligand interactions and its potential for drug discovery. Biochimica et Biophysica Acta (BBA)-Biomembranes, 2014. **1838**(1): p. 43-55.
- 127. Smith, S.M., Strategies for the Purification of Membrane Proteins, in Protein Chromatography: Methods and Protocols, D. Walls and S.T. Loughran, Editors. 2017, Springer New York: New York, NY. p. 389-400.
- 128. Kubicek, J., et al., *Expression and purification of membrane proteins*. Methods Enzymol, 2014. **541**: p. 117-140.
- 129. Cain, J.A., N. Solis, and S.J. Cordwell, *Beyond gene expression: the impact of protein post-translational modifications in bacteria*. Journal of proteomics, 2014. **97**: p. 265-286.
- 130. Bastian, O.W., et al., *Neutrophils contribute to fracture healing by synthesizing fibronectin+ extracellular matrix rapidly after injury.* Clinical Immunology, 2016. **164**: p. 78-84.
- 131. Strehl, R., et al., *Proliferating cells versus differentiated cells in tissue engineering*. Tissue engineering, 2002. **8**(1): p. 37-42.
- 132. Temu, T.M., et al., *The mechanism of ascorbic acid-induced differentiation of ATDC5 chondrogenic cells*. American Journal of Physiology-Endocrinology and Metabolism, 2010. **299**(2): p. E325-E334.
- 133. Szulc, W. and S. Zawadziński, *Post-traumatic infections of the musculoskeletal locomotor system; prophylaxis and treatment.* Polski tygodnik lekarski (Warsaw, Poland: 1960), 1991. **46**(30-31): p. 565-567.
- 134. Janz, T. and C. Pearson, *Vitamin D blood levels of Canadians*. Statistics Canada, 2015. **82-624-X**(Health at a Glance).